A Thesis for the Degree of Doctor of Philosophy in Pharmacy

Structure Determination of New Bioactive Secondary Metabolites from *Streptomyces*, *Actinomadura*, and *Deinococcus* Bacteria

August 2018

Bora Shin

Natural Products Science Major, College of Pharmacy
Doctoral Course in the Graduate School
Seoul National University

Abstract

Structure Determination of New Bioactive Secondary Metabolites from *Streptomyces*, *Actinomadura*, and *Deinococcus* Bacteria

Bora Shin
Natural Products Science Major
College of Pharmacy
Doctoral Course in the Graduate School
Seoul National University

1. Suncheonoside A-D, benzothioate glycoside from marine-derived *Streptomyces* sp.

A marine-derived *Streptomyces* strain, SSC21, was isolated from the sediment of Suncheon Bay, Republic of Korea. Chemical analysis of the bacterial strain resulted in the isolation of four new metabolites, suncheonosides A-D (**1**-**4**), each bearing a sulfur atom. The planar structures of the suncheonosides were identified as hexa-substituted benzothioate glycosides by combined spectroscopic analyses. Analysis of the configuration of the sugar moieties based on ROESY NMR correlations, 1-bond ^{1}H-^{13}C coupling constant analysis, and chemical derivatizations elucidated that the suncheonosides incorporate only L-rhamnose. Suncheonosides A, B, and D promoted adiponectin production in a concentration-dependent manner during adipogenesis in human mesenchymal stem cells, suggesting anti-diabetic potential.

2. JS8 A and B, novel bacterial flavonoid, from *Streptomyces* sp. associated with white grub *Protaetia brevitarsis seulensis*.

Investigation of secondary metabolites of bacteria associated with eukaryotic hosts has become a promising approach to discover novel bioactive compounds. In search for new bioactive chemotypes, I have been focusing on secondary metabolites of bacterial strains associated in the gut of a white grub of *Protaetia brevitarsis seulensis*. The secondary metabolite profiles of the 80 actinobacterial strains isolated from the gut of a *P. brevitarsis* grub were chemically analyzed by LC/MS. This chemical analysis led to the discovery of two new flavonoid-like compounds, which are dominantly found in plants but really uncommon as bacterial metabolites. The epimeric compounds JS8A and B (**6**-**7**) were purified by HPLC using a chiral column (a polysaccharide-based immobilizing cellulose to silica gel). Their structures were determined mainly by spectroscopic analysis of NMR and mass data. The absolute configurations were established by time-controlled acetylation followed by the application of the modified Mosher's method using MTPA. Moreover, the comparative full genome analysis of the strain JS8 and the producer (CNB-689) of actionflavoside, will be discussed along with their structures.

3. Actinomadurol, an antibacterial norditerpenoid from a rare actinomycete, *Actinomadura* sp. KC-191

A new secondary metabolite, actinomadurol (**13**), was isolated

along with the known compound JBIR-65 (**14**) from a rare actinomycete, *Actinomadura* strain KC 191. The structure of **13** was established as a rare member of the bacterial C-19 norditerpenoid class by NMR data and ECD calculations. The absolute configuration of **14**, which was previously reported without stereochemical analysis, was determined by using the modified Mosher's method and ECD calculations. Actinomadurol (**13**) exhibited potent antibacterial activity against pathogenic strains, such as *Staphylococcus aureus, Kocuria rhizophila* and *Proteus hauseri* (MIC = 0.39 ~ 0.78 μg/mL), whereas JBIR-65 (**14**) showed no antibacterial activity.

4. Deinococcucins A−D, aminoglycolipids from Deinococcus sp., a gut bacterium of the carpenter ant *Camponotus japonicus*.

Four new aminoglycolipids, deinococcucins A-D (**18-21**), were discovered from a *Deinococcus* sp. strain isolated from the gut of queen carpenter ants, *Camponotus japonicus*. The structures of deinococcucins A-D were elucidated as a combination of *N*-acetyl glucosamine, 2,3-dihydroxypropanoic acid, and an alkyl amine with a C_{16} or C_{17} hydrocarbon chain primarily based on 1D and 2D nuclear magnetic resonance (NMR) and mass spectroscopic data. The exact location of the olefinic double bond in deinococcucins C-D (**20-21**) was assigned based on the liquid chromatography-mass spectroscopy (LC/MS) data obtained after olefin metathesis. The absolute configurations of the *N*-acetyl glucosamine and 2,3-dihydroxy moieties were determined through gas chromatography-mass

spectroscopy (GC/MS) analysis of authentic samples and phenylglycine methyl ester (PGME)-derivatized products, respectively. Deinococcucins A and C displayed significant induction of quinone reductase in murine Hepa-1c1c7 cells.

Key words; rare actinomyces, strucuture determination, biosynthesis

Student number: 2012-23593

List of Contents

List of Tables

List of Figures

are noted in ppm in DMSO-d_6.

Figure 16. Effect of deinococcucins A-D (**18-21**) on the induction of QR in murine Hepa 1c1c7 cells.

I. Introduction

Marine-derived bioactive compounds are currently considered tremendous chemical resources for drug discovery.[1] Early marine natural products research primarily focused on marine invertebrates, ultimately resulting in the development of several marketed drugs. The representative anticancer drug Halaven was originally derived from a marine sponge, whereas the painkiller Prialt was derived from a cone snail.[2] In addition, the anticancer agent Yondelis was developed from a marine tunicate.[2] However, over the past five years, the number of publications about the chemistry of marine invertebrates has remained static or even decreased, whereas marine microorganisms are now increasingly spotlighted as an emerging source of new bioactive natural products.[3] Among marine-derived bacteria, actinobacteria constitute important and potential taxa with respect to chemical diversity.[4] The number of chemical reports on marine actinomycetes has rapidly increased over the past decade, and the rates of increase over the past five years are even higher.[3]

In our search for new bioactive compounds from marine actinobacteria,[5] I selectively isolated actinomycete strains from marine sediment samples from Suncheon Bay, Republic of Korea. Suncheon Bay is a tideland with high biodiversity that provides habitats for migratory birds, various plants and animals as well as microorganisms.[6] Actinomycete strains from Suncheon Bay sediments were subjected to chemical profiling by LC/MS analysis. Through the profiling process, one of the strains, *Streptomyces* sp. SSC21, was identified to produce a series of compounds, each containing a

sulfur atom, based on mass spectroscopic data ($[M+Na]^+$:$[M+2+Na]^+$ ≈ 100:5).[7] This information, along with corresponding UV and mass spectra, suggested that these compounds were unlikely to have been previously reported, thus prompting further chemical analysis. In this paper, I discuss the isolation and identification of the structures of the sulfur-bearing compounds, named suncheonosides A-D (**1**-**4**), and their biological activity with respect to insulin sensitivity.

Investigation of secondary metabolites of bacteria associated with eukaryotic hosts has become a promising approach to discover novel bioactive compounds. In search for new bioactive chemotypes, I have been focusing on secondary metabolites of bacterial strains associated in the gut of a white grub of Protaetia brevitarsis seulensis. The secondary metabolite profiles of the 80 actinobacterial strains isolated from the gut of a P. brevitarsis grub were chemically analyzed by LC/MS. This chemical analysis led to the discovery of two new flavonoid-like compounds, which are dominantly found in plants but really uncommon as bacterial metabolites. The epimeric compounds JS8A and B (**6**-**7**) were purified by HPLC using a chiral column (a polysaccharide-based immobilizing cellulose to silica gel). Their structures were determined mainly by spectroscopic analysis of NMR and mass data. The absolute configurations were established by time-controlled acetylation followed by the application of the modified Mosher's method using MTPA. Moreover, the comparative

full genome analysis of the strain JS8 and the producer (CNB-689) of actionflavoside, will be discussed along with their structures.

The discovery of new antibiotics is constantly required because of the continuing development of antibiotic resistance and the side effects of current antibiotics.[16] Microbial natural products remain the most propitious source of novel antibiotics. Filamentous actinobacteria have a unique ability to produce natural antibiotic compounds;[17] notably members of the genus *Streptomyces* which are the source of over 70% actinobacterial bioactive compounds.[18] However, recently rare actinobacteria, that is, representatives of genera with lower isolation rates than *Streptomyces* strains, are being increasingly recognized as a potential source of novel antibiotics[19] following the discovery of epoch-making antibacterial drugs, as exemplified by the isolation of erythromycin from *Saccharopolyspora erythraea*,[20] and vancomycin from *Amycolatopsis orientalis*.[21] In more recent times novel bioactive compounds have been isolated from rare actinobacteria classified in poorly studied genera such as *Salinispora*[22] and *Verrucosispora*.[23]

In our search for new bioactive compounds, I focused on the secondary metabolites of rare actinobacteria, as illustrated by the discovery of a structurally new benzofuran glycoside and indole alkaloids from an *Amycolatopsis* strain isolated from a marine sponge.[8] A continuation of these studies led us to *Actinomadura* strain KC 191 which was seen to inhibit neighboring bacterial colonies on isolation plates seeded with a

suspension of an agricultural soil sample. Extracts of strain KC 191 showed significant antibacterial activity against *Bacillus subtilis*, *Staphylococcus aureus, Kocuria rhizophila*, *Proteus hauseri* and *Salmonella enterica* strains (MIC = 0.39 ~ 3.12 μg/mL), prompting the scale-up of the culture. Comprehensive chemical analysis of the resultant extracts led to the identification of a new antibacterial norditerpenoid, actinomadurol (**13**), and its congener, JBIR-65 (**14**), which was previously reported albeit without stereochemical analysis.[25] Here, I report on the structural determination, including the absolute configurations of actinomadurol (**13**) and JBIR-65 (**14)** and their antibiotic activities.

Microbes in symbiotic insect ecosystems have recently been recognized as a tremendous reservoir of bioactive small molecules for drug discovery.[45-47] However, only a handful of insect systems have been investigated for microbial compounds, even though the class Insecta is estimated to contain approximately 5 million species in 28 orders.[48] Representative chemical studies on the bioactive small molecules produced by insect-associated microbes have involved the southern pine beetle *Dendroctonus frontali*[49-51] and the dung beetle *Copris tripartitus*[52-55] in the order Coleoptera, the fungus-growing termite *Macrotermes natalensis*[56-58] in the order Blattodea, the mantis *Tenodera aridifolia*[59] in the order Mantodea, the grasshopper *Oxya chinensis* in the order Orthoptera,[60,61] and the fungus-growing ants

(*Apterostigma dentigerum* and *Trachymyrmex cornetzi*)[62,63] and the wasps (*Sceliphron caementarium*[64,65] and *Philanthus triangulum*[66,67]) in the order Hymenoptera.

Hymenoptera, which harbors more than 125,000 described species and 220,000 estimated species, is one of the four most speciose insects.[68] This order distinctively encompasses most of the eusocial insects. Ants are common and representative eusocial insects belonging to the family Formicidae in the order Hymenoptera.[69] Their successful adaptation in diverse environments has been explained by their organized social life cycles. As highlighted in the pioneering chemical studies of symbiotic bacteria in fungus-growing ants,[62,63] bacterial associations with ants can be a general phenomenon. Therefore, the chemical investigation of bacterial secondary metabolites in ant ecosystems may be an efficient strategy to discover new bioactive small molecules. This study focused on the ecosystem of the carpenter ant, *Camponotus japonicus*, which is a dominant ant species in East Asia.[70] I collected carpenter ants in Seoul Grand Park, Republic of Korea, and isolated bacterial strains from the ant specimens. Chemical analysis of the bacterial metabolites by liquid chromatography-mass spectroscopy (LC/MS) revealed that strain SJN1, which was most closely related to *Deinococcus xinjiangensis* and isolated from the gut of queen specimens, produced a series of previously unreported compounds that were invisible under UV detection but distinctly detected in mass spectra ($[M+H]^+$ ions at *m*/*z* 531~547). Further scaling up the culture of

SJN1 and chromatographic isolation of these compounds by HPLC with refractive index (RI) detection resulted in the discovery of four new aminoglycolipids, deinococcucins A-D (**18-21**). Here, I report the structural determination, including the absolute configurations, and the biological activities of deinococcucins A-D (**18-21**), rare metabolites from the genus *Deinococcus*.

II. Studies on the secondary metabolites from *Streptomyces*, *Actinomadura*, and *Deinococcus* bacteria

1. Suncheonoside A-D, benzothioate glycoside from marine-derived *Streptomyces* sp.

II.1.1. Results and discussion

Suncheonoside A (**1**) was isolated as a white powder. The molecular formula of **1** was assigned as $C_{19}H_{28}O_7S$ based on HRFAB mass spectrometric data and ^1H and ^{13}C NMR data (Table 1). The ^1H and HSQC NMR spectra of **1** in pyridine-d_5 showed a proton at δ_H 5.77 directly bound to a dioxygenated carbon at δ_C 107.2, four methine protons between 4.87 ppm and 4.41 ppm correlated with oxygenated sp^3 carbons between 72.1 and 73.4, a methine proton (δ_H 3.39) attached to an aliphatic carbon (δ_C 32.1), three singlet methyl groups (δ_H 2.58- δ_C 11.4; δ_H 2.48-δ_C 14.2; δ_H 2.41- δ_C 12.8), and three doublet methyl groups (δ_H 1.72- δ_C 18.6; δ_H 1.41-δ_C 21.6; δ_H 1.38- δ_C 21.7). In contrast to the ^1H NMR spectrum, which showed only sp^3 carbon-bound protons, the ^{13}C NMR spectrum exhibited one carbonyl carbon at 197.3 ppm and six sp^2 carbons between 157.4 and 116.7 ppm, along with the five oxygenated carbons and seven aliphatic carbons observed in the HSQC NMR spectrum.

Given this information, the structure of compound **1** was determined by a combined analysis of COSY and HMBC NMR experiments. First, the HMBC spectrum clearly demonstrated the presence of a hexa-substituted benzenoid system. The position of one aryl methyl group (C-8) at δ_H 2.58 was assigned to C-3 based on three strong HMBC correlations of H_3-8 to C-3 (δ_C 116.7) and two oxygen-bearing carbons (C-2 at δ_C 152.4 and C-4 at δ_C 157.4). The other aryl methyl group (C-9) at δ_H 2.48 was determined to be

located at C-5 based on the distinct HMBC couplings of H_3-9 to one oxygen-bearing carbon (C-4 at δ_C 157.4) and two double-bond carbons (C-5 at δ_C 140.9 and C-6 at δ_C 120.5). The H_3-8/C-4 and H_3-9/C-4 HMBC correlations clearly secured the connectivity of C-3 to C-4. The COSY correlations of the aliphatic methine proton H-10 (δ_H 3.39) to two doublet methyl protons (H_3-11 at δ_H 1.38 and H_3-12 at δ_H 1.41) suggested the formation of an isopropyl group. The ^{1}H-^{13}C long-range coupling detected from these geminal methyl groups to C-6 placed the isopropyl group at C-6. The HMBC correlations from H-10 and H_3-9 to C-5 and C-6 established a C-5-C-6 linkage. The ring closure connectivity from C-1 to C-2 was deduced by the double-bond chemical shifts of these carbons and the number of double-bond carbons, thus indicating the formation of a six-membered aromatic system.

Analysis of the COSY and HMBC NMR data revealed a hexose structure. ^{1}H-^{1}H homonuclear couplings revealed the formation of a spin system from H-1′ (δ_H 5.77) to H_3-6′ (δ_H 1.72) COSY correlations. H-1′/C-5′ and H-5′/C-1′ HMBC correlations established that a hexose underwent ring closure. The hexose ring was connected to the hexa-substituted aromatic moiety through an ether functional group, based on the HMBC correlation from H-1′ to C-2. These assignments consequently left the C-1 position to be substituted by a functional group composed of an unused carbonyl carbon at δ_C 197.3, a singlet methyl group (δ_H 2.41-δ_C 12.8), and a sulfur atom. The HMBC

correlation from the singlet methyl protons to the carbonyl carbon suggested two possible functional groups, *S*-methyl methanethioate and ethanethioate. The chemical shift (δ_C 12.8) of the methyl group clearly indicated *S*-methyl methanethioate, thus assigning the position of the thioester carbon (C-7) as between C-1 and the *S*-methyl group (C-13). Therefore, the planar structure of suncheonoside A (**1**) was elucidated as a new benzothioate glycoside (Figure 1).

The relative configuration of the sugar was established by analyzing ^{1}H-^{13}C and ^{1}H-^{1}H coupling constants and ROESY NMR through-space correlations. The magnitude of $^{1}J_{CH}$ (170 Hz) between C-1′ and H-1′ was clearly indicative of an α-configuration,[8] placing the anomeric proton (H-1′) at an equatorial position. The large ^{1}H-^{1}H vicinal coupling constant (9.0 Hz) between H-3′ and H-4′ established their *anti*-relationship and, therefore, axial positions. The equatorial position of H-2′ was assigned based on the ROESY correlation between H-2′ and H-3′. The H-3′/H-5′ 1,3-ROESY correlation established an axial position for H-5′ and consequently an equatorial position for the C-6′ methyl group. This assignment was also supported by the H-4′/H_3-6′ ROESY correlation. Therefore, the hexose moiety was determined to be rhamnose (Figure 2).

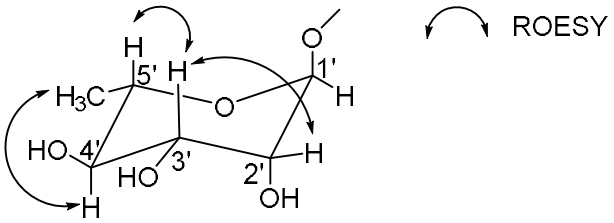

Figure 2. The observed strong ROESY correlations in the hexose moiety in **1**-**4**.

To date, rhamnose sugar has been found to occur only in the L-form in nature, and thus, this moiety has often been assumed to possess an L-configuration in nature without precise stereochemical verification.[8] To establish the absolute configuration of rhamnose in a rigorous manner, suncheonoside A **(1)** was first subjected to acid hydrolysis. The hydrolysate and authentic L- and D-rhamnose samples were separately derivatized with L-cysteine methyl ester hydrochloride and σ-tolyl isothiocyanate.[9] Based on LC/MS analysis of the derivatives, the rhamnose moiety in suncheonoside A was determined to possess an L-configuration.

Suncheonoside B (**2**) was purified as a white powder, the molecular formula of which was determined to be $C_{20}H_{30}O_7S$ based on the corresponding HRFAB mass spectrometric data and ^1H and ^{13}C NMR data (Table 1). The ^1H and ^{13}C NMR spectra of **2** in pyridine-d_5 were observed to be highly similar to those of **1**. Detailed examination of the 1D and 2D NMR data of **2** revealed the existence of the *S*-methyl benzothioate and rhamnose moieties analogous to those of **1**. The most noticeable difference in **2** compared to suncheonoside A was the occurrence of a methoxy group

(δ_H 3.68-δ_C 62.3). The group was readily accommodated by replacing the 4-OH hydroxy group in **2**, as indicated by the HMBC correlation of 4-OMe to C-4 (δ_C 157.8). The absolute configuration of rhamnose in suncheonoside B (**2**) was also assigned an L-configuration by the chemical derivatization and LC/MS analysis method discussed above. Therefore, the structure of suncheonoside B (**2**) was elucidated as a methoxy analog of **1** on C-4.

Suncheonoside C (**3**) was isolated as a white powder. Its molecular formula ($C_{20}H_{30}O_7S$) was determined to be identical to that of suncheonoside B (**2**) based on HRFAB mass spectrometric data and ^1H and ^{13}C NMR data (Table 1). The NMR, UV, and IR spectroscopic features of **3** were highly analogous to those of **2**. Further investigation of the ^1H, ^{13}C, COSY, HSQC, HMBC and ROESY NMR spectra indicated that the structure of suncheonoside C (**3**) was very similar to that of suncheonoside B (**2**), except for the positions of the methoxy group and the sugar moieties. The methoxy protons (δ_H 3.68) displayed an HMBC correlation to C-2 (δ_C 152.8), placing the methoxy group at C-2 whereas the H-1″/C-4 long-range coupling connected the sugar at C-4. Stereochemical analysis of the sugar moiety established that this unit is also L-rhamnose.

In addition to suncheonosides A-C (**1**-**3**), suncheonoside D (**4**) was purified as a white powder. The molecular formula of **4** was determined to be $C_{25}H_{38}O_{11}S$ based on HRFAB analysis and ^1H and ^{13}C NMR data (Table 1). Interpretation of the ^1H, ^{13}C, COSY, HSQC and HMBC NMR spectra

suggested that suncheonoside D (**4**) has a structure similar to the structures of other congeners that have *S*-methyl benzothioate and rhamnose moieties. Further analysis of 1D and 2D NMR data indicated that compound **4** possessed two hexoses that consisted of two anomeric protons (δ_H 5.68-δ_C 107.3 and δ_H 5.54-δ_C 106.5) and eight protons attached to oxygen-bearing carbons between 4.98 ppm and 4.44 ppm as well as two methyl groups (δ_H 1.66 and 1.66) not belonging to the benzothioate unit. These two hexoses were constructed mainly by COSY correlations (Figure 1) and connected to C-2 and C-4 in the benzothioate aglycone based on the H-1′/C-2 and H-1″/C-4 HMBC correlations. Analysis of the coupling constants $^1J_{CH}$ and $^3J_{HH}$ and ROESY correlations confirmed that these two units are rhamnose. The absolute configurations of the rhamnose moieties were also determined to both be L-configurations by chemical derivatization and chromatographic analysis, analogously to suncheonosides A-C.

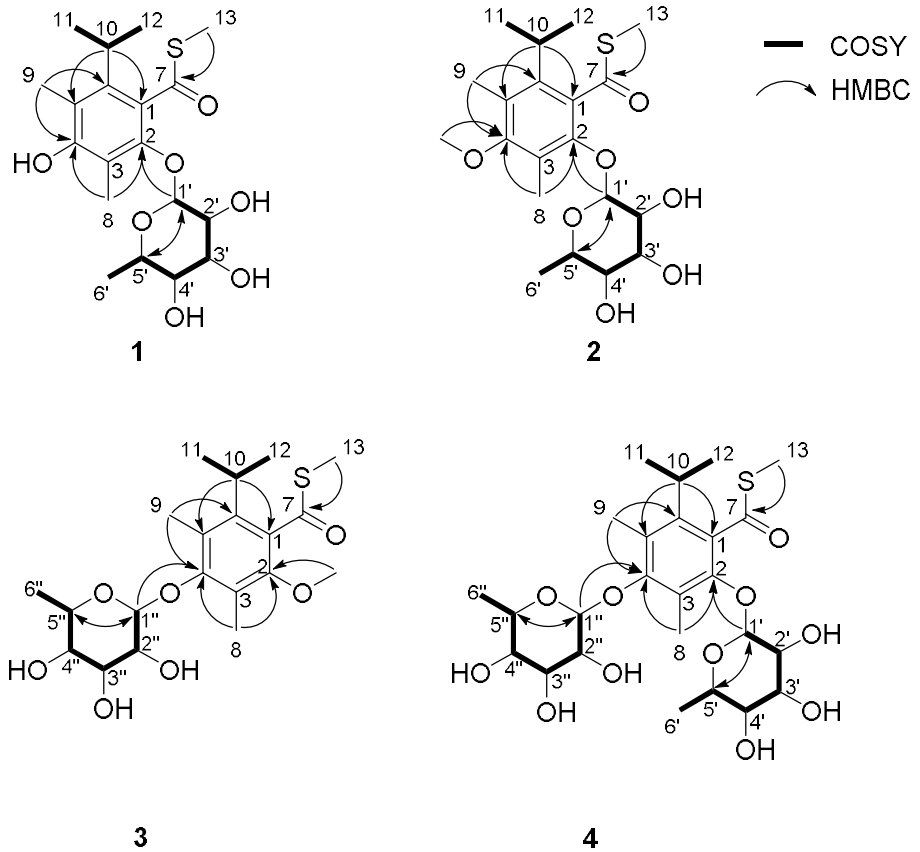

Figure 1. Key ^{1}H-^{1}H COSY and HMBC correlations of **1-4**.

The glycosidic bond conformations between the aglycone and the sugar moieties of the suncheonosides were analyzed using ROESY NMR correlations. In suncheonoside A (**1**), the H_3-8 showed ROESY correlations with H-3′ and H-5′. Based on these correlations, the C-8 methyl group, not the benzene ring, is located on the top of the rhamnose ring, possibly minimizing steric repulsion between the two rings (Figure 3). This conformation was also well supported by the energy-minimized structure and ^{1}H-^{1}H distances obtained through density functional theory (DFT) calculations (Figure 3).

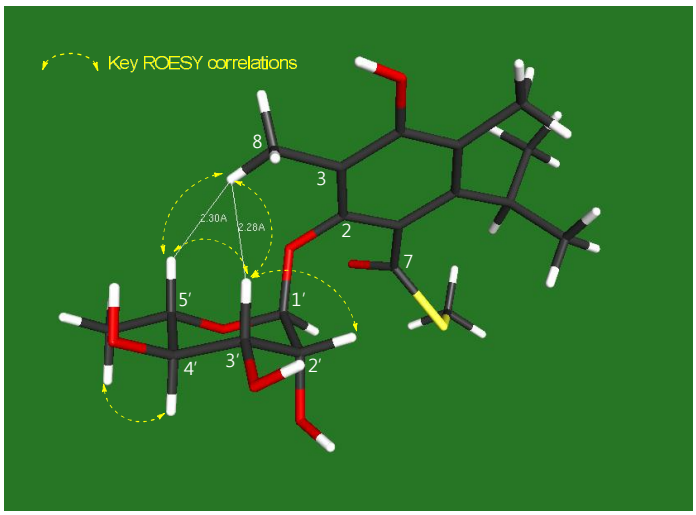

Figure 3. DFT-calculation-based minimum energy conformation of suncheonoside A (**1**) with the key ROESY correlations and distances between protons.

The conformation of suncheonoside B (**2**), an *O*-methyl version of **1**, is assumed to be analogous to that of **1**. In the case of suncheonoside C (**3**), H_3-8 displayed ROESY correlations with H-1″ and H-3″ and H_3-9 displayed ROESY correlations with H-1″ and H-5″. These observations illustrated that the C-8 and C-9 methyl groups are oriented toward the top face of the hexose where the axial protons H-3″ and H-5″ are located. This conformation was also supported by the DFT calculations (Supporting Information Figure S26). Finally, the conformation of suncheonoside D bearing two sugars at positions C-2 and C-4 of the aromatic ring was analyzed by ROESY correlations. H_3-8 of the aglycone part showed ROESY correlations with H-2′ and H-3′ in 2-rhamnose and with H-3″ in 4-rhamnose. In addition, H_3-9 was correlated with H-1″ and H-5″ in the ROESY

spectrum. These correlations are sufficiently rationalized by DFT calculations (Figure S27).

Hexa-substituted benzoid structures bearing a thioester are uncommon, with only a few examples observed in nature. Resorthiomycin I, which exhibits antitumor and antibiotic activities, is derived from *Streptomyces collinus*[10], and the anticancer enediyne compounds calicheamicins, derived from *Micromonospora echinospora*[11], are incorporated with hexa-substituted thiobenzoate moieties. Relatively recently, the aglycone of the suncheonosides *S*-methyl-2,4-hydroxy-6-isopropyl-3,5-dimethylbenzothioat (**5**) was reported from a marine-derived *Streptomyces* sp. without biological evaluation.[12] Hexa-substituted benzothioates are rarely found from sources other than actinobacteria featuring mortivinactin B from the fungus *Mortierella vinacea*[13] and polycarpamine B from the marine ascidian *Polycarpa auzata*.[14]

The biological activities of suncheonosides A-D (**1**-**4**) were investigated to improve the insulin sensitivity related to anti-diabetic drug discovery. In a phenotype-based assay for searching for new compounds to regulate adipogenesis in human bone marrow mesenchymal stem cells (hBM-MSCs), the suncheonosides (10 μM) promoted adipogenesis in hBM-MSCs (Figure 4a and 4b). When adipogenesis in hBM-MSC is induced by co-treatment with insulin, dexamethasone, and isobutylmethylxanthine (IBMX) (IDX medium), adipocyte differentiation can be promoted by a compound that

improves insulin sensitivity.[15] hBM-MSCs were treated with the suncheonosides (**1**-**4**) in IDX media for 6 days, and the level of lipid droplet formation in the hBM-MSCs was measured by Oil Red O (ORO) staining (Figure 4a and 4b). Suncheonosides A, B and D significantly promoted adipogenesis in hBM-MSCs by up to 107%, 65% and 75%, respectively, compared with the level observed in the IDX control. Suncheonoside C was likely to promote adipogenesis by up to 42%; however, the magnitude of this effect was above the statistical threshold (p = 0.05). To investigate the concentration dependency of the suncheonoside effect, the cell viability of hBM-MSCs was evaluated for the suncheonosides and their aglycone, which was obtained via enzymatic hydrolysis of suncheonoside A (Figure 4c). A concentration-effect analysis of suncheonosides A, B and D and the aglycone of suncheonoside A (**5**) was performed at concentrations of up to 100 μM because at this concentration, the compounds do not affect the viability of hBM-MSCs (Figure 4d). The adiponectin concentrations in the hBM-MSC culture media were measured by quantitative analysis (Figure 4d). Glibenclamide was used as a positive control drug because adiponectin production during adipogenesis in hBM-MSCs can be used to evaluate anti-diabetic drugs and improve insulin sensitivity.[15] Glibenclamide increased adiponectin production in a concentration-dependent manner during adipogenesis in hBM-MSCs and exhibited a plateau in activity at concentrations above 10 μM. The suncheonosides promoted adiponectin

production during adipogenesis in hBM-MSCs in a concentration-dependent manner relative to the adiponectin production observed for the IDX control. However, compared with the maximum activity of glibenclamide, the maximum levels at which suncheonosides A, B and D promoted adiponectin production were 43.9%, 46.9% and 37.8%, respectively. Notably, the concentration effect of the suncheonosides decreased at 100 μM. In addition, the aglycone of suncheonoside A (**5**) did not promote adiponectin production in hBM-MSCs compared with that of the IDX medium control, suggesting that the L-rhamnose moiety is essential to the pharmacological activity of the suncheonosides. Although the direct molecular target of the pharmacological activity of the suncheonosides has not been identified, these benzothioate rhamnose glycosides may be used as a chemical tool to elucidate the corresponding pharmacological mechanism and thereby improve insulin sensitivity for a new class of anti-diabetic drugs.

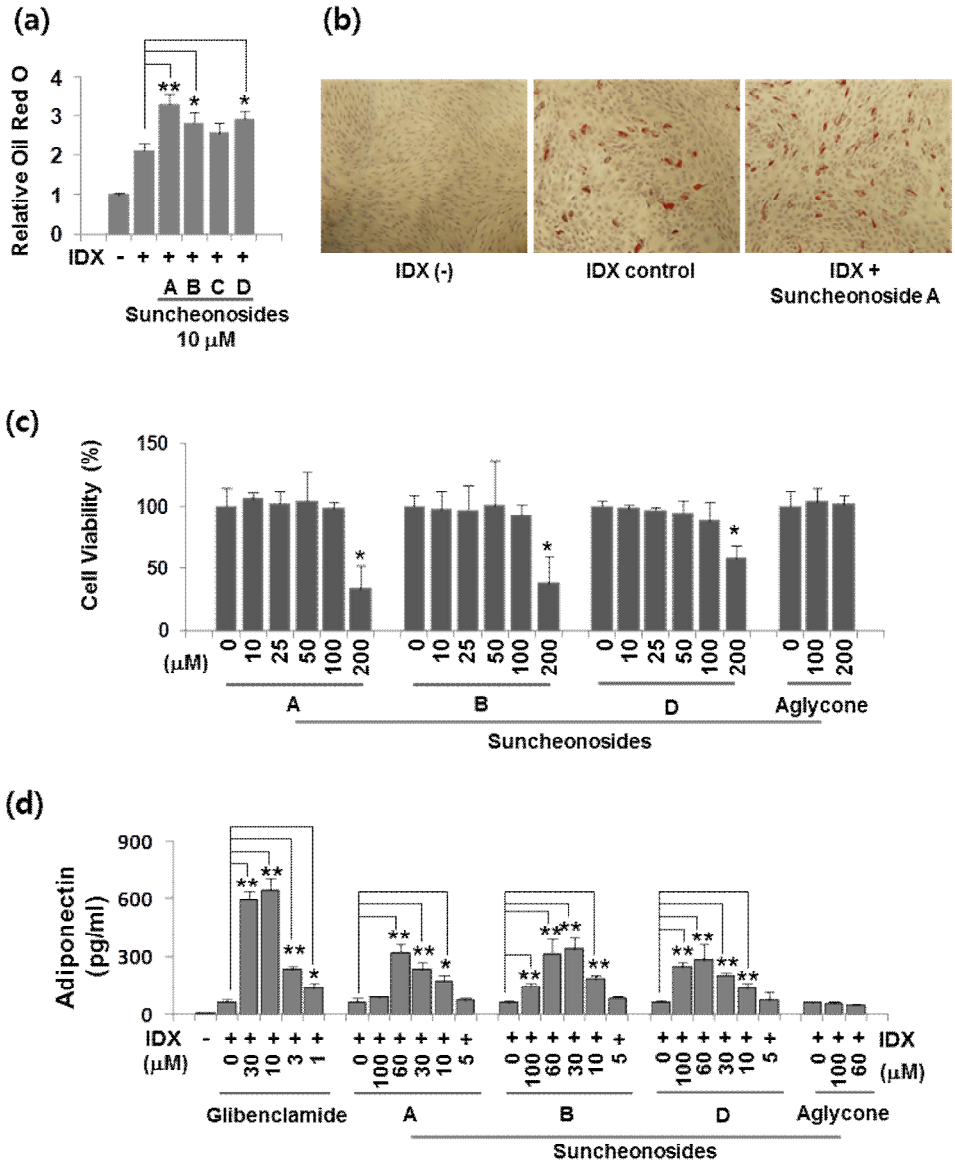

Figure 4. The effects of the suncheonosides on insulin sensitivity during adipogenesis in hBM-MSCs. (a) Adipogenesis of hBM-MSCs was induced by treating the adipocyte-differentiation-inducing medium supplemented with 10 μM of each suncheonoside in IDX medium. Suncheonosides A (**1**), B (**2**), and D (**4**) promoted adipogenesis by up to 107%, 65%, and 75%, respectively. (b) Differentiated adipocytes were visualized by co-staining with hematoxylin reagent on the ORO-stained adipocytes. (c) The hBM-MSC cell viability effects of suncheonosides A, B, and D. (d) The

concentration-dependent effect of suncheonosides A, B, D, and the aglycone of suncheonoside A (**5**) on the production of adiponectin was evaluated during adipogenesis in hBM-MSCs. Values represent the mean expression ± standard deviation (SD) (n = 3). * $P \leq 0.05$ and ** $P \leq 0.01$.

II.1.2 Experimental section

General Experimental Procedures. Optical rotations were determined using a JASCO P-1020 polarimeter. UV spectra were measured on a PerkinElmer Lambda 35 UV/VIS spectrophotometer. IR spectra were recorded using a Thermo NICOLET iS10 spectrometer. ^{1}H, ^{13}C, and 2D NMR spectra were obtained on Bruker Avance 600 MHz spectrometers at the National Center for Inter-university Research Facilities at Seoul National University (NCIRF). Low-resolution electrospray ionization source mass spectra were acquired with an Agilent Technologies 6130 quadrupole mass spectrometer coupled to an Agilent Technologies 1200 series high-performance liquid chromatography (HPLC) instrument. High-resolution fa st-atom bombardment (HRFAB) mass spectra were obtained using a J EOL JMS-600W high-resolution mass spectrometer at the NCIRF. Semi-preparative HPLC separations were achieved with a Gilson 305 pump and a Gilson UV/VIS-155 detector.

Bacterial Isolation. A sediment sample was collected from Suncheon Bay, Republic of Korea, in 2013. Dried sediment was spread onto the surface of actinomycete isolation medium (1 L of seawater, 18 g of agar, 100 mg/L cycloheximide), A4 medium (1 L of seawater, 18 g of agar, 100 mg/L cycloheximide), A5 medium (750 mL of seawater, 250 mL of distilled water, 18 g of agar, 100 mg/L cycloheximide), A6 medium (1 L of seawater, 18 g of agar, and 5 mg/L polymyxin B sulfate), A7 medium (1 L of seawater, 18

g of agar, and 5 mg/L kanamycin) and chitin-based agar plates using autoclaved foam plugs (2 cm in diameter). The plates were incubated at 25 °C for 3 weeks. The strain SSC21 was isolated from an actinomycete isolation medium plate. Colonies were repeatedly inoculated onto fresh agar plates to obtain a pure culture. 16S rDNA sequencing of the strain SSC21 was performed by COSMO Co., Ltd. A comparative sequence analysis indicated that strain SSC21 (GenBank accession number: KR007961) is most similar to *Streptomyces pulveraceus* (99% identity).

Cultivation and Extraction. The strain SSC21 was initially cultivated in 50 mL of modified K medium (2 g of yeast extract, 2 g of glucose, 3 g of mannitol, 5 g of starch, and 5 g of soytone in 1 L of distilled water). After the strain was cultivated for 5 days on a rotary shaker at 190 rpm and 30 °C, 10 mL of the culture was inoculated in 1 L of modified K medium in a 2.8-L Fernbach flask. The entire culture (72 L) was extracted twice with ethyl acetate. The EtOAc extract was concentrated *in vacuo* to yield 7 g of dry material.

Isolation of Suncheonosides A-D. One-half of the dried extract was fractionated with 150 mL each of 20%, 40%, 60%, 80%, and 100% MeOH in water using a packed C_{18} (20 g) column. After the fractionation, suncheonosides A-D (**1-4**) were found in the 20% and 40% MeOH/water fractions. Each fraction was then subjected to reversed-phase HPLC (Kromasil 100-5-C_{18} 250 × 10 mm, flow rate 2 mL/min, UV 280 nm detection, 50%–60% aqueous acetonitrile gradient with 0.1% formic acid

over 60 min). Under these purification conditions, suncheonoside A (**1**) (7 mg), suncheonoside B (**2**) (4 mg), suncheonoside C (**3**) (3 mg), and suncheonoside D (**4**) (7 mg) were purified with retention times of 25, 31, 30, and 20 min, respectively.

*Suncheonoside A (**1**):* white powder; $[\alpha]_D^{25}$ +62 (*c* 0.5, MeOH); UV (MeOH) λ_{max} (log ε) 206 (1.55) nm; IR (neat) ν_{max} 3351, 2751, 1681, 1272, 1038 cm^{-1}; for ^1H and ^{13}C NMR data, Table 1; HRFABMS *m/z* 423.1043 $[M+Na]^+$ (calcd for $C_{19}H_{28}O_7NaS$, 423.1055).

*Suncheonoside B (**2**):* white powder; $[\alpha]_D^{25}$ +82 (*c* 0.3, MeOH); UV (MeOH) λ_{max} (log ε) 207 (1.63) nm; IR (neat) ν_{max} 3941, 3397, 2938, 1689, 1342, 1130 cm^{-1}; for ^1H and ^{13}C NMR data, Table 1; HRFABMS *m/z* 437.1712 $[M+Na]^+$ (calcd for $C_{20}H_{30}O_7NaS$, 437.1730).

*Suncheonoside C (**3**)*: White powder; $[\alpha]_D^{25}$ +72 (*c* 0.5, MeOH); UV (MeOH) λ_{max} (log ε) 206 (1.62) nm; IR (neat) ν_{max} 3261, 2849, 1646, 1630, 1292, 1049 cm^{-1}; for ^1H and ^{13}C NMR data, Table 1; HRFABMS *m/z* 437.1712 $[M+Na]^+$ (calcd for $C_{20}H_{30}O_7NaS$, 437.1730).

*Suncheonoside D (**4**):* White powder; $[\alpha]_D^{25}$ +98 (*c* 0.3, MeOH); UV (MeOH) λ_{max} (log ε) 209 (1.84) nm; IR (neat) ν_{max} 3841, 3394, 2928, 1681, 1442, 1208, 1040 cm^{-1}; for ^1H and ^{13}C NMR data, Table 1; HRFABMS *m/z* 569.1843 $[M+Na]^+$ (calcd for $C_{25}H_{38}O_{11}NaS$, 569.1855).

Stereochemical analysis of rhamnose. Each of the suncheonosides A-D

(**1-4**) (2.0 mg quantity) was subjected to acid hydrolysis using 6 N HCl. Each hydrolysate was dissolved in pyridine (0.5 mL) containing L-cysteine methyl ester hydrochloride (0.5 mg) and heated to 60 °C for 1 h. One hundred microliters of a σ-tolyl isothiocyanate (0.5 mg) solution in pyridine (0.5 mL) was added to the mixture, which was then heated to 60 °C for 1 h. The reaction mixtures were directly analyzed using LC/MS (10%–100% aqueous acetonitrile gradient with 0.1% formic acid over 20 min). The hydrolysate derivatives of **1-4** were detected at 10.4, 10.6, 10.6, and 10.5 min, respectively. The retention times of the authentic rhamnose samples were 10.4 (L-rhamnose) and 9.3 (D-rhamnose) min under the same LC/MS conditions. Therefore, the absolute configurations of the rhamnose units in **1-4** were established as L-configurations.

Enzymatic hydrolysis. Suncheonoside A (**1**) (2.5 mg) was hydrolyzed in H_2O (2 mL) with naringinase (30 mg, from *Penicillium* sp.; ICN Biomedicals Inc.) at 40 °C for 24 h. The reaction mixture was extracted with $CHCl_3$. The $CHCl_3$ layer was chromatographed over a normal-phase silica gel (Waters Sep-Pak Vac 6 cc) with a solvent composed of a 30:1 mixture of $CHCl_3$-MeOH to yield the benzothioate aglycone (**5**, 1.5 mg) of **1**.

*Aglycone (**5**) of suncheonoside A (**1**):* ^{1}H NMR (600 MHz, pyridine-d_5) δ 3.47 (m, 1H), 2.58 (s, 3H), 2.50 (s, 3H), 2.38 (s, 3H), 1.45 (d, J = 7.1, 3H), and 1.45 (d, J = 7.1, 3H); ESI-MS *m/z* 255 $[M+H]^+$.

Computational Analysis. The ground-state geometries were optimized by

DFT calculations, using Turbomole 6.5 and the basis set def-SV(P) for all atoms at the B3LYP/DFT functional level; the ground states were further confirmed by harmonic frequency calculations.

Insulin sensitivity assay. The effect of the suncheonosides on insulin sensitivity was investigated in the adipogenesis model of hBM-MSCs as previously described.[15] hBM-MSCs were purchased from Lonza, Inc. (Walkersville, MD, USA). hBM-MSCs were maintained in Dulbecco's modified Eagle's medium (DMEM) with low glucose (1 g/L glucose) containing 10% fetal bovine serum (FBS) (Lonza), supplemented with antibiotics and Glutamax^{TM} (Invitrogen, Carlsbad, CA, USA). When hBM-MSCs were confluent in 24-well culture plates, adipogenesis was induced by exchanging the cell culture media with the adipocyte-differentiation-inducing medium, i.e., DMEM with high glucose (4.5 g/L glucose) supplemented with 10% FBS, 10 μg/mL insulin, 1 μM dexamethasone, and 0.5 mM 3-isobutyl-1-methylxanthine (IBMX) (IDX medium). After inducing adipogenesis in the hBM-MSCs, the IDX media were exchanged every 48 h. To evaluate cell viability, the hBM-MSCs were treated with 4-3-[4-iodophenyl]-2-4(4-nitrophenyl)-2H-5-tetrazolio-1,3-benzene disulfonate (WST-1; 10 μM pure solution, Roche, Indianapolis, IN, USA) and further incubated for 2 h. The absorbances of the samples were determined at 450 nm (A450). To measure the level of differentiated adipocytes in hBM-MSC culture, Oil Red O (ORO) staining was performed. Differentiated adipocytes

were washed in phosphate-buffered saline (PBS) and fixed for 30 minutes in 10% formalin solution in PBS. Fixed cells were washed in 60% isopropyl alcohol and stained at room temperature with Oil Red O (ORO) in 60% isopropyl alcohol. After 5 minutes of ORO staining, the cells were quickly washed with distilled water. To determine the adipogenic level, adsorbed ORO was dissolved with 100% isopropyl alcohol, and the absorbance was measured at 500 nm. To stain the nuclei of differentiated adipocytes, hematoxylin reagent was counter-stained. The differentiated adipocytes in hBM-MSC culture were observed and imaged using an Olympus IX71 inverted phase microscope (Olympus Co., Tokyo, Japan). To determine the concentrations of adiponectin in the cell culture supernatants of the hBM-MSCs, adiponectin ELISA was performed according to the manufacturer's instructions (R&D systems, Minneapolis, MN, USA).

Table 1. NMR data for suncheonosides A-D (**1-4**) in pyridine-d_5.

	Suncheonoside A (**1**)		Suncheonoside B (**2**)		Suncheonoside C (**3**)		Suncheonoside D (**4**)	
Position	δ_C, type	δ_H, mult (*J* in Hz)	δ_C, type	δ_H, mult (*J* in Hz)	δ_C, type	δ_H, mult (*J* in Hz)	δ_C, type	δ_H, mult (*J* in Hz)
1	127.5, C		132.0, C		131.6, C		131.6, C	
2	152.4, C		154.8, C		152.8, C		153.1, C	
2-OMe					61.9, CH_3	3.68, s		
3	116.7, C		123.7, C		124.5, C		123.4, C	
4	157.4, C		157.8, C		158.8, C		159.4, C	
4-OMe			62.3, CH_3	3.68, s				
5	140.9, C		141.9, C		140.7, C		141.6, C	
6	120.5, C		127.2, C		125.1, C		127.0, C	
7	197.3, C		196.7, C		197.0, C		197.5, C	
8	11.4, CH_3	2.58, s	11.0, CH_3	2.31, s	11.2, CH_3	2.31, s	11.9, CH_3	2.54, s
9	14.2, CH_3	2.48, s	14.5, CH_3	2.38, s	13.5, CH_3	2.38, s	12.8, CH_3	2.38, s
10	32.1, CH	3.39, m	32.0, CH	3.31, m	32.9, CH	3.31, m	32.5, CH	3.32, m
11	21.7, CH_3	1.38, d (7.0)	21.7, CH_3	1.31, d (7.0)	21.6, CH_3	1.31, d (7.0)	21.6, CH_3	1.28, d (7.0)
12	21.6, CH_3	1.41, d (7.0)	21.6, CH_3	1.29, d (7.0)	21.5, CH_3	1.29, d (7.0)	21.6, CH_3	1.28, d (7.0)
13	12.8, CH_3	2.41, s	12.7, CH_3	2.47, s	12.3, CH_3	2.47, s	14.6, CH_3	2.37, s
2-L-rhamnose								
1′	107.2, CH	5.77, br s	107.2, CH	5.57, br s			107.3, CH	5.68, br s
2′	72.3, CH	4.87, br s	72.2, CH	4.97, br s			72.2, CH	4.78, br s
3′	72.8, CH	4.68, d (9.0)	72.8, CH	4.72, dd (9.0, 3.0)			72.6, CH	4.62, dd (9.0, 3.0)
4′	73.4, CH	4.41, ddd (9.0, 9.0, 3.5)	73.4, CH	4.44, dd (9.0, 9.0)			73.4, CH	4.37, dd (9.5, 9.0)
5′	72.1, CH	4.62, dq (9.0, 6.0)	72.1, CH	4.68, m			72.0, CH	4.54, m
6′	18.6, CH_3	1.72, d (6.0)	18.6, CH_3	1.71, d (6.0)			18.7, CH_3	1.66, d (5.0)
2′-OH		7.15, d (3.0)						
3′-OH		6.80, br s						
4′-OH		7.0, d (3.5)						
4-L-rhamnose								
1″					106.4, CH	5.56, br s	106.5, CH	5.54, br s
2″					72.7, CH	4.96, br s	72.4, CH	4.98, br s
3″					73.0, CH	4.67, dd (9.0, 3.0)	72.7, CH	4.72, dd (9.0, 3.0)
4″					73.4, CH	4.43, t (9.0, 9.0)	73.3, CH	4.44, dd (9.0, 9.0)
5″					72.4, CH	4.66, m	72.6, CH	4.68, m
6″					18.7, CH_3	1.72, d (6.0)	18.7, CH_3	1.66, d (5.0)

2. JS8 A and B, novel bacterial flavonoid, from *Streptomyces* sp. associated with white grub *Protaetia brevitarsis seulensis*.

II .2.1. Results and discussion

JS8 A (**6**) was isolated as a as a colorless, non-crystalline solid. The molecular formula of **6** was assigned as $C_{22}H_{31}NO_8$ based on HRFAB mass spectrometric data and ^{1}H and ^{13}C NMR data (Table 2). Comprehensive analysis of the COSY, HMQC and HMBC NMR spectra for **6** defined three substructures, a 2, 3, 6-trideoxyaminosugar, a 2-methyl-3-hydroxy-butyramide, and an aglycone possessing a 5- hydroxymethyl-7, 8-dihydroxyflavonoid structure. HMBC correlations were effective in providing the substitution pattern of the pentasubstituted aromatic ring and in connecting substructures. Correlations from the C-6 proton (δ_H 7.09) to the C-8 and C-10 carbons (δ_C 170.0 and 112.8 repectively), from the C-11 methylene protons to the C-5, C-6 and C-10 carbons (δ_C 136.7, 105.8 and 112.8) served to position free hydroxyl and hydroxymethyl substituents. The connection of the ketone fragment to the C-10 carbon (δ_C 112.8) was indicated by a correlation from the C-3b proton (δ_H 2.65). The C-3b proton also correlated with C-1', thus leading to placement of the CH_2 substituent at C-2. The linkage of the glycoside at the C-7 hydroxyl was shown by the correlation of the anomerie proton (C-1", 5.80) to the C-7 carbon at δ_C 148.6. Furthermore, the sugar was confirmed to be in the pyranose by HMBC correlations from the anomeric proton to the C-5" carbon. Complete analysis of the NMR signals from the aminosugar led to its assignment as ristosamine. This was apparent from HMBC correlations from the C-3"

proton (δ_C 4.31) to the C-1''' amide carbonyl carbon (δ_C 169.5).(Figure 5)

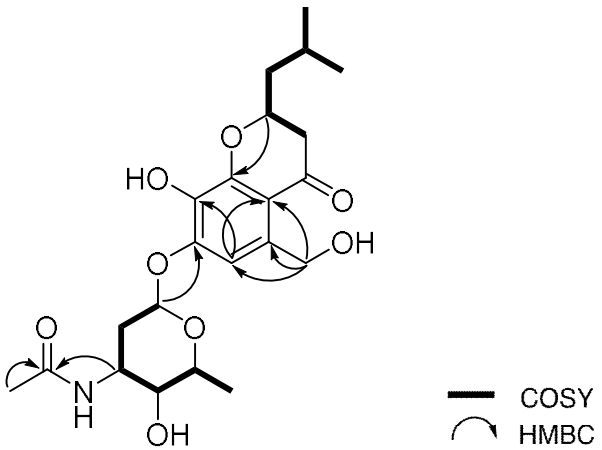

Figure 5. Key ^{1}H-^{1}H COSY and HMBC correlations of **6.**

JS8 B (**7**) was isolated as a as a colorless, non-crystalline solid as well as. The molecular formula of **7** was also assigned as $C_{22}H_{31}NO_8$ based on HRFAB mass spectrometric data and ^{1}H and ^{13}C NMR data. The ^{13}C NMR spectrum of **6**, showed two sets of partially overlapping ABX spin systems. For example, the ^{13}C NMR spectrum showed two methine carbon signals, at δ_C 94.0 and 94.1 which, on the basis of the formula for **6**, could only account for one carbon. Production of a perbenzoate derivative, followed by chiral column HPLC analysis using UV detection illustrated conclusively that **6** was a 50/50 mixture of diastereomers. With the exception of the above, all other proton and carbon signals of the mixture appeared at identical chemical shifts JS8 compounds (**6** and **7**) was racemized at the only aglycone chiral carbon (C-2).

Complete analysis of the NMR signals from the aminosugar led to its

assignment as ristosamine, a rare deoxyamino sugar first observed as a component of the vancomycin-related antibiotic, ristomycin. The relative stereochemistry of the ristosamine moiety was determined by coupling constant analysis. The magnitude of $^{1}J_{CH}$ (170 Hz) between C-1" and H-1" was clearly indicative of an α-configuration.[8] Complex couplings to the C-3" proton rendered analysis difficult. However, the coupling constants for the C-4" proton were clear (3.5 and 10.0 Hz). Irradiation of the C-3" proton signal resulted in a simplified doublet, with J = 10 Hz, for the C-4" proton. Therefore, the 3.5 coupling constant placed the C-3", C-4" and C-5" protons in equatorial, axial and axial configurations, respectively.

To determine the absolute configuration of JS8 A (**6**), the modified Mosher's method was applied.[11] Prior to this procedure, the time-controlled acetylation of **6** mainly yielded a tri-acetate product (**8**) esterified at the C-1, C-8 and C-11. The secondary hydroxy group at C-2' and C-4'' in **6** was then derivatized with *R*-(-) and *S*-(+)-α-methoxy-α-(trifluoromethyl)phenylacetyl chloride (MTPA-Cl) to yield the *S*- and *R*- MTPA esters (**9** and **10**), respectively. The ^{1}H chemical shifts of the relevant protons were assigned by analyzing the ^{1}H NMR spectra of **9** and **10**. Calculating the $\Delta\delta_{S-R}$ values established the absolute configuration of 2*S*. (Figure 6).

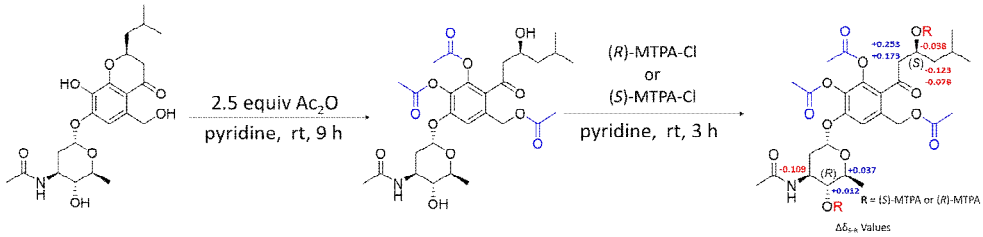

Figure 6. Stereochemical determination of the JS8 A (**6**) (application of time controlled acetylation and Modified mosher method).

Based on the absolute configuration of JS8 A and B, the assignment was further confirmed by comparing the experimental ECD spectrum of hydrosylate of JS8 A (**6**) and the calculated ECD spectra of the hydrosylate of JS8 A (**12**). The experimental ECD spectrum of **12** displayed positive Cotton effects at 220 and 290 nm, which is consistent with the calculated ECD spectrum of the 2*S* (Figure 7a) and the experimental ECD spectrum of **13** displayed negative Cotton effects at 220 and 290 nm, which is consistent with the calculated ECD spectrum of the 2*R* (Figure 7b). Therefore, the absolute configuration of JS8 A was established as 2*S* and the absolute configuration of JS8 B as 2*R* (Figure 7).

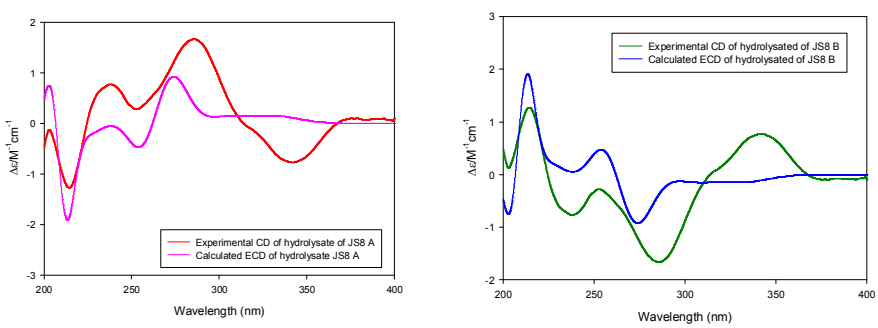

Figure 7. (a) Experimental CD spectra of hydrosylate of **11** and calculated ECD spectra of hydrosylate of **11.** (b) Experimental CD spectra

of hydrosylate of **12** and calculated ECD spectra of hydrosylate of **12.**

JS8 A and B are biosynthetically interesting because they are unusual bacterial metabolites. The only reported bacterial flavonoid producer is the strain CNB-689 which produces actinoflavoside (**13**). The comparative whole genome sequence analysis of the strain JS8 and the CNB-689 was conducted to find out the biosynthetic pathway of bacterial flavonoid. At first, we performed stable isotope labeling experiments to distinguish between the chalcone synthase (CHS) using 4-coumaroyl-CoA with three malonyl-CoA and aloesone synthase (ALS) using acetyl-CoA with six malonyl-CoA. The [2-^{13}C]sodium acetate was provided as a precursor to the JS8 A and ^{13}C NMR analysis of labeled sodium acetate-enriched JS8 A revealed the specific isotopic labeling of C11 at approximately 20% enrichment (Figure S14). And to confirm the incorporation of an isovaleryl-CoA as a starting unit, [1-^{13}C]sodium acetate was also labeled (Figure S15). As a result, the specific isotopic labeling of C2 and C3 were founded we could conclude isovaleryl-CoA is used as a starting unit. Moreover, due to the ALS pathway was traced by injection of stable isotope L-leucine (precursor of isovaleryl-CoA), the isotopically labeled products were analyzed by LC/MS and the product profiles formed in the presence of isovaleryl-CoA. The comparative whole genome sequence analysis of the strains JS8 and CNB-689 identified common putative gene clusters for bacterial flavonoid biosynthesis. Stable isotope labeling experiments using [1-^{13}C]sodium acetate, [2-^{13}C]sodium acetate, universally-labeled leucine

revealed that JS8A and B were produced through a biosynthetic pathway analogous to that for aloesone-type flavonoids in plants (Figure 8).

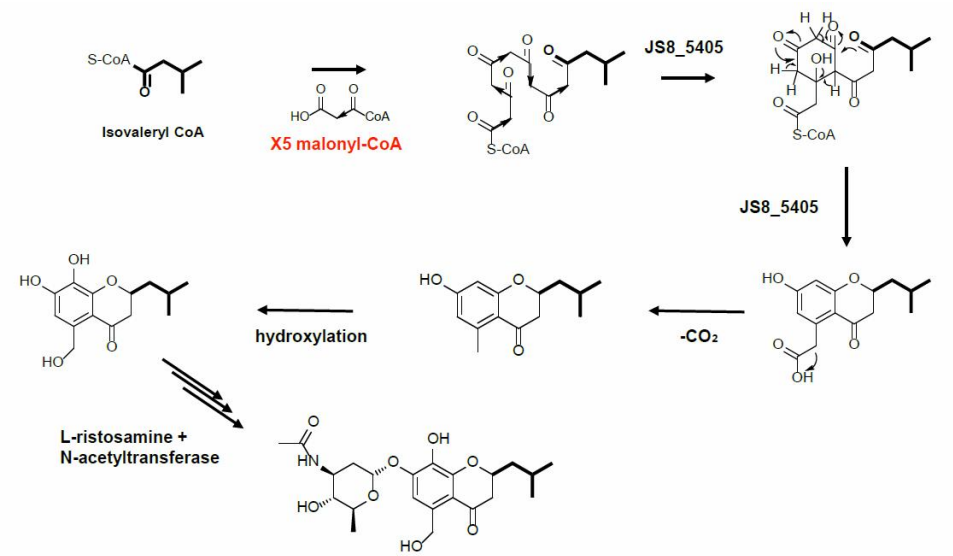

Figure 8. Proposed biosynthetic pathway of JS8 A.

II.2.2. Experimental section

General Experimental Procedures. Optical rotations were measured on a JASCO P1020 polarimeter with a 1 cm cell. UV spectra were acquired with a PerkinElmer Lambda 35 UV/VIS spectrophotometer and ECD spectra were recorded using an Applied Photopysics Chirascan-Plus circular dichroism spectrometer. IR spectra were recorded using a Thermo NICOLET iS10 spectrometer. ^{1}H, ^{13}C, and 2D NMR spectra were obtained on a Bruker Avance 850 MHz spectrometer at the the National Center for Inter-University Research Facilities (NCIRF) at Seoul National University. ^{1}H and ^{13}C NMR chemical shifts (δ_H and δ_C) were recorded in ppm. Low-resolution electrospray ionization source mass spectra were acquired with an Agilent Technologies 6130 quadrupole mass spectrometer coupled to an Agilent Technologies 1200 series high-performance liquid chromatography (HPLC) instrument. High-resolution electrospray ionization mass spectra (HRESIMS) were obtained using a Thermo Scientific Q high-resolution mass spectrometer at the NICEM (National Instrumentation Center for Environmental Management at Seoul National University). Semi-preparative HPLC separations achieved with a Gilson 305 pump and a Gilson UV/VIS 155 detector.

Isolation and Classification of a bacterial strain JS8. The bacterical strain JS8 was isolated from the gut of a *Protaetia brevitarsis seulensis* grub. A white grub specimen was washed with sterilized water and then soaked in

97% ethanol to remove the microbes on their exoskeleton. Only abdomen was extracted using a razor blade and the cuticle of the abdomen was removed. The intestinal parts were placed in a conical tube containing 20 mL of sterilized distilled water at 25 °C. The tube was vortexed, and 300-μL aliquots of the suspension were spread onto the surfaces of actinomycete isolation medium (1 L of distilled water, 22 g of actinomycete isolation medium, 18 g of agar, and 100 mg/L cycloheximide), A4 medium (1 L of distilled water, 18 g of agar, and 100 mg/L cycloheximide), A6 medium (1 L of distilled water, 18 g of agar, and 5 mg/L polymyxin B sulfate), A7 medium (1 L of distilled water, 18 g of agar, and 5 mg/L kanamycin) and chitin-based agar medium (1 L of distilled water, 4 g of chitin, 18 g of agar, and 100 mg/L cycloheximide) plates using autoclaved foam plugs (2 cm in diameter) and spreaders. The plates were incubated at 25 °C for 3 weeks. Strain JS8 was isolated from a actinomycete isolation medium plate. Colonies were repeatedly inoculated onto fresh YEME agar (1 L of distilled water, 18 g of agar, 4 g of yeast extract, 4 g of glucose, and 10 g of malt extract) plates to obtain a pure culture.

Cultivation and Isolation. The strain was cultivated in 50 mL of modified K medium (2 g of yeast, 2 g of glucose, 3 g of mannitol, 5 g of soytone, 5 g of starch and 1 g of calcium carbonate in 1 L of distilled H_2O). After culturing the strain for 5 days on a rotary shaker at 190 rpm and 30 °C, 10 mL of the culture was inoculated into 1 L of modified K medium in a 2.8 L Fernbach flask. The entire culture (24 L) was extracted twice with EtOAc

then concentrated in vacuo to yield 30 g of dry material. After extraction, the extract was directly subjected to reversed-phase high-performance liquid chromatography (HPLC; Kromasil 100-5-C_{18} 250 × 10 mm, flow rate 2 mL/min, UV 280 nm detection, 58% aqueous MeOH isocratic). Under these purification conditions, JS8 A (**1**) and B (**2**) were purified together with retention times of 32 min. For further purification, two epimeric compounds were isolated by normal-phase high-performance liquid chromatography (HPLC; CTK Chiralpak IB 250 × 4.6 mm, flow rate 1 mL/min, UV 280 nm detection, n-Hexane/Ethanol = 80/20 isocratic). Finally, JS8 A (**1**, 12 mg) and JS8 B (**2**, 12 mg) were isolated as pure compounds as retention times of 16 min and 20 min, respectively.

JS8 A (6): Colorless, non-crystalline solid; $[\alpha]^{25}_{D}$ -45.0 (*c* 0.5, MeOH); UV (MeOH) λ_{max} (log ε) 261 (2.46) nm; ECD (*c* 4.3 × 10^{-4} M, MeOH) λ_{max} ($\Delta\varepsilon$) 220 (10.4), 312 (1.6) nm; IR (neat) ν_{max} 3360, 1660 cm^{-1}; ^{1}H and ^{13}C NMR data in Table 2; ESI MS *m*/*z* 436.1756 $[M-H]^-$ (calcd for $C_{22}H_{30}NO_8$, *m*/*z* 436.1753).

JS8 B (7): Colorless, non-crystalline solid; $[\alpha]^{25}_{D}$ -80.0 (*c* 0.1, MeOH); UV (MeOH) λ_{max} (log ε) 255 (2.13) nm; ECD (*c* 4.3 × 10^{-4} M, MeOH) λ_{max} ($\Delta\varepsilon$) 248 (3.12), 330 (1.36) nm; IR (neat) ν_{max} 3300, 1580^{-1}; ESI MS *m*/*z* 436.1756 $[M-H]^-$ ($C_{22}H_{30}NO_8$, *m*/*z* 436.1753).

Acetylation of 6. JS8 A (**6**, 4 mg) was dissolved in pyridine (2 mL), and a stock solution of acetic anhydride was prepared in pyridine (0.42 μM: 80 μL

acetic anhydride in 2 mL pyridine). The stock solution was added to the JS8 A solution gradually in 10 or 20 μL aliquots, and the reaction was monitored by liquid chromatography/mass spectrometry (LC/MS). The reaction solution was cooled when the acetic anhydride solution was added, and the mixture was stirred at room temperature. When 400 μL of the stock solution in total had been applied for 9 h. The reaction was halted by adding 10 μL of water. The acetate of JS8 A (**3**, 3.4 mg) was purified through reversed-phase HPLC (Kromasil 100-5-C_{18} 250 × 10 mm, flow rate 2 mL/min, UV 280 nm detection, 75% aqueous MeOH isocratic, retention time 20 min). The molecular formula ($C_{28}H_{39}NO_{12}$) of the desired product, an acetate of JS8 A (**3**), was confirmed by electrospray mass spectrometry (ESI MS) ($[M+H]^+$ *m/z* at 581) and ^{1}H NMR data spectroscopy.

Acetate (8) of JS8 A (6): ^{1}H NMR (600 MHz, CD_3OD) δ 6.17 (br s, 1H), 5.75 (dd, *J* = 17.5, 10.5, 1H), 4.89 (dd, *J* = 17.5, 1.0, 1H), 4.85 (dd, *J* = 10.5, 1.0, 1H), 4.75 (m , 2H), 4.28 (s, 1H), 3.42 (m, 1H), 2.78 (dd, *J* = 18.0, 4.5, 1H), 2.71 (m, 2H), 2.61 (dd, *J* = 18.0, 14.0, 1H), 2.46 (d, *J* = 18.0, 1H), 2.19 (s, 3H), 1.91 (d, *J* = 18.0, 1H), 1.52 (m, 2H), 1.02 (s, 3H), and 0.98 (s, 3H).

MTPA Esterification of JS8 A Acetate (8). Acetate (**8**) was prepared in two 40 mL vials (two 1.7 mg samples), which were dried completely under high vacuum for 12 h. First, freshly distilled anhydrous pyridine (1 mL) was prepared prior to the addition of a catalytic amount of dimethylaminopyridine to the solution. *R*-(-) and *S*-(+)-MTPA chloride (10

μL) were added separately and the mixture stirred at room temperature. After 3 h, the reaction was quenched with 0.5 mL of MeOH. The products were then purified using reversed-phase HPLC (Kromasil 100-5-C_{18} 250 × 10 mm, flow rate 2 mL/min, UV 280 nm detection) under gradient conditions ranging from 60% to 100% aqueous acetonitrile. The *S*-MTPA (**9)** and *R*-MTPA (**10**) esters eluted at 27.0 and 27.5 min, respectively. The molecular formulae ($C_{48}H_{53}F_6NO_{16}$) of the MTPA esters were confirmed by ESI MS ($[M+H]^+$ *m/z* at 1014) and ^{1}H NMR spectroscopy. The ^{1}H chemical shifts around the stereogenic centers of the derivatives were assigned by ^{1}H NMR spectra of **9** and **10**.

***S*-MTPA ester (9) of acetate (8):** ^{1}H NMR (600 MHz, DMSO-d_6) δ 7.25-7.15 (m, 5H), 6.10 (br s, 1H), 5.75 (dd, *J* = 17.5, 10.5, 1H), 5.18 (s, 1H), 4.74 (dd, *J* = 17.5, 1.0, 1H), 4.70 (dd, *J* = 10.5, 1.0, 1H), 4.60 (m , 2H), 3.49 (s, 3H), 3.46 (m, 1H), 2.74 (dd, *J* = 18.0, 4.5, 1H), 2.71 (m, 2H), 2.63 (dd, *J* = 18.0, 14.0, 1H), 2.46 (d, *J* = 18.0, 1H), 2.19 (s, 3H), 1.91 (d, *J* = 18.0, 1H), 1.52 (m, 2H), 1.01 (s, 3H), and 0.95 (s, 3H).

***R*-MTPA ester (10) of acetate (8):** ^{1}H NMR (600 MHz, DMSO-d_6) δ 7.26-7.10 (m, 5H), 6.08 (br s, 1H), 5.72 (dd, *J* = 17.5, 10.5, 1H), 5.21 (s, 1H), 4.76 (dd, *J* = 17.5, 1.0, 1H), 4.72 (dd, *J* = 10.5, 1.0, 1H), 4.62 (m , 2H), 3.49 (s, 3H), 3.45 (m, 1H), 2.75 (dd, *J* = 18.0, 4.5, 1H), 2.72 (m, 2H), 2.64 (dd, *J* = 18.0, 14.0, 1H), 2.47 (d, *J* = 18.0, 1H), 2.18 (s, 3H), 1.89 (d, *J* = 18.0, 1H), 1.50 (m, 2H), 1.02 (s, 3H), and 0.97 (s, 3H).

Computational Analysis. The ground-state geometries were optimized by DFT calculations using Turbomole 6.5 with the basis set def-SV(P) for all atoms at the functional B3LYP/DFT level. The ground states were further confirmed by harmonic frequency calculations. The calculated ECD data corresponding to the optimized structures were obtained with TD-DFT at the functional B3LYP/DFT level at the basis set def2-TZVPP for all atoms. The CD spectra were simulated by overlapping each transition, where σ is the width of the band at 1/e height. ΔE_i and R_i are the excitation energies and rotatory strengths for transition i, respectively. In the current work, the value of σ was 0.10 eV.

$$\Delta\epsilon(E) = \frac{1}{2.297 \times 10^{-39}} \frac{1}{\sqrt{2\pi\sigma}} \sum_{i}^{A} \Delta E_i R_i e^{[-(E-\Delta E_i)^2/(2\sigma)^2]}$$

Measurment of labeles precursor incorporation rate using [2-^{13}C]sodium acetate and [1-^{13}C]sodium acetate. [2-^{13}C]sodium acetate and [1-^{13}C]sodium acetate were purchased from Sigma Aldrich Korea. [2-^{13}C]sodium acetate (1.0 g/l) was added to the JS8 strain liquid culture. JS8 A and B labled with [2-^{13}C]sodium acetate were purified via reversed-phase HPLC (Kromasil 100-5-C_{18} 250 × 10 mm, flow rate 2 mL/min, UV 280 nm detection) using an isocratic of 58% aqueous methanol. And for further purification, JS8 A and B were isolated by normal-phase high-performance liquid chromatography (HPLC; CTK Chiralpak IB 250 × 4.6 mm, flow rate 1 mL/min, UV 280 nm detection, n-Hexane/Ethanol = 80/20 isocratic). JS8 A and B were eluted at 16 and 19 min, respectively. Also, [1-^{13}C]sodium

acetate (1.0 g/l) was added to the JS8 strain liquid culture and JS8 A and B labled with [1-^{13}C]sodium acetate. After purification labeled JS8 A and B were assigned by ^{1}H NMR spectra and incoportation ratio were calculated.

Measurment of labeles precursor of universally-labeled leucine

Universally-labele leucine (L-Leucine-$^{13}C_6$,^{15}N) from Sigma Aldirch Korea was feeding with liquid culture of JS8 strain. The isotopically labeled products were analyzed by liquid chromatography/mass spectrometry (LC/MS) under a gradient solvent system (flow rate: 0.7 mL/min; UV detection: 210, 230, 254, 280, and 360 nm; 10% to 100% aqueous acetonitrile [CH_3CN/H_2O] with 0.1% formic acid over 20 min).

Table 2. NMR data for JS8 (**6**) in DMSO-d_6.

Position	δ_C, type	δ_H, mult (*J* in Hz)
2	75.7, CH	4.51, m
3	43.8, CH_2	2.65, dd (16.5, 11.0)
		2.6, dd (16.5, 5.4)
4	192.7, C	
5	136.7, C	
6	105.8, CH	7.09, s
7	148.6, C	
8	170.0, C	
9	151.6, C	
10	112.8, C	
11	61.6, CH_2	4.74, d (4.0)
1′	43.1, CH_2	1.79, 1.45, m
2′	23.2, CH	1.97, m
3′	23.3, CH3	0.93, d (6.5)
4′	22.2, CH_3	0.92, d (6.5)
1′′	94.0, CH	5.8, t (5.6)
2′′	32.7, CH_2	2.04, m
3′′	45.2, CH	4.31, m
4′′	70.5, CH	3.29, dd (10.0, 3.5)
5′′	66.2, CH	3.71, dq (16.5, 10.0)
6′′	17.8, CH_3	1.06, d (6.3)
1′′′	169.5, C	
2′′′	22.9, CH_3	1.02, s
8-OH		7.68
11-OH		5.07
3′′-NH		8.68
4′′-OH		4.93

[a] ^1H and ^{13}C NMR were recorded at 850 and 212.5 MHz, respectively.

3. Actinomadurol, an antibacterial norditerpenoid from a rare actinomycete, *Actinomadura* sp. KC-191

II.3.1. Results and discussion

Actinomadurol (**13**) was isolated as a colorless oil yielding an $[M-H]^-$ ion at *m/z* 317.1756 in its high-resolution electrospray ionization mass spectrum (HRESIMS). The exact mass was consistent with the molecular formula $C_{19}H_{26}O_4$ while the molecular formula provided seven unsaturation equivalents. The infrared (IR) absorption peaks at 3360 and 1660 cm^{-1} indicated the presence of hydroxy and carbonyl functional groups, respectively. The ^{13}C NMR spectrum revealed the presence of 19 carbon signals, which were classified by the DEPT spectrum as two sp^3 methyls (δ_C 24.3 and 12.6), five sp^3 methylenes (δ_C 63.2, 41.2, 35.1 29.3, and 25.9), three sp^3 methines (δ_C 82.1, 68.6, and 40.3), two sp^3 quaternary carbons (δ_C 49.0 and 35.4), one sp^2 methylene (δ_C 110.3), two sp^2 methines (δ_C 149.8 and 121.3), three fully substituted sp^2 carbons (δ_C 169.5, 140.1, and 129.3), and one carbonyl carbon (δ_C 201.4). Three double bonds (six olefinic sp^2 carbons) and one carbonyl group accounted for four unsaturations thereby suggesting that actinomadurol (**13**) contains three rings in its structure.

The $^1J_{CH}$ direct connectivities between protons and carbons were established by analyzing the HSQC spectrum and the tabulated ^1H and ^{13}C NMR spectral data for **13**, which are listed in Table 4. The planar structure of actinomadurol (**13**) was elucidated by analyzing COSY and HMBC spectra (Figure 9). The COSY correlations between the olefinic H-15 (δ_H 5.83) and H_2-16 (δ_H 4.94 and 4.83) peaks revealed the existence of a

terminal methylene. Two methylenes were shown to be connected by ^{1}H-^{1}H coupling between H_2-11 (δ_H 2.54 and 2.34) and H_2-12 (δ_H 1.47 and 1.38) signals in the COSY spectrum. The ^{1}H-^{13}C long-range couplings from the H_3-17 (δ_H 1.02) singlet to the quaternary C-13 (δ_C 35.4) signal, C-12 (δ_C 35.1) and the C-14 (δ_C 41.2) methylene resonances, and the olefinic C-15 (δ_C 149.8) peak established the connectivities of C-11 through to C-17. A 4-methyl-4-vinylcyclohex-1-ene moiety was constructed by the HMBC correlations from the H_2-14 (δ_H 2.22 and 1.91) signals to the C-8 (δ_C 129.3) and C-9 (δ_C 140.1) resonances and from the H_2-12 peak to the C-9 signal.

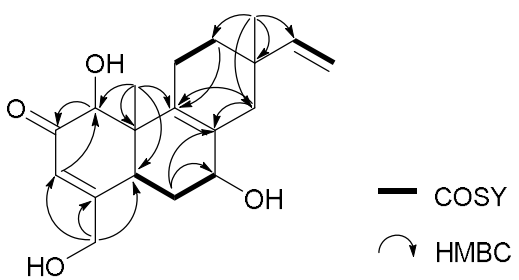

Figure 9. Key ^{1}H-^{1}H COSY and HMBC correlations of **13.**

Correlations between the peaks of the methine H-5 (δ_H 3.13) and methylene H_2-6 (δ_H 1.99 and 1.87) were observed in the COSY spectrum, connecting C-5 and C-6. Another cyclohexene partial structure was elucidated based on the HMBC couplings from the H_3-18 (δ_H 0.86) singlet to an oxymethine C-1 (δ_C 82.1), a quaternary C-10 (δ_C 49.0), and olefinic C-9 (δ_C 140.1) and a methine C-5 (δ_C 40.3) and from the H-6 resonance to C-7

(δ_C 68.6) and C-8.

The hydroxymethyl H_2-19 peaks (δ_H 4.31 and 4.26) displayed $^2J_{CH}$ and $^3J_{CH}$ correlations to the olefinic fully substituted C-4 (δ_C 169.5), the olefinic methine C-3 (δ_C 121.3), and the aliphatic methine C-5 (δ_C 40.3) signals. The HMBC correlations between the signals of H-3 (δ_H 6.35) and C-1 and between the resonances of the oxymethine H-1 (δ_H 4.28) and the ketone C-2 (δ_C 201.4) established the presence of the last six-membered ring moiety. Consequently, the structure of actinomadurol (**13**) was determined as a new C-19 norditerpenoid that is structurally similar to the pimarane class.

JBIR-65 (**14**) was obtained as a major secondary metabolite during the purification of actinomadurol (**1**). ^{1}H and ^{13}C NMR spectra of **14** exhibited analogous features to those of **13**. The structure of JBIR-65 (**2**) was confirmed as a previously reported secondary metabolite by comparison of the NMR data (Table S1) with the literature.[25] The original source of the compound was a sponge associated *Actinomadura* strain.[25]

The relative configuration of actinomadurol (**13**) was determined by analyzing ^{1}H-^{1}H coupling constants and NOESY NMR correlations (Figure 10). The H-5 signal (dd, J = 13.5, 2.0 Hz) showed a large coupling with the H-6β peak (ddd, J = 13.5, 13.5, 4.0), clearly indicating their pseudo-axial positions. The H-1/H-5 NOESY correlation revealed that H-1 is located in a pseudo-axial position. The carbinol H-7 peak possesses only small coupling constants (dd, J = 4.0, 2.0), indicating its pseudo-equatorial position. The H-

11α signal showed a strong 1,3-NOESY correlation with the H_3-17 peak, whereas H-11β displayed a clear NOESY correlation with the H_3-18 resonance, revealing that the C-17 and C-18 methyl groups exist pseudo-axially on opposite faces. Thus, the relative configuration of **13** was determined to be 1*S**, 5*R**, 7*R**, 10*S**, and 13*R**.

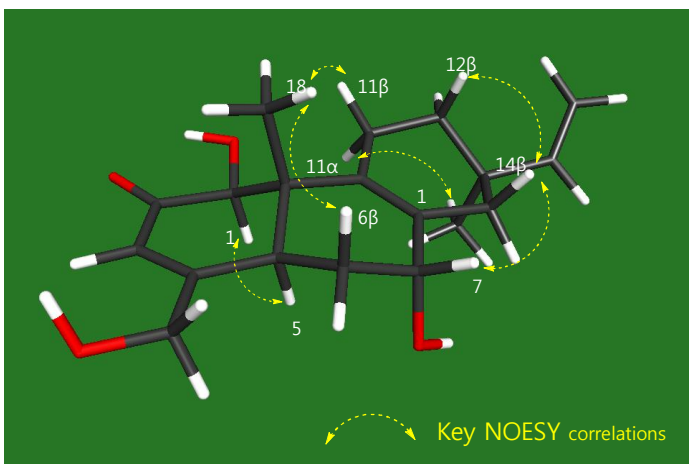

Figure 10. The strong NOESY correlations observed in **13**.

The relative configuration of JBIR-65 (**14**), which is the 6-oxo-form of **13**, has not been previously reported. Consequently, its configuration was analyzed using ^{1}H-^{1}H coupling constants and NOESY correlations, as for **13**. However, for compound **14**, I could not determine the configuration of C-13 because of the overlapping signals of the two methylenes at H_2-11 and H_2-12, even in the 900 MHz ^{1}H NMR spectrum (Table S1 and Figure S8). Eventually, I obtained two possible relative configurations (1*S**, 5*R**, 10*S**, and 13*R**; 1*S**, 5*R**, 10*S**, and 13*S**).

To determine the absolute configuration of JBIR-65 (**14**), the modified

Mosher's method was applied.[26] Prior to this procedure, the time-controlled acetylation of **13** mainly yielded a mono-acetate product (**15**) esterified at the primary alcohol at C-19. The secondary hydroxy group at C-1 in **13** was then derivatized with *R*-(-) and *S*-(+)-α-methoxy-α-(trifluoromethyl)phenylacetyl chloride (MTPA-Cl) to yield the *S*- and *R*-MTPA esters (**16** and **17**), respectively. The ^{1}H chemical shifts of the relevant protons were assigned by analyzing the ^{1}H NMR spectra of **16** and **17**. Calculating the $\Delta\delta_{S-R}$ values established the absolute configuration of 1*S* (Figure 11).

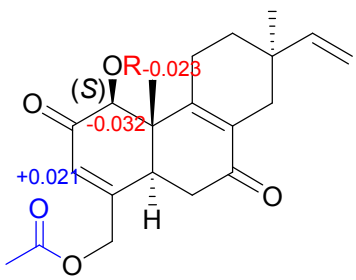

4: **R** = (*S*)-MTPA
5: **R** = (*R*)-MTPA

Figure 11. $\Delta\delta_{S-R}$ values in ppm of **16** and **17** in DMSO-d_6.

Although the C-5 and C-10 stereogenic centers in **14** were determined as 5*R* and 10*S*, respectively, based on the relative configuration of the left ring of **14**, the absolute configuration of C-13 could not be assigned: the relative configuration of this center was not established because of the overlapping ^{1}H NMR resonances of H-11α/H-11β and H-12α/H-12β (Table S1). Therefore, I determined the last stereogenic center by calculating the electronic circular dichroism (ECD) spectra of the two possible

configurations (1*S*, 5*R*, 10*S*, and 13*R*; 1*S*, 5*R*, 10*S*, and 13*S*).[27] These spectra were calculated using time-dependent density-functional theory (TD-DFT) at the B3LYP/def2-TZVPP//B3LYP/def-SV(P) level for all atoms. The experimental ECD spectrum of **14** showed a negative Cotton effect at 248 nm, which corresponded better to the calculated ECD spectrum for the 1*S*, 5*R*, 10*S* and 13*R* configuration than to that of the 13*S* configuration (Figure S17). Therefore, the absolute configuration of **14** was finally assigned as 1*S*, 5*R*, 10*S* and 13*R*.

Based on the absolute configuration of **14**, actinomadurol (**13**), which shares a common biosynthetic origin with **14**, presumably possesses a 1*S*, 5*R*, 7*R*, 10*S*, and 13*R* configuration. This assignment was further confirmed by comparing the experimental ECD spectrum of **13** and the calculated ECD spectra of the two possible enantiomers of **13**. The experimental ECD spectrum of **13** displayed positive Cotton effects at 220 and 310 nm, which is consistent with the calculated ECD spectrum of the 1*S*, 5*R*, 7*R*, 10*S*, and 13*R* configuration, whereas its enantiomer (1*R*, 5*S*, 7*S*, 10*R*, and 13*S*) showed an opposite calculated ECD spectrum (Figure S18). Therefore, the absolute configuration of actinomadurol (**13**) was established as 1*S*, 5*R*, 7*R*, 10*S*, and 13*R*.

Because the extract of *Actinomadura* strain KC 191 showed significant antibacterial activity, the biological activities of actinomadurol (**13**) and JBIR-65 (**14**) were evaluated against diverse pathogenic bacteria. As previously reported,[25] JBIR-65 did not display any antibacterial activity

(MIC > 100 μg/mL) in our tests. However, actinomadurol exhibited significant inhibitory activities comparable to or even stronger than those of the positive control ampicillin against *Staphylococcus aureus*, *Bacillus subtilis*, *Kocuria rhizophila*, *Proteus hauseri*, and *Salmonella enterica* (MIC = 0.39 ~ 3.12 μg/mL), but not against *Escherichia coli* (MIC > 100 μg/mL) (Table 3). Based on the antibacterial assay result the reduction of a ketone functional group (**14**) to a secondary alcohol (**13**) at C-7 was apparently the cause of the significant antibacterial activity. An attempt to reduce the ketones at C-2 and C-7 in JBIR-65 (**14**) with $NaBH_4$ to produce actinomadurol analogues with secondary alcohols at C-2/C-7 was unsuccessful because JBIR-65 was degraded during reduction.

Further biological evaluations of **13** and **14** using cytotoxicity assays against various cancer cell lines (A549, HCT116, SNU638, SK-HEP1, MDA-MB231 and K562) were performed. Compounds **13** and **14** did not inhibit the growth of the tested cancer cell lines, even at high concentrations (IC_{50} > 100 μg/mL). In addition, the two compounds did not display any inhibitory activity against *Candida albicans*, *Aspergillus fumigatus*, *Trichophyton rubrum*, *Trichophyton mentagrophytes* (MIC > 100 μg/mL) as well as against *Candida albicans*-derived isocitrate lyase (ICL), a key enzyme in microbial biosynthesis.[28]

Table 3. Antibacterial activities of Actinomadurol (**13**) and JBIR-65 (**14**)

	Antibacterial activity (MIC, μg/mL)					
	S. aureus	*B. subtilis*	*K. rhizophila*	*P. hauseri*	*S. enterica*	*E. coli*
1	0.78	1.56	0.39	0.78	3.12	>100
2	>100	>100	>100	>100	>100	>100
Ampicillin	3.12	1.56	0.79	1.56	3.12	6.25

Bacterial diterpenoids have been reported only rarely since the discovery of the first examples, the gibberellins from *Rhizobium phaseoli* in 1988,[29] and most of these compounds were discovered from streptomycete actinobacteria.[30] Diterpenoids have been even more infrequently isolated from rare actinobacteria. Brasilicardins A-D, tricyclic diterpenoids with cytotoxic and immunosuppressive activities, were isolated from *Nocardia brasiliensis*[31] while tuberculosinol and the isotuberculosinols, which play key roles in pathogenesis, were isolated from *Mycobacterium tuberculosis*.[32] Another rare actinobacterium, *Verrucosispora gifhornesis,* produced the gifhornenolones, which are norditerpenoids with potent inhibitory activity against the androgen receptor.[33] In turn, actinomadurol (**13**) and JBIR-65 (**14**) are rare members of the bacterial norditerpenoid metabolite series. To the best of our knowledge, aside from the gifhornenolones, only two similar series of bacterial norditerpenoids have been reported as C-16 norditerpenoid antibiotics, namely the platensimycins[34] and the platenicins[35] from *Streptomyces platenesis* strains.

In summary, our chemical investigation of *Actinomadura* sp. KC 191 revealed a new antibacterial secondary metabolite, actinomadurol (**13**), and the absolute configuration of JBIR-65 (**14**). The potent antibacterial activity

of **13** and its unique 19-norditerpenoid carbon backbone provide a new scaffold for antibiotic discovery. The discovery of this rare diterpenoid from the relatively uninvestigated actinobacterial genus *Actinomadura* underpins the importance of extending chemical studies to members of rare actinobacterial taxa.

II.3.2. Experimental section

General Experimental Procedures. Optical rotations were determined with a JASCO P1020 polarimeter using a 1 cm cell. UV spectra were measured on a PerkinElmer Lambda 35 UV/VIS spectrophotometer and ECD spectra were recorded using an Applied Photopysics Chirascan-Plus circular dichroism spectrometer. IR spectra were recorded using a Thermo NICOLET iS10 spectrometer. ^{1}H, ^{13}C, and 2D NMR spectra were obtained on a Bruker Avance 900 MHz spectrometer at the Korea Basic Science Institute (KBSI) in Ochang. ^{1}H and ^{13}C NMR chemical shifts (δ_H and δ_C) were recorded in ppm. Low-resolution electrospray ionization source mass spectra were acquired with an Agilent Technologies 6130 quadrupole mass spectrometer coupled to an Agilent Technologies 1200 series high-performance liquid chromatography (HPLC) instrument. High-resolution electrospray ionization mass spectra (HRESIMS) were obtained using a Thermo Scientific Q high-resolution mass spectrometer at the NICEM (National Instrumentation Center for Environmental Management at Seoul National University). Semi-preparative HPLC separations achieved with a Gilson 305 pump and a Gilson UV/VIS 155 detector.

Isolation and Classification of an Actinobacterial strain KC 191. Strain KC 191 was isolated from a soil sample taken from Palace Leas hay meadow plot 6 at Cockle Park Experimental Farm, Northumberland, UK (National Grid Reference NZ 202912) using starch-casein agar,[36]

supplemented with cycloheximide and nystatin (at 25 μg/mL), a medium known to favor the selective isolation of streptomycetes.[37] Biomass for the comparative 16S rRNA gene sequence analyses was grown in shake flasks of glucose-yeast extract-malt extract broth (ISP medium 2) at 28 °C for 7 days, harvested by centrifugation and washed twice in distilled water.[37] Genomic DNA was extracted from the resultant biomass, and polymerase chain reaction (PCR) amplification and 16S rRNA gene sequencing achieved using previously described procedures.[38] The nearly complete 16S rRNA gene sequence (1392 nucleotides [nt]) of strain KC 191 was aligned manually against corresponding sequences of representatives of the genus *Actinomadura* using MEGA 5.0 software (MEGA software, Philadelphia, PA, USA)[39] and phylogenetic trees inferred by using the neighbor-joining,[40] maximum-likelihood[41] and maximum-parsimony.[42] The Jukes & Cantor model[43] was used to generate evolutionary distance matrices for the neighbor-joining data. The resultant tree topologies were evaluated by bootstrap analysis[44] based on 1000 resampled datasets using MEGA 5.0. The strain shared a phyletic line within a subclade which also encompassed the type strains of *Actinomadura glauciflava*, *Actinomadura masheskhailensis* and *Actinomadura mexicana*, a relationship that was supported by all of the tree-making algorithms and by a high bootstrap value (Figure S19). The strain was most closely related to *A. mexicana* A290^{T}, these strains shared a 16S rRNA gene sequence similarity of 99.6%, a value which corresponded to 6 nucleotide differences at 1386 locations.

Consequently, strain KC 191 (GenBank accession number KU936908) forms the nucleus of a potentially novel species within the genus *Actinomadura*.

Cultivation and Isolation. The strain was cultivated in 50 mL of yeast extract-malt extract (YEME) medium (4 g of yeast, 4 g of glucose, and 10 g of malt in 1 L of distilled H_2O). After culturing the strain for 7 days on a rotary shaker at 190 rpm and 30 °C, 10 mL of the culture was inoculated into 1 L of YEME medium in a 2.8 L Fernbach flask. The entire culture (80 L) was extracted twice with EtOAc then concentrated in vacuo to yield 5 g of dry material. After extraction, the extract was fractionated by C_{18} reversed-phase vacuum flash chromatography using a sequential mixture of MeOH and H_2O as the eluent (five fractions eluted with a MeOH/H_2O gradient from 20% to 100%). After fractionation, compounds **1** and **2** were found in the 60% and 80% MeOH/H_2O fractions. Each fraction was then subjected to reversed-phase high-performance liquid chromatography (HPLC; Kromasil 100-5-C_{18} 250 × 10 mm, flow rate 2 mL/min, UV 254 nm detection, 68% aqueous MeOH isocratic). Under these purification conditions, actinomadurol (**1**) and JBIR-65 (**2**)[10] were purified with retention times of 30 and 25 min, respectively.

Actinomadurol (13): Colorless oil; $[\alpha]^{25}_{D}$ -45.0 (*c* 0.5, MeOH); UV (MeOH) λ_{max} (log ε) 261 (2.46) nm; ECD (*c* 4.3 × 10^{-4} M, MeOH) λ_{max} ($\Delta\varepsilon$) 220 (10.4), 312 (1.6) nm; IR (neat) ν_{max} 3360, 1660 cm^{-1}; ^{1}H and ^{13}C NMR data in Table 4; ESI MS *m/z* 317.1756 $[M-H]^-$ (calcd for $C_{19}H_{25}O_4$, *m/z*

317.1753).

JBIR-65 (14): Colorless oil; $[\alpha]^{25}_{D}$ -80.0 (*c* 0.1, MeOH); UV (MeOH) λ_{max} (log ε) 255 (2.13) nm; ECD (*c* 4.3 × 10^{-4} M, MeOH) λ_{max} ($\Delta\varepsilon$) 248 (3.12), 330 (1.36) nm; IR (neat) ν_{max} 3300, 1580^{-1}; ESI MS *m/z* 317.1753 $[M+H]^+$ (calcd for $C_{19}H_{25}O_4$, *m/z* 317.1736).

Acetylation of 14. JBIR-65 (**14**, 4 mg) was dissolved in pyridine (2 mL), and a stock solution of acetic anhydride was prepared in pyridine (0.42 μM: 80 μL acetic anhydride in 2 mL pyridine). The stock solution was added to the JBIR-65 solution gradually in 10 or 20 μL aliquots, and the reaction was monitored by liquid chromatography/mass spectrometry (LC/MS). The reaction solution was cooled when the acetic anhydride solution was added, and the mixture was stirred at room temperature. When 400 μL of the stock solution in total had been applied for 7 h, the reaction yielded 85% of the mono-acetate (**15**) of JBIR-65. The reaction was halted by adding 10 μL of water. The acetate of JBIR-65 (**15**, 3.4 mg) was purified through reversed-phase HPLC (Kromasil 100-5-C_{18} 250 × 10 mm, flow rate 2 mL/min, UV 254 nm detection, 75% aqueous MeOH isocratic, retention time 20 min). The molecular formula ($C_{21}H_{26}O_5$) of the desired product, an acetate of JBIR-65 (**3**), was confirmed by electrospray mass spectrometry (ESI MS) ($[M+H]^+$ *m/z* at 359) and ^{1}H NMR data spectroscopy.

Acetate (15) of JBIR-65 (14): ^{1}H NMR (600 MHz, CD_3OD) δ 6.17 (br s, 1H), 5.75 (dd, *J* = 17.5, 10.5, 1H), 4.89 (dd, *J* = 17.5, 1.0, 1H), 4.85 (dd, *J* =

10.5, 1.0, 1H), 4.75 (m , 2H), 4.28 (s, 1H), 3.42 (m, 1H), 2.78 (dd, *J* = 18.0, 4.5, 1H), 2.71 (m, 2H), 2.61 (dd, *J* = 18.0, 14.0, 1H), 2.46 (d, *J* = 18.0, 1H), 2.19 (s, 3H), 1.91 (d, *J* = 18.0, 1H), 1.52 (m, 2H), 1.02 (s, 3H), and 0.98 (s, 3H).

MTPA Esterification of JBIR-65 Acetate (15). Acetate (**15**) was prepared in two 40 mL vials (two 1.7 mg samples), which were dried completely under high vacuum for 12 h. First, freshly distilled anhydrous pyridine (1 mL) was prepared prior to the addition of a catalytic amount of dimethylaminopyridine to the solution. *R*-(-) and *S*-(+)-MTPA chloride (10 μL) were added separately and the mixture stirred while gradually increasing the temperature from 45 °C to 65 °C. After 2.5 h, the reaction was quenched with 0.5 mL of MeOH. The products were then purified using reversed-phase HPLC (Kromasil 100-5-C_{18} 250 × 10 mm, flow rate 2 mL/min, UV 254 nm detection) under gradient conditions ranging from 60% to 100% aqueous acetonitrile. The *S*-MTPA (**16**) and *R*-MTPA (**17**) esters eluted at 27.0 and 27.5 min, respectively. The molecular formulae ($C_{31}H_{33}F_3O_7$) of the MTPA esters were confirmed by ESI MS ($[M+H]^+$ *m/z* at 575) and ^{1}H NMR spectroscopy. The ^{1}H chemical shifts around the stereogenic centers of the derivatives were assigned by ^{1}H NMR spectra of **16** and **17**.

***S*-MTPA ester (16) of acetate (15):** ^{1}H NMR (600 MHz, DMSO-d_6) δ 7.25-7.15 (m, 5H), 6.10 (br s, 1H), 5.75 (dd, *J* = 17.5, 10.5, 1H), 5.18 (s,

1H), 4.74 (dd, *J* = 17.5, 1.0, 1H), 4.70 (dd, *J* = 10.5, 1.0, 1H), 4.60 (m , 2H), 3.49 (s, 3H), 3.46 (m, 1H), 2.74 (dd, *J* = 18.0, 4.5, 1H), 2.71 (m, 2H), 2.63 (dd, *J* = 18.0, 14.0, 1H), 2.46 (d, *J* = 18.0, 1H), 2.19 (s, 3H), 1.91 (d, *J* = 18.0, 1H), 1.52 (m, 2H), 1.01 (s, 3H), and 0.95 (s, 3H).

***R*-MTPA ester (17) of acetate (15):** ^{1}H NMR (600 MHz, DMSO-d_6) δ 7.26-7.10 (m, 5H), 6.08 (br s, 1H), 5.72 (dd, *J* = 17.5, 10.5, 1H), 5.21 (s, 1H), 4.76 (dd, *J* = 17.5, 1.0, 1H), 4.72 (dd, *J* = 10.5, 1.0, 1H), 4.62 (m , 2H), 3.49 (s, 3H), 3.45 (m, 1H), 2.75 (dd, *J* = 18.0, 4.5, 1H), 2.72 (m, 2H), 2.64 (dd, *J* = 18.0, 14.0, 1H), 2.47 (d, *J* = 18.0, 1H), 2.18 (s, 3H), 1.89 (d, *J* = 18.0, 1H), 1.50 (m, 2H), 1.02 (s, 3H), and 0.97 (s, 3H).

Computational Analysis. The ground-state geometries were optimized by DFT calculations using Turbomole 6.5 with the basis set def-SV(P) for all atoms at the functional B3LYP/DFT level. The ground states were further confirmed by harmonic frequency calculations. The calculated ECD data corresponding to the optimized structures were obtained with TD-DFT at the functional B3LYP/DFT level at the basis set def2-TZVPP for all atoms. The CD spectra were simulated by overlapping each transition, where σ is the width of the band at 1/e height. ΔE_i and R_i are the excitation energies and rotatory strengths for transition *i*, respectively. In the current work, the value of σ was 0.10 eV.

$$\Delta\epsilon(E) = \frac{1}{2.297 \times 10^{-39}} \frac{1}{\sqrt{2\pi}\sigma} \sum_{i}^{A} \Delta E_i \, R_i \, e^{[-(E-\Delta E_i)^2/(2\sigma)^2]}$$

Antibacterial Assays. The *in vitro* antimicrobial activities of the

compounds were assessed against three representative Gram-positive bacteria, viz. *Staphylococcus aureus* (ATCC 6538p), *Bacillus subtilis* (ATCC 6633), and *Kocuria rhizophila* (NBRC 12708), and three Gram-negative bacteria, viz. *Proteus hauseri* (NBRC 3851), *Salmonella enterica* (ATCC 14028) and *Escherichia coli* (ATCC 25922). The resultant data are presented in Table 3 as MIC values. The bacteria were grown overnight in LB broth at 37 °C harvested by centrifugation and then washed twice with sterile distilled water. Stock solutions of the compounds were prepared in DMSO. Each stock solution was diluted with Standard method broth (Difco) to prepare serial two-fold dilutions in the range of 100 to 0.8 μg/mL. Ten microliters of broth containing approximately 10^5 colony-forming units (cfu)/mL of the test bacteria were added to each well of a 96 well microtiter plate. The culture plates were incubated for 24 h at 37 °C.

Table 4. ^{1}H and ^{13}C NMR data for Actinomadurol (**13**) in CD_3OD[a]

Position	δ_C, type	δ_H, mult (*J* in Hz)
1	82.1, CH	4.28, s
2	201.4, C	
3	121.3, CH	6.35, br s
4	169.5, C	
5	40.3, CH	3.13, dd (13.5, 2.0)
6α	29.3, CH_2	1.99, ddd (13.5, 2.0,
6β		2.0)
		1.87, ddd (13.5, 13.5,
		4.0)
7	68.6, CH	3.84, dd (4.0, 2.0)
8	129.3, C	
9	140.1, C	
10	49.0, C	
11α	25.9, CH_2	2.54, m
11β		2.34, m
12α	35.1, CH_2	1.38, m
12β		1.47, m
13	35.4, C	
14α	41.2, CH_2	1.91, d (18.0)
14β		2.22, d (18.0)
15	149.8, CH	5.83, dd (17.5, 11.0)
16a	110.3, CH_2	4.94, dd (17.5, 1.0)
16b		4.83, dd (11.0, 1.0)
17	24.3, CH_3	1.02, s
18	12.6, CH_3	0.86, s
19a	63.2, CH_2	4.31, m
19b		4.26, m

[a] ^{1}H and ^{13}C NMR were recorded at 900 and 225 MHz, respectively.

4. Deinococcucins A−D, aminoglycolipids from *Deinococcus* sp., a gut bacterium of the carpenter ant *Camponotus japonicus*.

II.4.1. Results and discussion

Deinococcucin A (**18**) was isolated as an amorphous, colorless oil and contained an $[M+H]^+$ ion at *m/z* 533.3756 in its high-resolution electrospray ionization mass spectroscopy (HRESIMS) data. The exact mass was consistent with the molecular formula $C_{27}H_{52}N_2O_8$, which provided three unsaturation equivalents. The infrared (IR) absorption peaks at 3360 and 1640 cm^{-1} indicated the presence of hydroxy and amide functional groups, respectively. The ^{13}C nuclear magnetic resonance (NMR) data revealed the presence of 27 carbon signals, which were classified from the HSQC spectrum as two sp^3 methyl (δ_C 22.8 and 13.9), 17 sp^3 methylene (δ_C 69.6-29.1), six sp^3 methine (δ_C 97.1, 72.6, 70.8, 70.8, 70.4 and 53.4) carbons and two carbonyl carbons (δ_C 171.1 and 169.3).

The $^1J_{CH}$ direct connectivities between protons and carbons were established by analyzing the HSQC spectrum and the tabulated ^1H and ^{13}C NMR spectral data for **18**, which are listed in Table 5. The planar structure of deinococcucin A (**18**) was elucidated by analyzing its COSY and HMBC data (Figure 12), revealing a hexose structure. The ^1H-^1H homonuclear couplings demonstrated the formation of a spin system from H-1′ (δ_H 4.62) to H_2-6′ (δ_H 3.55 and 3.47). H-1′/C-5′ and H-5′/C-1′ HMBC correlations established the closure of the hexose ring. The exchangeable protons of 2′-NH (δ_H 7.56), 3′-OH (δ_H 4.78), 4′-OH (δ_H 5.00), and 6′-OH (δ_H 4.45) were assigned in this hexose spin system based on the ^1H-^1H COSY correlations.

In addition, the HMBC correlations from 2′-NH and H_3-8′ (δ_H 1.85) to the amide carbon C-7′ (δ_C 169.3) established an *N*-acetyl group at the C-2′ position. Another spin system was identified from the H-1/H-2 and H-2/2-OH COSY correlations. The $^2J_{CH}$ coupling from H-2 to the carbonyl carbon C-3 constructed a 2,3-dihydroxypropanoic acid moiety. The last partial structure was identified as an alkyl amine hydrophobic chain starting from the NH group. The amide proton 3-NH showed a COSY correlation to H_2-4. The lipophilic chain composed of highly overlapped methylene protons and a terminal methyl group (δ_H 0.85; δ_C 13.9) was deduced based on the molecular formula, the overlapped COSY correlations among the methylene protons, and the clear COSY correlation from a methylene proton (H_2-18) to the methyl group (H_3-19).

The three partial structures, a hexose ring, 2,3-dihydroxypropanoic acid, and an alkyl amine hydrocarbon chain, were assembled based on the HMBC correlations. The hexose ring was connected to 2,3-dihydroxypropanoic acid through an ether based on the H-1′/C-1 and H-1/C′-1 HMBC correlations. The HMBC correlations from H-2 and 3-NH to the carbonyl carbon C-3 at δ_C 171.1 secured the connectivity from 2,3-dihydroxypropanoic acid to the hydrocarbon chain unusually starting at an NH group and not at a carbonyl carbon. Therefore, the planar structure of deinococcucin A (**1**) was elucidated as a new aminoglycolipid (Figure 12).

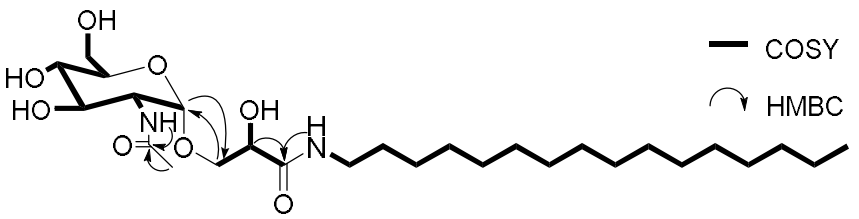

Figure 12. Key ^{1}H-^{1}H COSY and HMBC correlations of **18.**

Deinococcucin B (**19**) was purified as a colorless oil with a molecular formula of $C_{28}H_{54}N_2O_8$ determined from its HRESIMS data. The 1D and 2D NMR spectroscopic data of **19** (Table 5) displayed almost identical features to those of **18**. Careful analysis of the NMR data disclosed the presence of one additional sp^3 methylene carbon in the lipid chain of **19** compared to **18**, thus determining the structure of **19** as an analogue of **18** with a C_{16} alkyl chain.

Deinococcucin C (**20**) was obtained as a colorless oil, and its molecular formula was deduced to be $C_{27}H_{50}N_2O_8$ based on its HRESIMS data. Careful comparison of the NMR spectroscopic data (Table 6) revealed that the ^{1}H and ^{13}C NMR spectra of **3** in DMSO-d_6 were very similar to those of **18** but that deinococcucin C (**20**) bears two overlapped sp^2 methine carbons (δ_C 129.0), indicating that **3** possesses a double bond in the hydrocarbon chain. Further analysis of its 2D NMR spectra, including COSY, HSQC, and HMBC data, indicated that the structure of deinococcucin C (**20**) was analogous to that of **18** with an olefinic double bond in its chain. However, the overlapped ^{1}H and ^{13}C NMR resonances of the hydrocarbon chain

hampered the determination of the exact position and the geometry of the double bond, which required further analysis.

For the exact assignment of the double bond position, a recently developed method utilizing olefin cross-metathesis and subsequent LC/MS analysis was applied.[71] Cross-metathesis of **20** with methyl acrylate using the 2nd-generation Hoveyda-Grubbs catalyst yielded a UV-detectable product (Figure 13). The double bond positions could be simply deduced by comparing the mass changes between deinococcucin C ($[M+H]^+$ at *m/z* 531) and the cross-metathesis product in the LC/MS data (Figure 13). The molecular mass of the deinococcucin C-derived cross-metathesis product was 504 ($[M+H]^+$ at *m/z* 505), indicating a 26-Dalton decrease from the mass of deinococcucin C. This result can be easily explained by the removal of a C_6H_{13} group (85 Daltons) and the addition of a CO_2CH_3 group (59 Daltons) in the metathesis partner, methyl acrylate, during cross-metathesis, thus placing the double bond position at the seventh carbon from the chain terminus. Therefore, the double bond position was unequivocally established between C-12 and C-13.

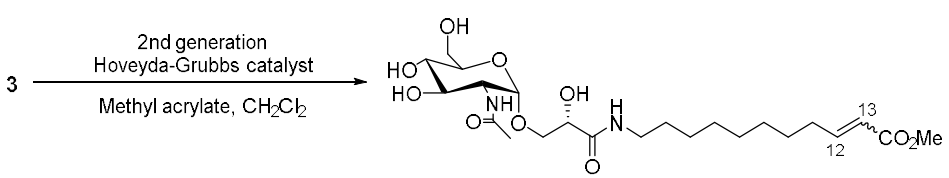

Figure 13. Olefin cross-metathesis of deinococcucin C (**20**).

Regarding the geometry of the double bond, the ^1H-^1H coupling constant

between H-12 and H-13 could not be measured because these two protons overlap at δ_H 5.33. Instead, the ^{13}C chemical shifts were used to establish the configuration of the olefinic bond. Reportedly, the aliphatic carbons flanking a Z-olefin in a long hydrocarbon chain resonate at δ_C 28~30, while those next to an *E*-double bond appear at δ_C 42~43, clearly distinguishing the *E*/*Z* geometries.[72,73] The chemical shifts of C-11 and C-14 were detected at δ_C 28.5, thus assigning the 12*Z* configuration.

Deinococcucin D (**21**) was isolated as a colorless oil. The molecular formula was assigned as $C_{28}H_{52}N_2O_8$ based on its HRESIMS data. Similar to the relationship between deinococcucins A (**18**) and C (**20**), deinococcucin D (**21**) has two more sp^2 methine (δ_C 129.6) and two less sp^3 methylene carbons compared to **19**. Detailed analysis of the 2D NMR spectra (Table 6) indicated that deinococcucin D also possesses an olefinic double bond in the lipid chain similar to **20**. The location and geometry of the double bond in **21** were determined as 12*Z* by cross-metathesis and ^{13}C chemical shift analysis, as shown for **20**.

The relative configuration of the hexose ring was established by analyzing the ^1H-^{13}C and ^1H-^1H coupling constants and the ROESY NMR through-space correlations. The magnitude of $^1J_{CH}$ (170 Hz) between C-1′ and H-1′ was clearly indicative of an α-configuration,[7] placing the anomeric proton (H-1′) in an equatorial position. The large ^1H-^1H vicinal coupling constant (8.5 Hz) between H-2′ and H-3′ established their *anti*-relationship

and, therefore, axial positions. In addition, H-4′ was assigned an axial position based on $^{3}J_{HH}$ (10.0 Hz) between H′-3 and H′-4. Lastly, the ^{1}H-^{1}H coupling constant (9.0 Hz) of the H-5′ doublet determined its axial position, and the H-2′/H-4′ ROESY correlation confirmed their relative configurations. Therefore, the hexose moiety was determined to be *N*-acetyl glucosamine (Figure 14).

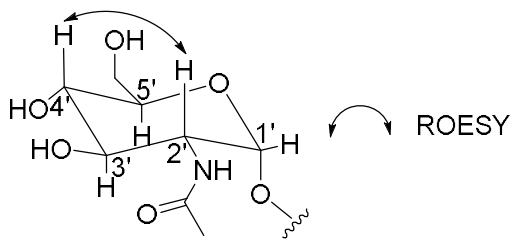

Figure 14. Strong ROESY correlations observed in the hexose moiety of **18**.

To determine the absolute configuration of the glucosamine moiety in deinococcucin A (**18**), the compound was subjected to acid hydrolysis yielding glucosamine which was derivatized using hexamethyldisilazane (HMDS) and TMS-Cl and analyzed by gas chromatography-mass spectroscopy (GC/MS). The derivative of glucosamine from *N*-acetyl glucosamine in **18** exhibited a retention time that was consistent with that of the authentic D-glucosamine derivative.[75]

To determine the absolute configuration of deinococcucin A (**18**), the phenylglycine methyl ester (PGME) method was applied.[76] Prior to this procedure, acid hydrolysis of **18** mainly yielded a 2,3-dihydroxypropanoic acid (**22**). The carboxylic acid group at C-1 in **22** was then derivatized with

S- or *R*-PGME to yield the *S*- or *R*-PGME amide (**22a** and **22b**), respectively. The ^{1}H chemical shifts of the relevant protons were assigned by analyzing the ^{1}H NMR spectra of **22a** and **22b**. Calculating the $\Delta\delta_{S-R}$ values established the absolute configuration as 2*R* (Figure 15).

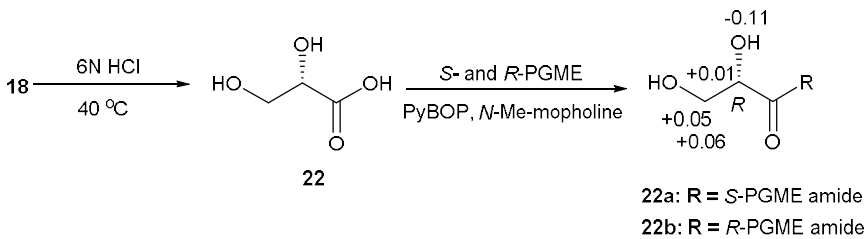

Figure 15. Degradation of **18** to 2,3-dihydroxypropanoic acid (**22**) and derivatization of **22** to *S*-and *R*-PGME amides. $\Delta\delta_{S-R}$ values of **22a** and **22b** are noted in ppm in DMSO-d_6.

The biological activities of deinococcucins A-D (**18**–**21**) were evaluated in several ways. Deinococcucins A-D (**18**–**21**) were neither cytotoxicity against human cancer cell lines (IC_{50} > 10 μM) or active against Gram positive and negative bacteria or fungi (MIC > 128 μM) (See the supporting information.).

Cancer chemoprevention is considered to play an important role in decreasing the risk of cancer development, involving the prevention, delay or reversal of carcinogenesis. One important cancer prevention strategy is to enhance the deactivation of radicals and electrophiles via phase II enzymes.[77] Quinone reductase (QR), a representative phase II detoxification enzyme, is known to function as a cancer chemopreventative.[78] The QR activity in Hepa 1c1c7 cells was enhanced in a dose-dependent manner over

a concentration range of 2.5–20 μM deinococcucins A (**18**) and C (**20**) without causing cytotoxicity. Deinococcucin C (**20**) induced QR activity by 1.8, 2.2, 2.5, and 2.7 fold, and deinococcucin A (**18**) induced significant QR activity by 1.2, 1.3, 1.6, and 1.9 fold at concentrations of 2.5, 5, 10, and 20 μM, respectively, as shown in Figure 16. However, no significant effects of deinococcucins B (**19**) and D (**21**) were observed (Figure 16).

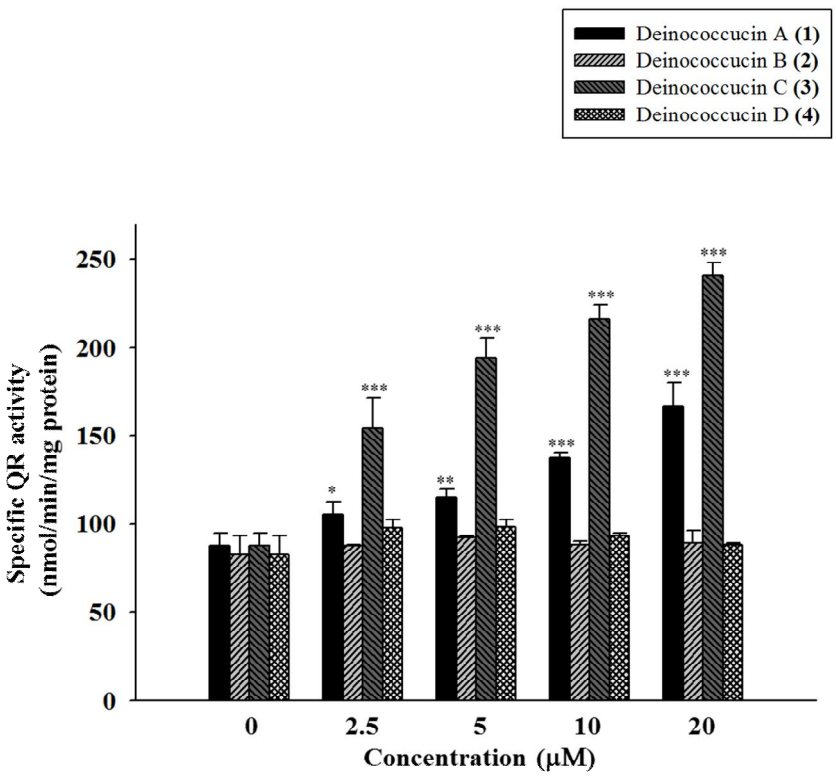

Figure 16. Effect of deinococcucins A-D (**18-21**) on the induction of QR in murine Hepa 1c1c7 cells. Cells were grown for 24 h and then exposed to the test compounds for 24 h. QR activities were measured in the cell lysates by reduction of a tetrazolium dye and expressed as nmol/min/mg protein. Values are the mean ±SD of four determinations. $P < 0.05$ (*), $P < 0.01$ (**) and $P < 0.001$ (***) indicate statistically significant differences from the

control group.

Reports on the chemistry of the genus *Deinococcus* are sparse. From the representative species *D. radiodurans*, a radiation-resistant species deinoxanthin was reported as a red pigment possibly responsible for the antioxidant activity of this species against hydroxy radicals produced by photochemical reactions.[79] The other class of compounds from *D. radiodurans* consists of phosphoglycolipids.[80,81] The deinococcucins are structurally most similar to the glucosamine-containing phosphoglycolipids, of which the gross structures were proposed in mixtures without rigorous spectroscopic analysis or biological evaluation.[82] Our report of the new aminoglycolipids deinococcucins A-D is the first full characterization of glycolipids, including the determination of the exact double bond position and the absolute configuration, from the genus *Deinococcus*. The similar structural features of the phosphoglycolipids from *D. radiodurans* and of the deinococcucins from the *Deinococcus* sp. that is most closely related to *D. xinjiangensis*, which is a phylogenetically distant species from *D. radiodurans* (Figure S28), indicate that the backbone of the deinococcucins could be a basic structural backbone of glycolipids in this genus.

II.4.2. Experimental section

General Experimental Procedures. Optical rotations were measured using a Jasco P-1020 polarimeter. IR spectra were recorded using a Thermo Nicolet iS10 spectrometer. ^{1}H, ^{13}C, and 2D NMR spectra were obtained on a Bruker Avance 600 MHz spectrometer at the National Center for Inter-University Research Facilities at Seoul National University (NCIRF). Low-resolution electrospray ionization source mass spectra were acquired with an Agilent Technologies 6130 quadrupole mass spectrometer coupled with an Agilent Technologies 1200 series high-performance liquid chromatography (HPLC) instrument. High-resolution electrospray ionization (HRESI) mass spectra were acquired using a Thermo Scientific Q high-resolution mass spectrometer at the National Instrumentation Center for Environmental Management at Seoul National University. Semi-preparative HPLC separations were achieved with a Gilson 305 pump and a Shodex 101 RI detector.

Collection of Carpenter Ants. Ant specimens were collected around a pond called Bandoji at the Seoul Zoo in Seoul Grand Park, Gwacheon-si, Gyeonggi-do on the mating flight season (April 2015). Ant nests under rocks were excavated by a spade and a short half-moon hoe. Collected specimens were identified as Japanese carpenter ant *Camponotus japonicus* (Hymenoptera: Formicidae) in the field based on external morphological characteristics. These collected ants were divided into several containers

using brushes and tweezers and transferred to the laboratory at Seoul National University on the same day.

Isolation and Classification of Strain SJN 1. Sixty queen ant specimens were washed with sterilized water and then soaked in 97% ethanol to remove the microbes on their exoskeleton. The queen ants were cut into three parts (head, thorax, and abdomen) using a razor blade. The cuticle of the abdomen was removed, and the intestinal parts were placed in a conical tube containing 20 mL of sterilized distilled water at 25 °C. The tube was vortexed, and 300-μL aliquots of the suspension were spread onto the surfaces of actinomycete isolation medium (1 L of distilled water, 22 g of actinomycete isolation medium, 18 g of agar, and 100 mg/L cycloheximide), A4 medium (1 L of distilled water, 18 g of agar, and 100 mg/L cycloheximide), A6 medium (1 L of distilled water, 18 g of agar, and 5 mg/L polymyxin B sulfate), A7 medium (1 L of distilled water, 18 g of agar, and 5 mg/L kanamycin) and chitin-based agar medium (1 L of distilled water, 4 g of chitin, 18 g of agar, and 100 mg/L cycloheximide) plates using autoclaved foam plugs (2 cm in diameter) and spreaders. The plates were incubated at 25 °C for 3 weeks. Strain SJN1 was isolated from a chitin-based agar plate. Colonies were repeatedly inoculated onto fresh YEME agar (1 L of distilled water, 18 g of agar, 4 g of yeast extract, 4 g of glucose, and 10 g of malt extract) plates to obtain a pure culture. Strain SJN1 was identified as a *Deinococcus* sp. most closely related to *D. xinjiangensis* based on its 16S rDNA sequence. (GenBank accession number: MF102142).

Analysis of 16S rDNA sequences constructed a neighbor-joining phylogenetic tree to show the relationship between isolate SJN1 and the type strains of closely related species of the genus *Deinococcus* (Figure S28).

Cultivation and Isolation. The strain was cultivated in 50 mL of modified K medium (2 g of yeast, 2 g of glucose, 3 g of mannitol, 5 g of soytone, 5 g of starch and 1 g of calcium carbonate in 1 L of distilled H_2O). After culturing the strain for 3 days on a rotary shaker at 180 rpm and 30 °C, 10 mL of the culture was inoculated into 1 L of modified K medium in a 2.8-L Fernbach flask and incubated at 180 rpm and 30 °C for 7 days. The entire culture (80 L) was extracted twice with ethyl acetate (EtOAc) and then concentrated *in vacuo* to yield 5 g of dry material. After extraction, the extract was fractionated by C_{18} reversed-phase vacuum flash chromatography using a sequential mixture of MeOH and H_2O as the eluent (five fractions eluted with an MeOH/H_2O gradient from 20% to 100%). After fractionation, deinococcucins A-D (**18-21**) were found in the 80% and 100% MeOH/H_2O fractions. Each fraction was then subjected to reversed-phase HPLC (250 × 10 mm Kromasil 100-5-C_{18} column, flow rate of 2 mL/min, RI detection, isocratic elution with 70% aqueous acetonitrile). Each compound was further purified (250 × 10 mm Kromasil 100-5-C_{18} column, flow rate of 2 mL/min, RI detection, isocratic elution with 82% aqueous MeOH) to yield deinococcucins A-D (**18-21**) (20, 15, 10, and 10 mg with the yields of 0.25, 0.18, 0.13, 0.13 mg/L) at retention times of 29,

55, 31 and 76 min, respectively.

Deinococcucin A (18): Colorless oil; $[\alpha]^{25}_{D}$ -25.0 (*c* 0.5, MeOH); IR (neat) ν_{max} 3360, 1640 cm^{-1}; ^{1}H and ^{13}C NMR data in Table 5; ESI MS *m*/*z* 533.3756 $[M+H]^{+}$ (calcd for $C_{27}H_{53}N_2O_8$, *m*/*z* 533.3753).

Deinococcucin B (19): Colorless oil; $[\alpha]^{25}_{D}$ -25.0 (*c* 0.5, MeOH); IR (neat) ν_{max} 3280, 1690 cm^{-1}; ^{1}H and ^{13}C NMR data in Table 5; ESI MS *m*/*z* 547.3946 $[M+H]^{+}$ (calcd for $C_{28}H_{55}N_2O_8$, *m*/*z* 547.3943).

Deinococcucin C (20): Colorless oil; $[\alpha]^{25}_{D}$ -17.0 (*c* 0.5, MeOH); IR (neat) ν_{max} 3300, 1630 cm^{-1}; ^{1}H and ^{13}C NMR data in Table 6; ESI MS *m*/*z* 531.3650 $[M+H]^{+}$ (calcd for $C_{27}H_{51}N_2O_8$, *m*/*z* 531.3649).

Deinococcucin D (21): Colorless oil; $[\alpha]^{25}_{D}$ -35.0 (*c* 0.5, MeOH); IR (neat) ν_{max} 3350, 1640 cm^{-1}; ^{1}H and ^{13}C NMR data in Table 6; ESI MS *m*/*z* 545.3750 $[M+H]^{+}$ (calcd for $C_{28}H_{53}N_2O_8$, *m*/*z* 545.3748).

Determination of the Double Bond Position in Deinococcucins C (20) and D (21). 0.5 mg of deinococcucins C (**20**) or D (**21**) was dissolved in a 10:1 mixture of CH_2Cl_2 and methyl acrylate (0.5 mL) to which 50 μg (5 mol%) of 2nd-generation Hoveyda-Grubbs catalyst was subsequently added. The reaction mixture was stirred at room temperature for 2 h and injected into the LC/MS system without any treatment (100 × 4.6 mm Phenomenex C_{18} (2) column, gradient elution from 10 to 100% aqueous acetonitrile with 0.1% formic acid over 20 min and 100% acetonitrile with 0.1% formic acid after 20 min). The metathesis products of **20** and **21** commonly yielded an

$[M+H]^+$ ion at *m/z* 505 at a retention time of 9.2 min in the LC/MS analysis. The double bond positions of **20** and **21** were determined using the previously reported method based on the mass spectrometric data.[72]

Analysis of the Absolute Configuration of *N*-Acetyl Glucosamine in Deinococcucin A (18). Deinococcucin A (3 mg) was dissolved in 3 N HCl (0.5 mL) and stirred at 80 °C for 2 h. After the solution had cooled to rt, the HCl was evaporated *in vacuo* to yield the hydrolysate that contained glucosamine originating from *N*-acetyl glucosamine. HMDS and TMS-Cl (50 μL, v/v = 2:1) were added to the hydrolysate in pyridine (0.5 mL). After being stirred at 60 °C for 30 min, the mixture was dried *in vacuo* and separated using H_2O and CH_2Cl_2 (1 mL, v/v = 1:1). The CH_2Cl_2 layer was injected into a gas chromatograph equipped with an HP5 column (0.32 mm × 30 m). The injector and detector temperatures were maintained at 200 °C. During the analysis, the temperature of the GC column was controlled as follows: 60 °C for 3 min, 60–200 °C at 4 °C/min, and 200 °C for 3 min. The glucosamine derivative from the hydrolysate of **18** was detected at a retention time of 32.77 min. Authentic D-glucosamine and L-glucosamine samples were treated and analyzed using the same procedures. The derivatives of D-glucosamine and L-glucosamine were detected at 32.77 min and 32.85 min, respectively. Co-injection of the silylated derivative of the hydrolysate and authentic D-glucosamine gave a single peak at 32.76 min, thereby determining the absolute configuration of the glucosamine in **18** as the D-form.

Acid Hydrolysis of Deinococcucin A (18). Deinococcucin A (**18**) (5.5 mg) was hydrolyzed in 6 N HCl (0.5 mL) at 40 °C. After 2 h, the reaction vial was cooled in ice water for 3 min. Then, the HCl was removed *in vacuo*, and the dry material was resuspended in 0.5 mL of H_2O and dried three times to completely remove the residual HCl. The reaction mixture was extracted with $CHCl_3$. The $CHCl_3$ layer was chromatographed over normal-phase silica gel (Waters Sep-Pak Vac 6 cc) using a solvent composed of a 30:1 mixture of $CHCl_3$-MeOH to yield the 2,3-dihydroxypropanoic acid (**22**, 2.0 mg).

2,3-Dihydroxypropanoic Acid (22): ^{1}H NMR (600 MHz, DMSO-d_6) δ 9.5 (s, OH), 6.1 (s, OH), 4.9 (s, OH), 4.47 (t, J = 5.0, 1H), 4.04 (dd, J = 12.5, 5.5, 1H) and 3.72 (dd, J = 12.5, 5.5, 1H).

PGME Amide Derivatization of 2,3-Dihydroxypropanoic Acid (22). First, 2 mg of 2,3-dihydroxypropanoic acid (**22**) from deinococcucin A (**18**) was dried under high vacuum for 24 h and dissolved in 500 μL of dimethylformamide (DMF). To the DMF solution of 2,3-dihydroxypropanoic acid (**22**) and *S*- or *R*-PGME were added benzotriazolyloxy-tris[pyrrolidino]-phosphonium hexafluorophosphate (PyBOP) (4.4 mg, 8.4 μmol) and *N*-methylmorpholine (100 μL) at room temperature. After stirring for 1 h, 5% HCl solution and (1 mL) and EtOAc (2 mL) were added to the reaction mixture. The EtOAc layer was washed with saturated $NaHCO_3$ solution and brine. The *S*- or *R*-PGME amide

products ($[M+H]^+$ *m*/*z* 254) were observed in LC/MS analysis (100 × 4.6 mm, 5 μm, Phenomenex C_{18} (2) column; gradient elution from 10 to 100% aqueous acetonitrile with 0.1% formic acid over 20 min). After the reaction mixture was dried, the *S*- and *R*-PGME amide products (**22a** and **22b**) were purified by reserved-phase HPLC (250 × 10 mm, 5 μm, Kromasil C_{18} column; flow rate of 2 mL/min; UV detection at 254 nm; 50-100% aqueous acetonitrile gradient), eluting at retention times of 28 and 30 min, respectively.

(*S*)-PGME Amide of 2,3-Dihydroxypropanoic Acid (22a): ^{1}H NMR (600 MHz, DMSO-d_6) δ 8.58 (s, NH), 7.29-7.24 (m, 5H), 5.63 (s, 1H), 5.11 (s, OH), 4.54 (t, J = 6.5, 1H), 3.95 (dd, J = 12.0, 7.5, 1H), 3.88 (s, OH), 3.73 (s, 3H), and 3.58 (dd, J = 12.0, 7.5, 1H).

(*R*)-PGME Amide of 2,3-Dihydroxypropanoic Acid (22b): ^{1}H NMR (600 MHz, DMSO-d_6) δ 8.60 (s, NH), 7.31-7.26 (m, 5H), 5.61 (s, 1H), 5.22 (s, OH), 4.53 (t, J = 6.5, 1H), 3.90 (dd, J = 12.0, 7.5, 1H), 3.87 (s, OH), 3.71 (s, 3H), and 3.52 (dd, J = 12.0, 7.5, 1H).

QR Assays. The QR activities were determined spectrophotometrically using a previously reported modified microtiter method with murine Hepa-1c1c7 cells.[38] In this assay, 0.1% dimethyl sulfoxide (DMSO) was used as a negative control, and β-naphthoflavone (2 μM) was used as a positive control.

Table 5. ^{1}H and ^{13}C NMR Data for Deinococcucins A (**18**) and B (**19**) in DMSO-d_6[a]

	Deinococcucin A (**18**)		Deinococcucin B (**19**)	
Position	δ_C, type	δ_H, mult (J in Hz)	δ_C, type	δ_H, mult (J in Hz)
1	69.6, CH_2	3.63, m 3.45, m	69.6, CH_2	3.63, m 3.49, m
2	70.8, CH	3.97, dd (5.5, 3.0)	70.8, CH	4.00, dd (5.5, 3.0)
3	171.1, C		171.1, C	
4	38.2, CH_2	3.02, m	38.5, CH_2	3.05, m
5	29.1, CH_2	1.35, m	29.4, CH_2	1.40, m
6	26.1, CH_2	1.22, m	26.4, CH_2	1.23, m
7-16	28.9-28.4, 10CH_2	1.26-1.15, m	28.9-28.3, 10CH_2	1.31-1.19, m
17	31.0, CH_2	1.37, m	28.3, CH_2	1.13, m
18	22.4, CH_2	1.24, m	31.2, CH_2	1.41, m
19	13.9, CH_3	0.85, t (6.5)	22.0, CH_2	1.20, m
20			14.0, CH_3	0.85, t (5.5)
2-OH		5.52, br s		5.50, br s
3-NH		7.76, t (5.5)		7.76, t (5.5)
1′	97.1, CH	4.62, d (3.5)	97.0, CH	4.61, d (3.5)
2′	53.4, CH	3.67, dd (8.5, 3.5)	53.4, CH	3.67, dd (8.5, 3.5)
3′	70.8, CH	3.44, dd (10.0, 8.5)	70.7, CH	3.41, dd (10.0, 8.5)
4′	70.4, CH	3.12, ddd (10.0, 9.0, 2.5)	70.4, CH	3.16, ddd (10.0, 9.0, 2.5)
5′	72.6, CH	3.35, ddd (9.0, 5.0, 2.5)	72.7, CH	3.37, ddd (9.0, 5.0, 2.5)
6′	60.6, CH_2	3.55, m 3.47, m	60.5, CH_2	3.57, m 3.46, m
7′	169.3, C		169.2, C	
8′	22.8, CH_3	1.85, s	22.6, CH_3	1.85, s
2′-NH		7.56, d (8.5)		7.60, d (8.5)
3′-OH		4.78, br s		4.78, br s
4′-OH		5.00, br s		5.00, br s
6′-OH		4.45, dd (12.0, 3.5)		4.45, dd (12.0, 3.5)

[a] ^{1}H and ^{13}C data were recorded at 600 and 125 MHz, respectively.

Table 6. ^{1}H and ^{13}C NMR Data for Deinococcucins C (**20**) and D (**21**) in DMSO-d_6[a]

	Deinococcucin C (**20**)		Deinococcucin D (**21**)	
Position	δ_C, type	δ_H, mult (*J* in Hz)	δ_C, type	δ_H, mult (*J* in Hz)
1	69.6, CH_2	3.63, m	69.6, CH_2	3.62, m
		3.49, m		3.47, m
2	70.8, CH	4.00, dd	70.6, CH	4.00, dd
		(5.5, 3.0)		(5.5, 3.0)
3	171.1, C		171.0, C	
4	38.2, CH_2	3.06, m	38.2, CH_2	3.05, m
5	29.1, CH_2	1.39, m	29.1, CH_2	1.40, m
6	26.1, CH_2	1.22, m	26.1, CH_2	1.22, m
7-10	28.9-28.4, 4CH_2	1.33-1.26, m	28.9-28.4, 4CH_2	1.35-1.25, m
11	28.5, CH_2	1.97, m	28.3, CH_2	1.95, m
12-13	129.0, 2CH	5.33, m	129.6, 2CH	5.32, m
14	28.5, CH_2	1.97, m	28.3, CH_2	1.95, m
15-17	31.0-29.9, 3CH_2	1.33-1.26, m	29.9-29.4, 3CH_2	1.35-1.25, m
18	22.4, CH_2	1.26, m	31.2, CH_2	1.28, m
19	13.9, CH_3	0.85, t (6.5)	22.0, CH_2	1.26, m
20			14.0, CH_3	0.84, t (6.5)
2-OH		5.45, br s		5.50, br s
3-NH		7.73, t (5.5)		7.78, t (5.5)
1′	97.1, CH	4.62, d (3.5)	97.0, CH	4.61, d (3.5)
2′	53.4, CH	3.67, dd	53.4, CH	3.67, dd
		(8.5, 3.5)		(8.5, 3.5)
3′	70.8, CH	3.44, dd	70.7, CH	3.41, dd
		(10.0, 8.5)		(10.0, 8.5)
4′	70.4, CH	3.16, ddd	70.4, CH	3.16, ddd
		(10.0, 9.0, 2.5)		(10.0, 9.0, 2.5)
5′	72.6, CH	3.39, ddd	72.7, CH	3.37, ddd
		(9.0, 5.0, 2.5)		(9.0, 5.0, 2.5)
6′	60.6, CH_2	3.58, m	60.5, CH_2	3.57, m,
		3.47, m		3.46, m
7′	169.3, C		169.2, C	
8′	22.8, CH_3	1.85, s	22.6, CH_3	1.85, s
2′-NH		7.52, d (8.5)		7.60, d (8.5)
3′-OH		4.78, br s		4.78, br s
4′-OH		5.00, br s		5.00, br s
6′-OH		4.45, dd		4.45, dd
		(12.0, 3.5)		(12.0, 3.5)

[a] ^{1}H and ^{13}C data were recorded at 600 and 125 MHz, respectively.

Ⅲ. Conclusion

In our search for new bioactive compounds from marine actinobacteria,[5] I selectively isolated actinomycete strains from marine sediment samples from Suncheon Bay, Republic of Korea. Suncheon Bay is a tideland with high biodiversity that provides habitats for migratory birds, various plants and animals as well as microorganisms.[6] Actinomycete strains from Suncheon Bay sediments were subjected to chemical profiling by LC/MS analysis. Through the profiling process, one of the strains, *Streptomyces* sp. SSC21, was identified to produce a series of compounds, each containing a sulfur atom, based on mass spectroscopic data ($[M+Na]^+$:$[M+2+Na]^+$ ≈ 100:5).[7] This information, along with corresponding UV and mass spectra, suggested that these compounds were unlikely to have been previously reported, thus prompting further chemical analysis. In this paper, I discuss the isolation and identification of the structures of the sulfur-bearing compounds, named suncheonosides A-D (**1**-**4**), and their biological activity with respect to insulin sensitivity.

The secondary metabolite profiles of the 80 actinobacterial strains isolated from the gut of a P. brevitarsis grub were chemically analyzed by LC/MS. This chemical analysis led to the discovery of two new flavonoid-like compounds, which are dominantly found in plants but really uncommon as bacterial metabolites. The epimeric compounds JS8A and B (**6**-**7**) were purified by HPLC using a chiral column (a polysaccharide-based immobilizing cellulose to silica gel). Their structures were determined mainly by spectroscopic analysis of NMR and mass data. The absolute

configurations were established by time-controlled acetylation followed by the application of the modified Mosher's method using MTPA. Moreover, the comparative full genome analysis of the strain JS8 and the producer (CNB-689) of actionflavoside, will be discussed along with their structures.

In our search for new bioactive compounds, I focused on the secondary metabolites of rare actinobacteria, as illustrated by the discovery of a structurally new benzofuran glycoside and indole alkaloids from an *Amycolatopsis* strain isolated from a marine sponge.[8] A continuation of these studies led us to *Actinomadura* strain KC 191 which was seen to inhibit neighboring bacterial colonies on isolation plates seeded with a suspension of an agricultural soil sample. Extracts of strain KC 191 showed significant antibacterial activity against *Bacillus subtilis*, *Staphylococcus aureus, Kocuria rhizophila*, *Proteus hauseri* and *Salmonella enterica* strains (MIC = 0.39 ~ 3.12 μg/mL), prompting the scale-up of the culture. Comprehensive chemical analysis of the resultant extracts led to the identification of a new antibacterial norditerpenoid, actinomadurol (**13**), and its congener, JBIR-65 (**14**), which was previously reported albeit without stereochemical analysis.[25] Here, I report on the structural determination, including the absolute configurations of actinomadurol (**13**) and JBIR-65 (**14)** and their antibiotic activities.

This study focused on the ecosystem of the carpenter ant, *Camponotus japonicus*, which is a dominant ant species in East Asia.[70] I collected

carpenter ants in Seoul Grand Park, Republic of Korea, and isolated bacterial strains from the ant specimens. Chemical analysis of the bacterial metabolites by liquid chromatography-mass spectroscopy (LC/MS) revealed that strain SJN1, which was most closely related to *Deinococcus xinjiangensis* and isolated from the gut of queen specimens, produced a series of previously unreported compounds that were invisible under UV detection but distinctly detected in mass spectra ($[M+H]^+$ ions at *m*/*z* 531~547). Further scaling up the culture of SJN1 and chromatographic isolation of these compounds by HPLC with refractive index (RI) detection resulted in the discovery of four new aminoglycolipids, deinococcucins A-D (**18-21**). Here, I report the structural determination, including the absolute configurations, and the biological activities of deinococcucins A-D (**18-21**), rare metabolites from the genus *Deinococcus*.

References

1. Molinski, T. F.; Dalisay, D. S.; Lievens, S. L.; Saludes, J. P. *Nat. Rev. Drug Disc*. **2009**, *8*, 69-85.
2. (a) Gerwick, W. H.; Moore, B. S. *Chem. Biol*. **2012**, *19*, 85-98. (b) Liu, Y. J. Mar. *Sci. Res. Dev*. **2012**, *2*, e106.
3. Blunt, J. W.; Copp, B. R.; Keyzers, R. A.; Munro, M. H. G.; Prinsep, M. R. *Nat. Prod. Rep*. **2015**, *32*, 116-211.
4. Fenical, W.; Jensen, P. R. *Nat. Chem. Biol*. **2006**, *2*, 666-673.
5. (a) Um, S.; Kim, Y.-J.; Kwon, H.; Wen, H.; Kim, S.-H.; Kwon, H. C.; Park, S.; Shin, J.; Oh, D.-C. *J. Nat. Prod*. **2013**, *76*, 873-879. (b) Bae, M.; Kim, H.; Shin, Y.; Kim, B. Y.; Lee, S. K.; Oh, K.-B.; Shin, J.; Oh, D.-C. *Mar. Drugs* **2013**, *11*, 2882-2893. (c) Ko, K.; Lee, S.-H.; Kim, S.-H.; Kim, E.-H.; Oh, K.-B.; Shin, J.; Oh, D.-C. *J. Nat. Prod*. **2014**, *77*, 2099-2104. (d) Bae, M.; Kim, H.; Moon, K.; Nam, S.-J.; Shin, J.; Oh, K.-B.; Oh, D.-C. *Org. Lett*. **2015**, *17*, 712-715.
6. Kar, D. *Wetlands and Lakes of the World*; Springer India, 2014; p. 465.
7. Pretsch, E.; Bühlmann, P.; Affolter, C. *Structure Determination of Organic Compounds—Tables of Spectral Data*, Springer: New York, USA, 2000.
8. Kwon, Y.; Kim, S.-H.; Shin, Y.; Bae, M.; Kim, B.-Y.; Lee, S. K.; Oh, K.-B.; Shin, J.; Oh, D.-C. *Mar. Drugs* **2014**, *12*, 2326-2340.

9. Liao, L.; Won, T. H.; Kim, Y. H.; Shin, J. *J. Sep. Sci*. **2014**, *37*, 505-514.
10. (a) Tahara, M.; Okabe, T.; Furihata, K.; Tanaka, N.; Yamaguchi, H.; Nishimura, T.; Suzuki, H. *J. Antibiot*. **1990**, *43*, 135-137. (b) Tahara, M.; Okabe, T.; Furihata, K.; Tanaka, N.; Yamaguchi, H.; Nishimura, T.; Suzuki, H. *J. Antibiot*. **1991**, *44*, 255.
11. Lee, M. D.; Manning, J. K.; Williams, D. R.; Kuck, N. A.; Testa, R. T.; Borders, D. B. *J. Antibiot*. **1989**, *42*, 1070-1087.
12. Mahyudin, N. A.; Blunt, J. W.; Cole, A. L. J.; Munro, M. H. G. *J. Biomed. Biotech*. **2012**, *2012*, 894708.
13. Soman, A. G.; Gloer, J. B.; Wicklow, D. T. *J. Nat. Prod*. **1999**, *62*, 386-388.
14. Lindquist, N.; Fenical, W. *Tetrahedron Lett*. **1990**, *31*, 2389-2392.
15. Shin, D. W.; Kim, S. N.; Lee, S. M.; Lee, W.; Song, M. J.; Park, S. M.; Lee, T. R.; Baik, J.-H.; Kim, H. K.; Hong, J.-H.; Noh, M. *Biochem. Pharmacol*. **2009**, *77*, 125-133.
16. Fischbach, M. A.; Walsh, C. T. *Science* **2009**, *325*, 1089-1093.
17. Baltz, R. H. *Curr. Opin. Pharmacol*. **2008**, *8*, 557-563.
18. Bérdy, J. *J. Antibiot*. **2012**, *65*, 385-395.
19. Tiwari, K.; Gupta, R. K. *Crit. Rev. Biotechnol*. **2012**, *32*, 108-132.
20. Kibwage, I. O.; Janssen, G.; Busson, R.; Hoogmartens, J.; Vanderhaeghe, H.; Verbist, L. *J. Antibiot*. **1987**, *40*, 1-6.
21. McCormick, M. H.; Stark, W. M.; Pittenger, G. E.; Mcguire, J. M.

Antibiot. Ann. **1956**, *3*, 606-611.

22. Jensen, P. R.; Moore, B. S.; Fenical, W. *Nat. Prod. Rep*. **2015**, *32*, 738-751.
23. Wang, Q.; Song, F.; Xiao, X.; Huang, P.; Li, L.; Monte, A.; Abdel-Mageed, W. M.; Wang, J.; Guo, H.; He, W.; Xie, F.; Dai, H.; Liu, M.; Chen, C.; Xu, H.; Liu, M.; Piggott, A. M.; Liu, X.; Capon, R. J.; Zhang, L. *Angew. Chem., Int. Ed*. **2013**, *52*, 1231-1234.
24. Takagi, M.; Motohashi, K.; Khan, S. T.; Hashimoto, J.; Shin-ya, K. *J. Antibiot*. **2010**, *63*, 401-403.
25. Seco, J. M.; Quinoa, E.; Riguera, R. *Tetrahedron: Asymmetry* **2001**, *12*, 2915-2925.
26. Berova, N.; Bari, L. D.; Pescitelli, G. *Chem. Soc. Rev*. **2007**, *36*, 914-931.
27. Lorenz, M. C.; Fink, G. R. *Nature* **2001**, *412*, 83-86.
28. (a) Atzom, R.; Crozier, A.; Wheeler, C.; Sandberg, G. *Planta* **1988**, *175*, 532-538. (b) Bottini, R.; Cassan, F.; Piccoli, P. *Appl. Microbiol. Biotechnol*. **2004**, *65*, 497-503.
29. Smanski, M. J.; Peterson, R. M.; Huang, S.-X.; Shen, B. *Curr. Opin. Chem. Biol*. **2012**, *16*, 132-141.
30. (a) Komaki, H.; Tanaka, Y.; Yazawa, K.; Takagi, H.; Ando, A.; Nagata, Y.; Mikami, Y. *J. Antibiot*. **2000**, *53*, 75-77. (b) Komatsu, K.; Tsuda, M.; Shiro, M.; Tanaka, Y.; Mikami, Y.; Kobayashi, *J. Bioorg. Med. Chem*. **2004**, *12*, 5545-5551. (c) Usui, T.; Nagumo, Y.;

Watanabe, A.; Kubota, T.; Komatsu, K.; Kobayashi, J.; Osada, H. *Chem. Biol*. **2006**, *13*, 1153-1160.

31. Mann, F. M.; Xu, M.; Chen, X.; Fulton, D. B.; Russell, D. G.; Peters, R. J. *J. Am. Chem. Soc*. **2009**, *131*, 17526-17527.
32. Shirai, M.; Okuda, M.; Motohashi, K.; Imoto, M.; Furihata, K.; Matsuo, Y.; Katsuta, A.; Shizuri, Y.; Seto, H. *J. Antibiot*. **2010**, *63*, 245-250.
33. Singh, S. B.; Jayasuriya, H.; Ondeyka, J. G.; Herath, K. B.; Zhang, C.; Zink, D. L.; Tsou, N. N.; Ball, R. G.; Basilio, A.; Genilloud, O.; Diez, M. T.; Vicente, F.; Pelaez, F.; Young, K.; Wang, J. *J. Am. Chem. Soc*. **2006**, *128*, 11916-11920.
34. Jayasuriya, H.; Herath, K. B.; Zhang, C.; Zink, D. L.; Basilio, A.; Genilloud, O.; Diez, M. T.; Vicente, F.; Gonzalez, I.; Salazar, O.; Pelaez, F.; Cummings, R.; Ha, S.; Wang, J.; Singh, S. B. *Angew. Chem., Int. Ed*. **2007**, *46*, 4684-4688.
35. Küster, E.; Williams, S. T. *Nature* **1964**, *30*, 928-929.
36. Shirling, E. B.; Gottlieb, D. *Int. J. Syst. Bacteriol*. **1966**, *16*, 313-340.
37. Kim, B.-Y.; Zucchi, T. D.; Fiedler, H.-P.; Goodfellow, M. *Int. J. Syst. Evol. Microbiol*. **2012**, *62*, 966-970.
38. Tamura, K.; Peterson, D.; Peterson, N.; Stecher, G.; Nei, M.; Kumar, S. *Mol. Biol. Evol*. **2011**, *28*, 2731-2739.
39. Saitou, N.; Nei, M. *Mol. Biol. Evol*. **1987**, *4*, 406-425.

40. Felsenstein, J. *J. Mol. Evol*. **1981**, *17*, 368-376.

41. Fitch, W. M. *Syst. Zool*. **1971**, *20*, 406-416.

42. Jukes, T. H.; Cantor, C. R. *Evolution of protein molecules: In Mammalian Protein Metabolism*; Academic Press: New York, 1969; p. 21-132.

43. Felsenstein, *J. Evolution* **1985**, *39*, 783-791.

44. Ramadhar, T. R.; Beemelmanns, C.; Currie, C. R.; Clardy, J. *J. Antibiot*. **2014**, *67*, 53-58.

45. Dossey, A. T. *Nat. Prod. Rep*. **2010**, *27*, 1737-1757.

46. Choi, H.; Oh, D.-C. *Arch. Pharm. Res*. **2015**, *38*, 1591-1605.

47. Novotny, V.; Basset, Y.; Miller, S. E.; Weiblen, G. D.; Bremer, B.; Cizek, L.; Drozd, P. *Nature* **2002**, *416*, 841-844.

48. Scott, J. J.; Oh, D.-C.; Yuceer, M. C.; Klepzig, K. D.; Clardy, J.; Currie, C. R. *Science* **2008**, *322*, 63.

49. Oh, D.-C.; Scott, J. J.; Currie, C. R.; Clardy, J. *Org. Lett*. **2009**, *11*, 633-636.

50. Blodgett, J. A. V.; Oh, D.-C.; Cao, S.; Currie, C. R.; Clardy, J. *Prod. Natl. Acad. Sci. U.S.A.* **2010**, *107*, 11692-11697.

51. Um, S.; Bach, D.-H.; Shin, B.; Ahn, C.-H.; Kim, S.-H.; Bang, H.-S.; Oh, K.-B.; Lee, S. K.; Shin, J.; Oh, D.-C. *Org. Lett*. **2016**, *18*, 5792-5795.

52. Um, S.; Park, S. H.; Kim, J.; Park, H. J.; Ko, K.; Bang, H.-S.; Lee, S. K.; Shin, J.; Oh, D.-C. *Org. Lett*. **2015**, *17*, 1272-1275.

53. Kim, S.-H.; Ko, H.; Bang, H.-S.; Park, S.-H.; Kim, D.-G.; Kwon, H. C.; Kim, S. Y.; Shin, J.; Oh, D.-C. *Bioorg. Med. Chem. Lett*. **2011**, *21*, 5715-5718.

54. Kim, S.-H.; Kwon, S. H.; Park, S.-H.; Lee, J. K.; Bang, H.-S.; Nam, S.-J.; Kwon, H. C.; Shin, J.; Oh, D.-C. *Org. Lett*. **2013**, *15*, 1834-1837.

55. Kim, K. H.; Ramadhar, T. R.; Beemelmanns, C.; Cao, S.; Poulsen, M.; Currie, C. R.; Clardy, J. *Chem. Sci*. **2014**, *5*, 4333-4338.

56. Beemelmanns, C.; Ramadhar, T. R.; Kim, K. H.; Klassen, J. L.; Cao, S.; Wyche T. P.; Hou, Y.; Poulsen, M.; Bugni, T. S.; Currie, C. R.; Clardy, J. *Org. Lett*. **2017**, *19*, 1000-1003.

57. Um, S.; Fraimout, A.; Sapountzis, P.; Oh, D.-C.; Poulsen, M. *Sci. Rep*. **2013**, *3*, 3250.

58. Zhang, Y.-L.; Ge, H. M.; Zhao, W.; Dong, H.; Xu, Q.; Li, S. H.; Li, J.; Zhang, J.; Song, Y. C.; Tan, R. X. *Angew. Chem. Int. Ed*. **2008**, *47*, 5823-5826.

59. Guo, Z. K.; Liu, S. B.; Jiao, R. H.; Wang, T.; Tan, R. X.; Ge, H. M. *Bioorg. Med. Chem. Lett*. **2012**, *22*, 7490-7493.

60. Guo, Z. K.; Zhang, G. F.; Jiao, R. H.; Shen, Yan.; Xu, Q.; Tan, R. X.; Ge, H. M. *Planta Med*. **2012**, *78*, 988-994.

61. Oh, D.-C.; Poulsen, M.; Currie, C. R.; Clardy, J. *Nat. Chem. Biol*. **2009**, *5*, 391-393.

62. Sit, C. S.; Ruzzini, A. C.; Van Arnam, E. B.; Ramadhar, T. R.;

Currie, C. R.; Clardy, J. *Prod. Natl. Acad. Sci. U.S.A*. **2015**, *112*, 13150-13154.

63. Oh, D.-C.; Poulsen, M.; Currie, C. R.; Clardy, J. *Org. Lett*. **2011**, *13*, 752-755.
64. Poulsen, M.; Oh, D.-C.; Clardy, J.; Currie, C. R. *PLoS One* **2011**, *6*, e16763.
65. Kaltenpoth, M.; Gottler, W.; Herzner, G.; Strohm, E. *Curr. Biol*. **2005**, *15*, 475-479.
66. Kroiss, J.; Kaltenpoth, M.; Schneider, B.; Schwinger, M.-G.; Hertweck, C.; Maddula, R. K.; Strohm, E.; Svatos, A. *Nat. Chem. Biol*. **2010**, *6*, 261-263.
67. Mayhew, P. J. *Biol. Rev. Camb. Philos. Soc*. **2007**, *82*, 425-454.
68. Johnson, B. R.; Borowiec, M. L.; Chiu, J. C.; Lee, E. K.; Atallah, J.; Ward, P. S. *Curr. Biol*. **2013**, *23*, 1-5.
69. Zientz, E.; Feldhaar, H.; Stoll, S.; Gross, R. *Arch. Microbiol*. **2005**, *184*, 199-206.
70. Kwon, Y.; Lee, S.; Oh, D.-C.; Kim, S. *Angew. Chem. Int. Ed*. **2011**, *50*, 8275-8278.
71. Stothers, J. B. *Carbon-13 NMR Spectroscopy*, Academic Press; New York, USA, 1972.
72. Kim, S. Y.; Choi, Y. -H.; Huh, H.; Kim, J.; Kim, Y. C.; Lee, H. S. *J. Nat. Prod*. **1997**, *60*, 274-276.
73. Moon, K.; Ahn, C.-H.; Shin, Y.; Won, T. H.; Ko, K.; Lee, S. K.; Oh,

K.-B.; Shin, J.; Nam, S.-I.; Oh, D.-C. *Mar. Drugs* **2014**, *12*, 2526-2538.

74. Yabuuchi, T.; Kusumi, T. *J. Org. Chem*. **2000**, *65*, 397-404.
75. Cuendet, M.; Oteham, C. P.; Moon, R. C.; Pezzuto, J. M. *J. Nat. Prod*. **2006**, *69*, 460-463.
76. Ross, D.; Kepa, J. K.; Winski, S. L.; Beall, H. D.; Anwar, A.; Siegel, D. *Chem.-Biol. Interact*. **2000**, *129*, 77-97.
77. Lemee, L.; Peuchant, E.; Clerc, M.; Brunner, M.; Pfander, H. *Tetrahedron* **1997**, *53*, 919-926.
78. Anderson, R.; Hansen, K. *J. Biol. Chem*. **1985**, *260*, 12219-12223.
79. Huang, Y.; Anderson, R. *J. Biol. Chem*. **1989**, *264*, 18667-18672.
80. Park, H. J.; Lee, Y. W.; Park, H. H.; Lee, Y. S.; Kwon, I. B.; Yu, J. H. *Eur. J. Cancer Prev*. **1998**, *7*, 465-471.

APPENDIX A:

NMR Spectroscopic Data

List of Figures

Figure S21. ^{1}H NMR spectrum (600 MHz) of acetate (**15**) of JBIR-65 (**14**).

Figure S22. ^{1}H NMR spectrum (600 MHz) of *S*-MTPA ester (**16**) for JBIR-65 (**14**).

Figure S23. ^{1}H NMR spectrum (600 MHz) of *R*-MTPA ester (**17**) for JBIR-65 (**14).**

Figure S24. ^{1}H NMR spectrum (600 MHz) of deinococcucin A (**18**).

Figure S25. ^{13}C NMR spectrum (150 MHz) of deinococcucin A (**18**).

Figure S26. ^{1}H NMR spectrum (600 MHz) of deinococcucin B (**19**).

Figure S27. ^{13}C NMR spectrum (150 MHz) of deinococcucin B (**19**).

Figure S28. ^{1}H NMR spectrum (600 MHz) of deinococcucin C (**20**).

Figure S29. ^{13}C NMR spectrum (150 MHz) of deinococcucin C (**20**).

Figure S30. ^{1}H NMR spectrum (600 MHz) of deinococcucin D (**21**).

Figure S31. ^{13}C NMR spectrum (150 MHz) of deinococcucin D (**21**).

Figure S32. ^{1}H NMR spectrum (600 MHz) of 2,3-dihydroxy-propanoic acid (**22**)**.**

Figure S33. ^{1}H NMR spectrum (600 MHz) of (*S*)-PGME amide (**22a**) of 2,3-dihydroxy-propanoic acid (**22**).

Figure S34. ^{1}H NMR spectrum (600 MHz) of (*R*)-PGME amide (**22b**) of 2,3-dihydroxy-propanoic acid (**22)**.

Figure S1. [1]H NMR spectrum (600 MHz) of suncheonoside A (**1**) in pyridine-d_5.

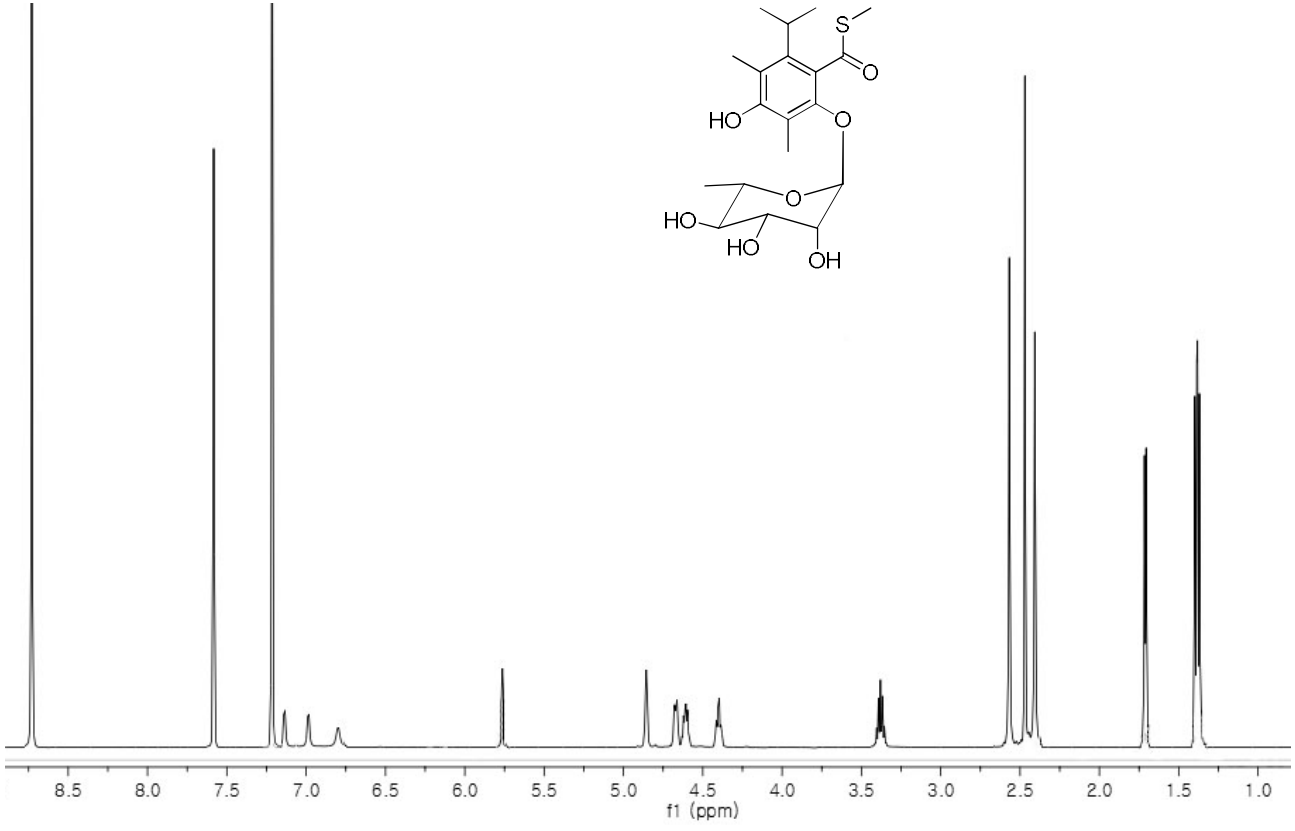

Figure S2. ^{13}C NMR spectrum (150 MHz) of suncheonoside A (**1**) in pyridine-d_5.

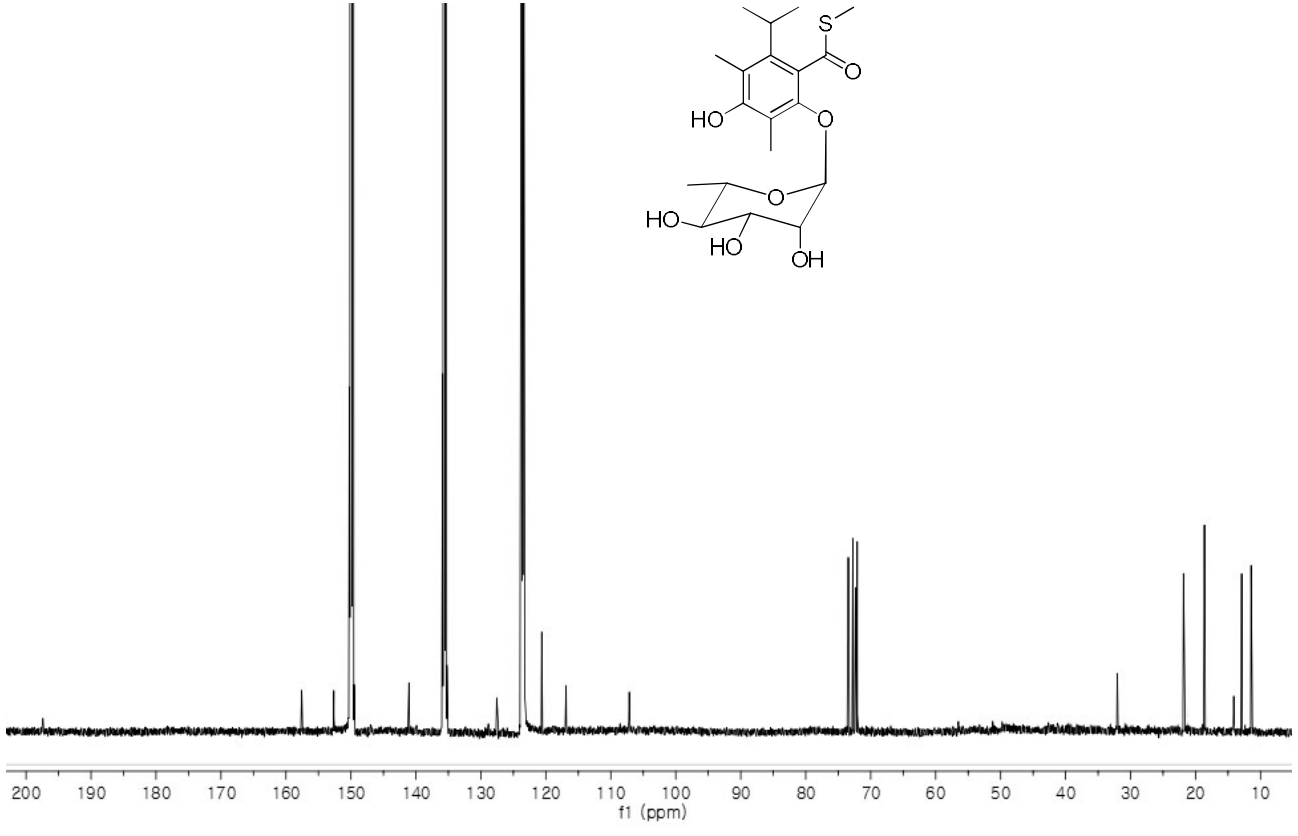

Figure S3. ^{1}H NMR spectrum (600 MHz) of suncheonoside B (**2**) in pyridine-d_5

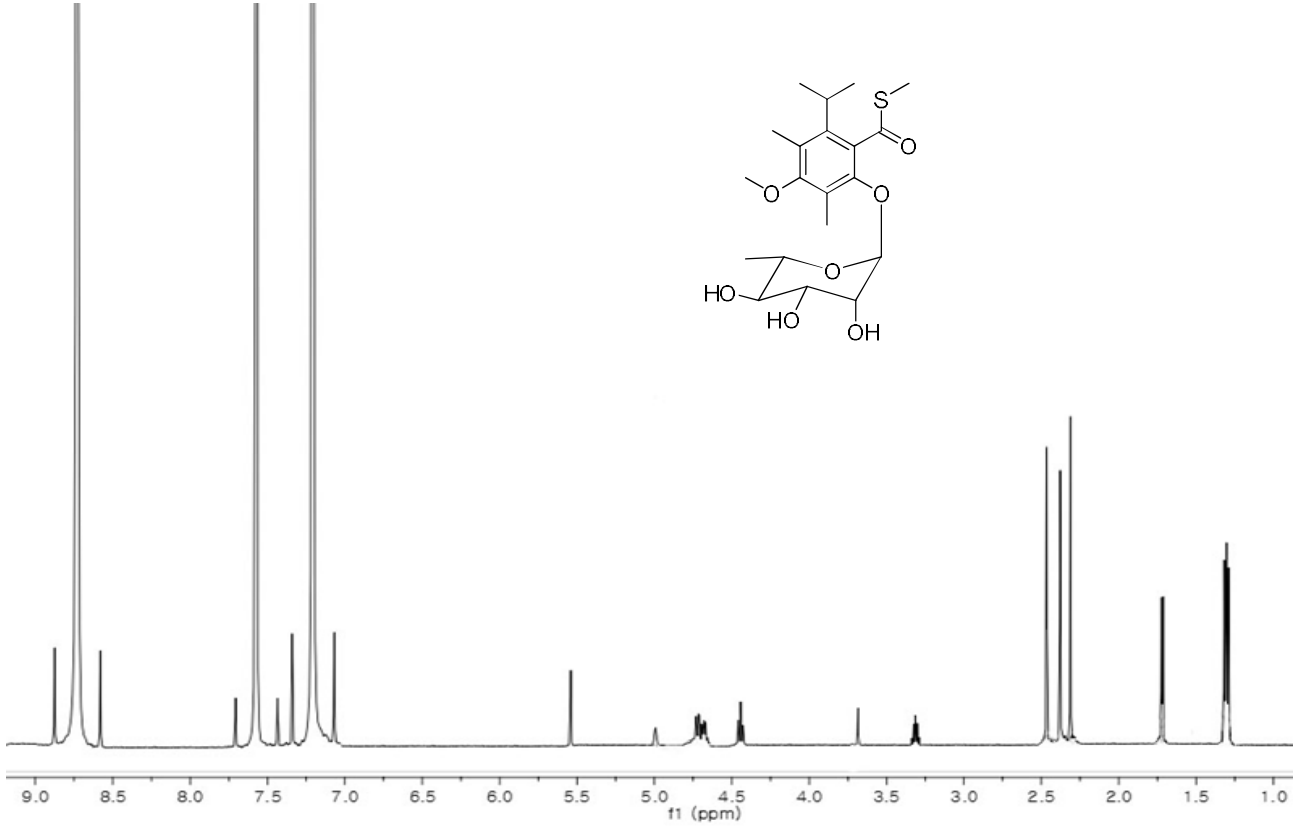

Figure S4. ^{13}C NMR spectrum (150 MHz) of suncheonoside B (**2**) in pyridine-d_5.

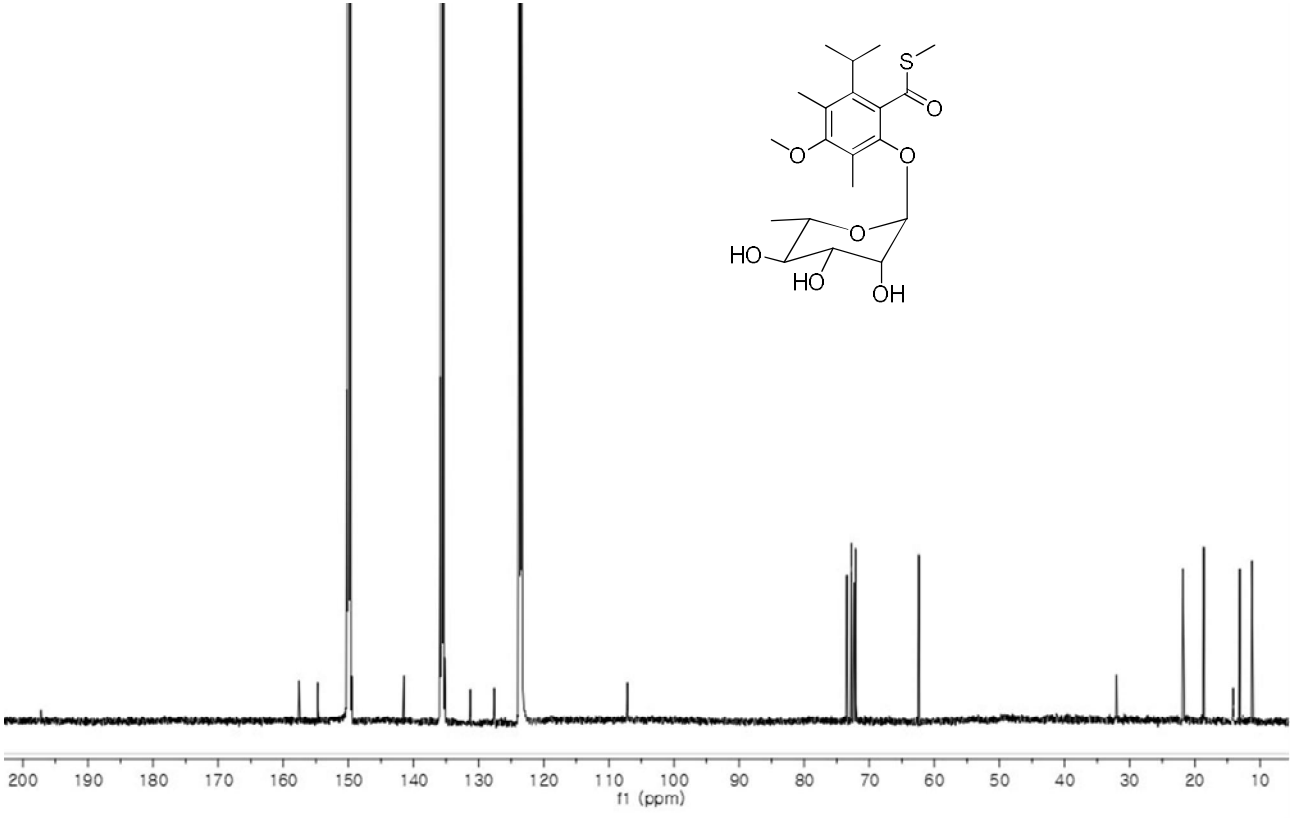

Figure S5. ^{1}H NMR spectrum (600 MHz) of suncheonoside C (**3**) in pyridine-d_5.

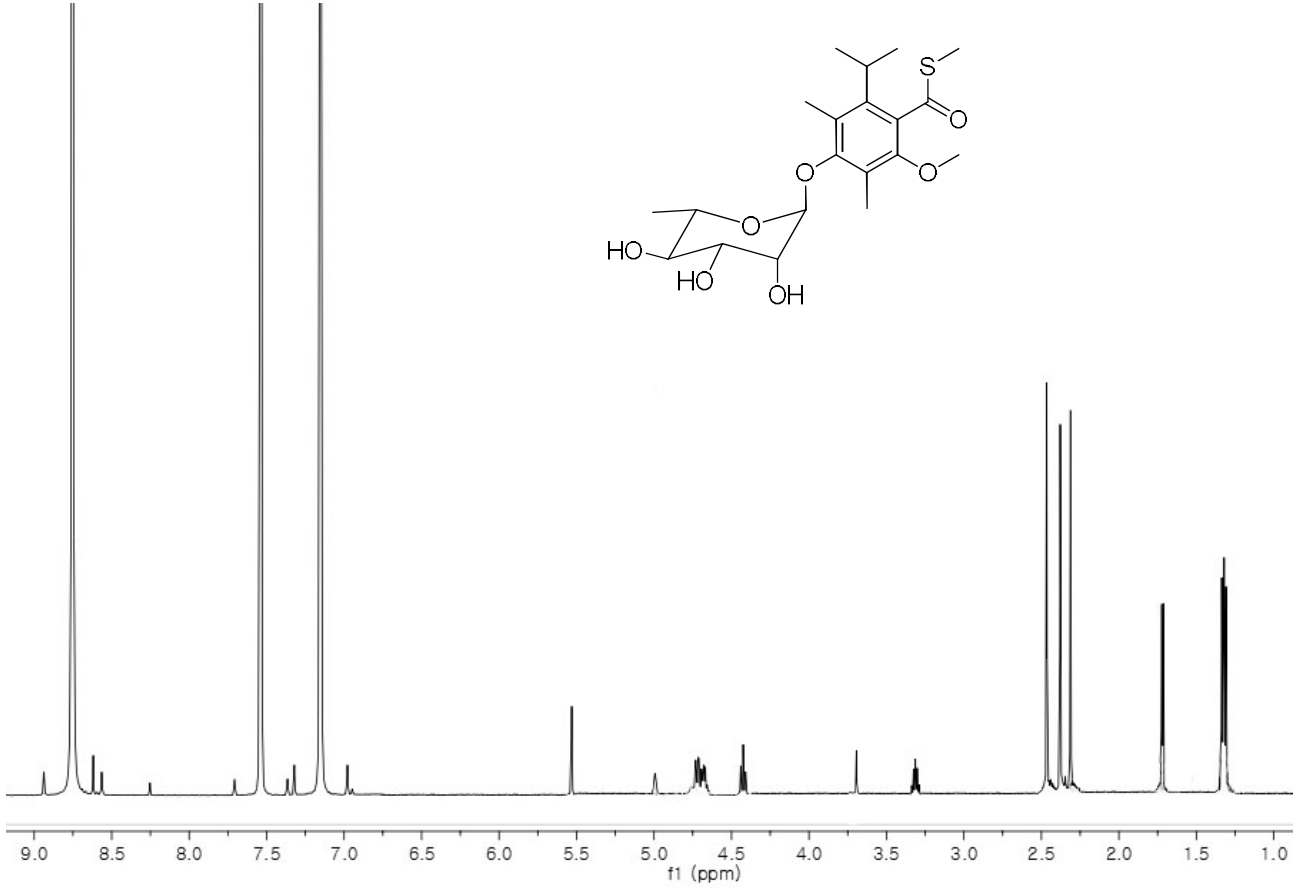

Figure S6. ^{13}C NMR spectrum (150 MHz) of suncheonoside C (**3**) in pyridine-d_5.

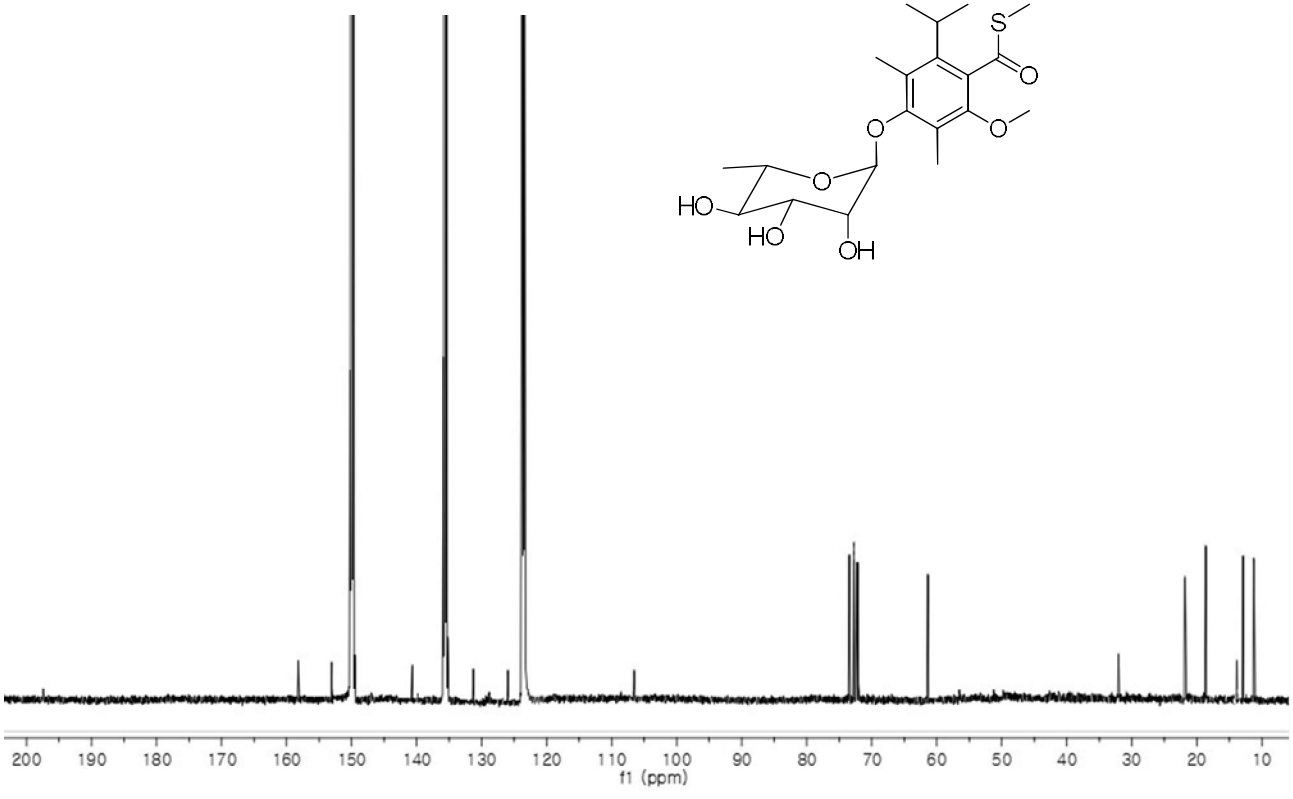

Figure S7. ^{1}H NMR spectrum (600 MHz) of suncheonoside D (**4**) in pyridine-d_5.

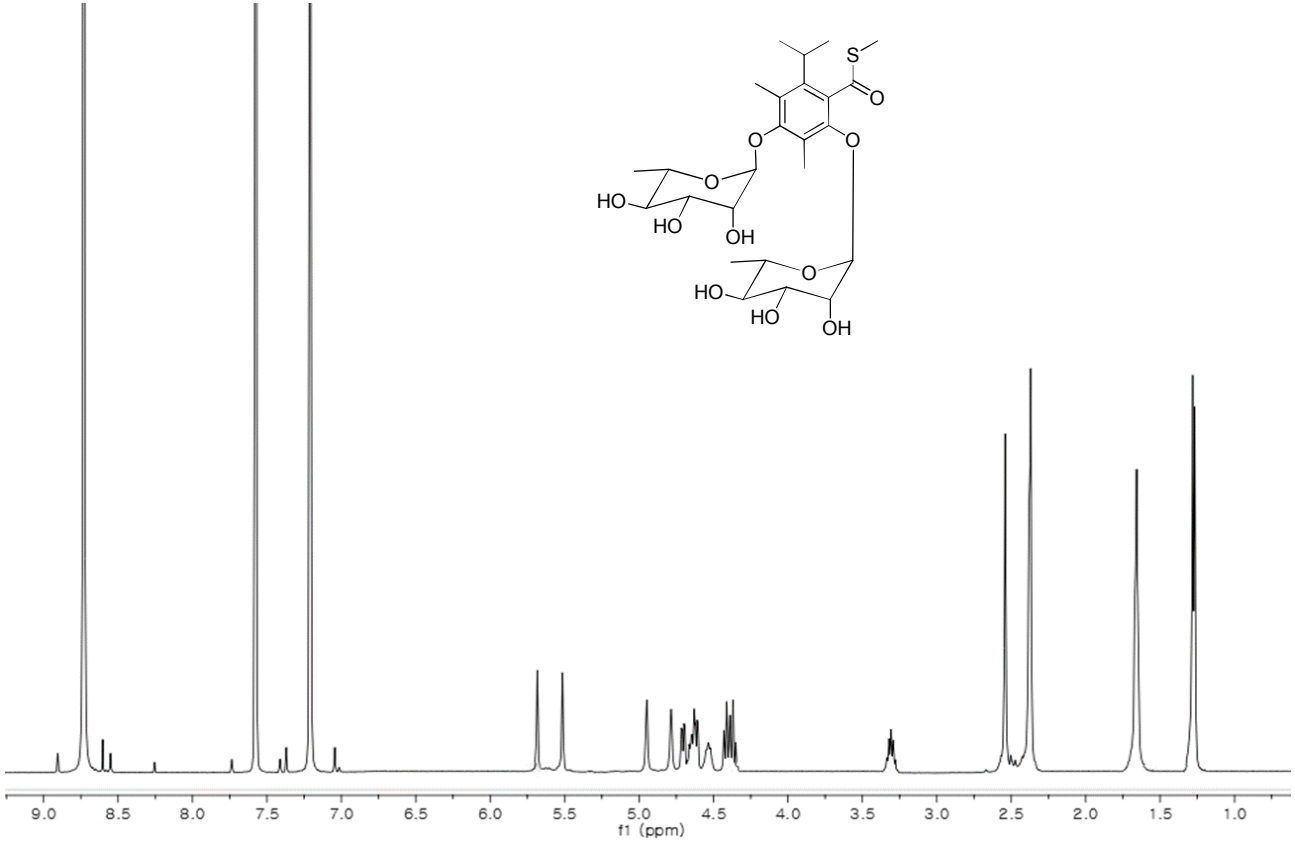

Figure S8. ^{13}C NMR spectrum (150 MHz) of suncheonoside D (**4**) in pyridine-d_5.

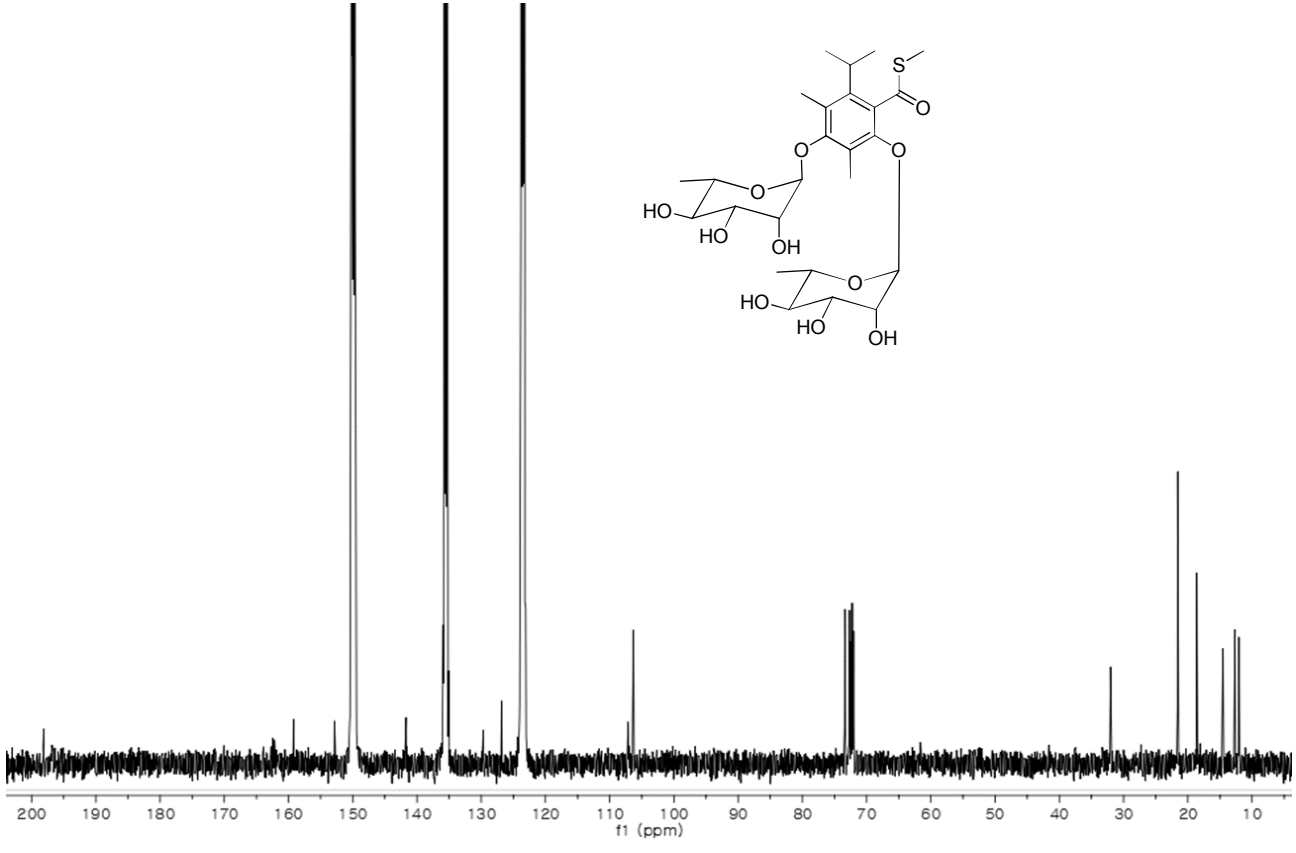

Figure S9. ^{1}H NMR spectrum (600 MHz) of enzymatic hydrolysis (**5**) in pyridine-d_5.

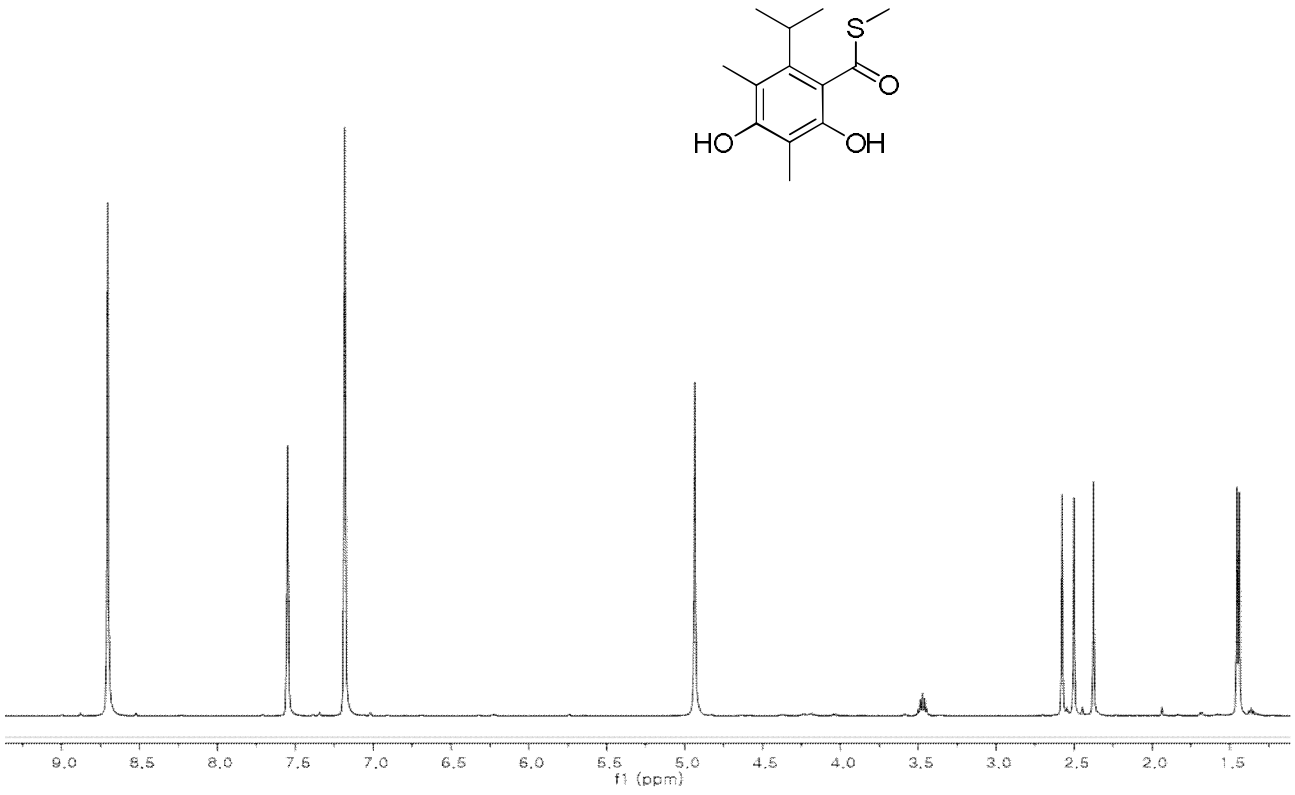

Figure S10. ^{1}H NMR spectrum (850 MHz) of JS8 A (**6**) in DMSO-d_6.

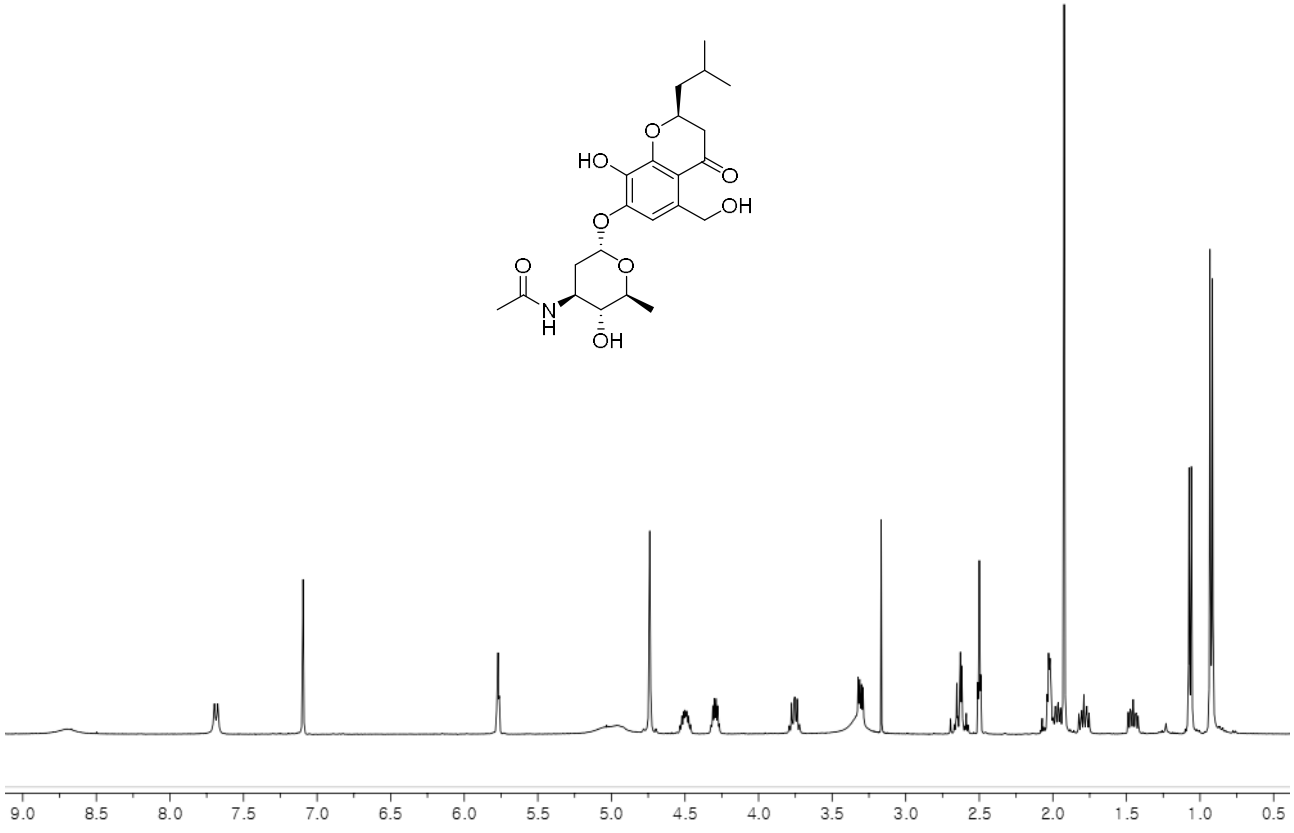

Figure S11. ^{13}C NMR spectrum (212.5 MHz) of JS8 A (**6**) in DMSO-d_6.

.

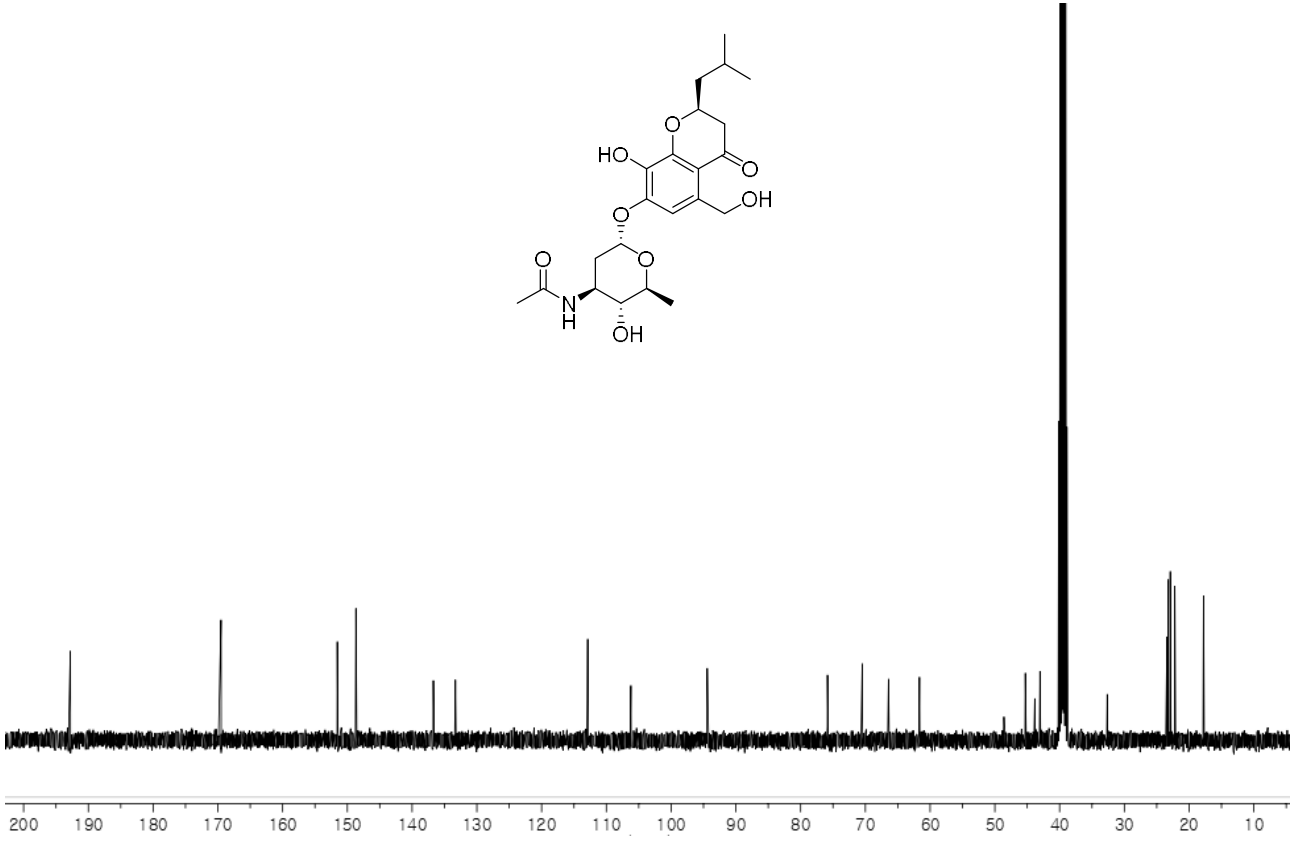

Figure S12. ^{1}H NMR spectrum (850 MHz) of JS8 B (**7**) in DMSO-d_6.

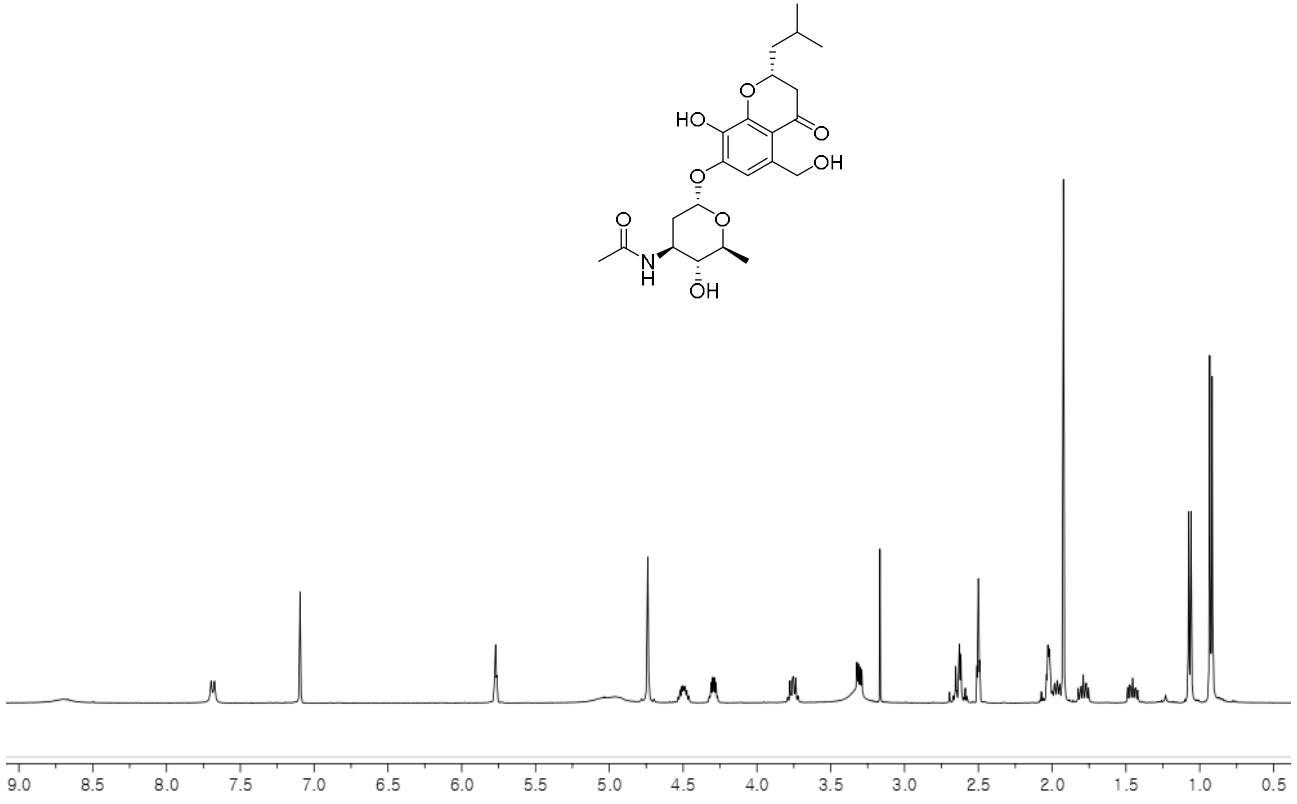

Figure S13. ^{13}C NMR spectrum (212.5 MHz) of JS8 B (**7**) in DMSO-d_6.

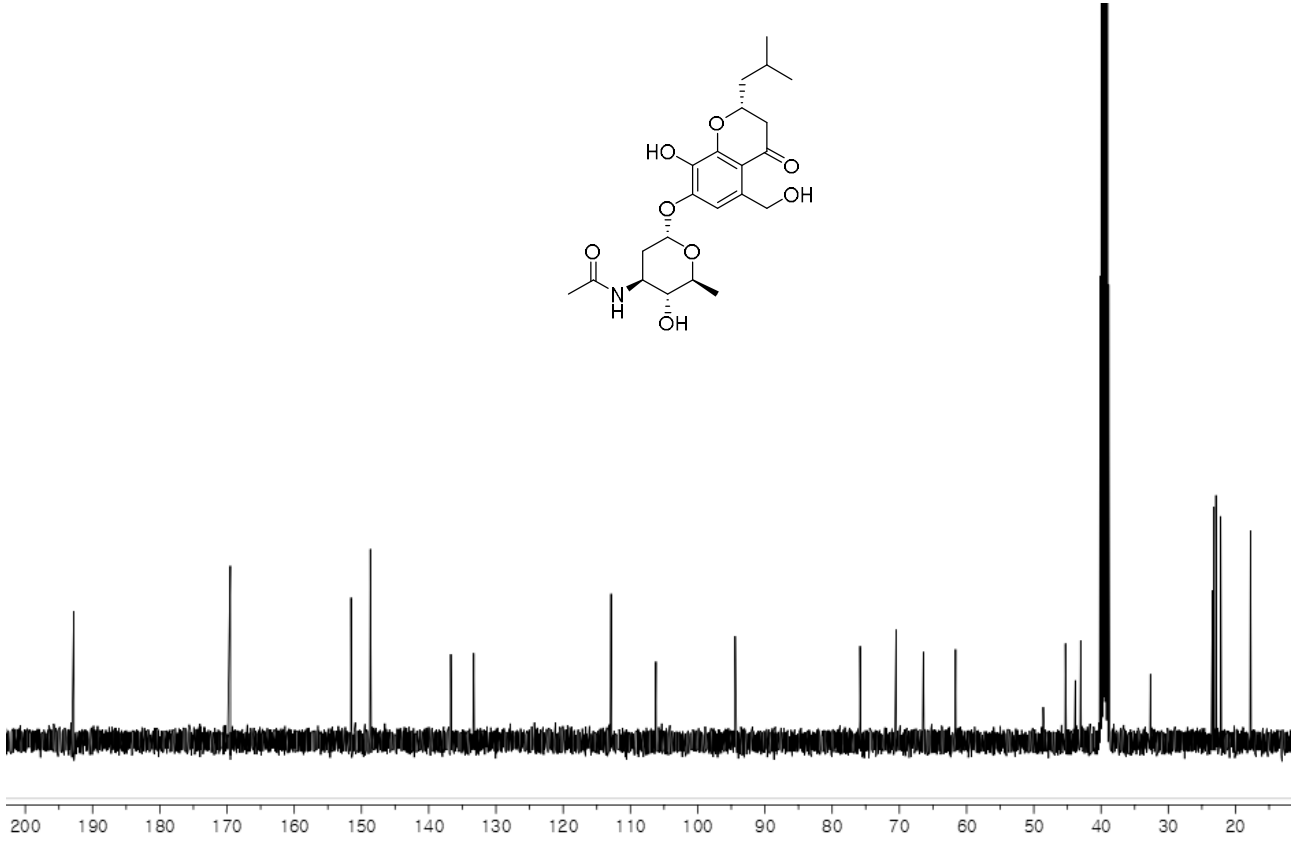

Figure S14. ^{13}C NMR spectrum (212.5 MHz) of JS8 A (**6**) labeled with [2-^{13}C]sodium acetate.

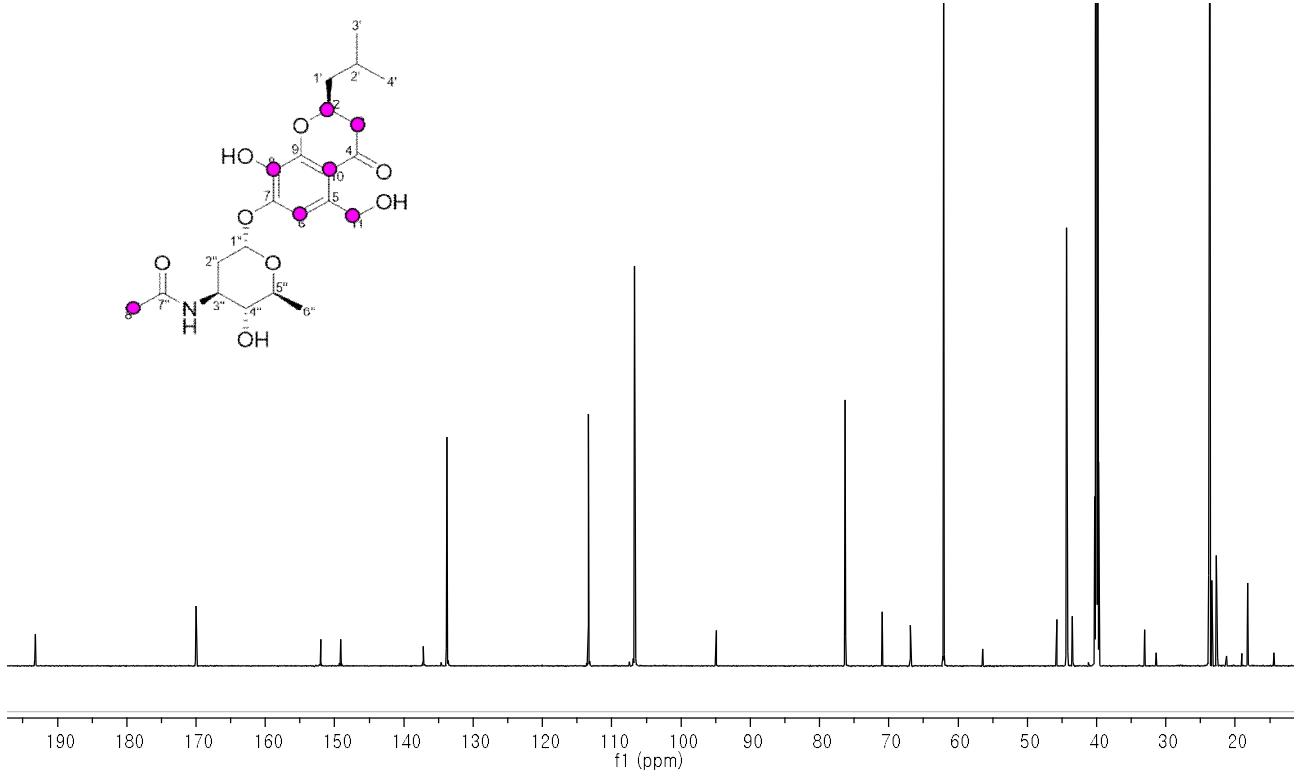

Figure S15. ^{13}C NMR spectrum (212.5 MHz) of JS8 A (**6**) with labeled [1-^{13}C]sodium acetate.

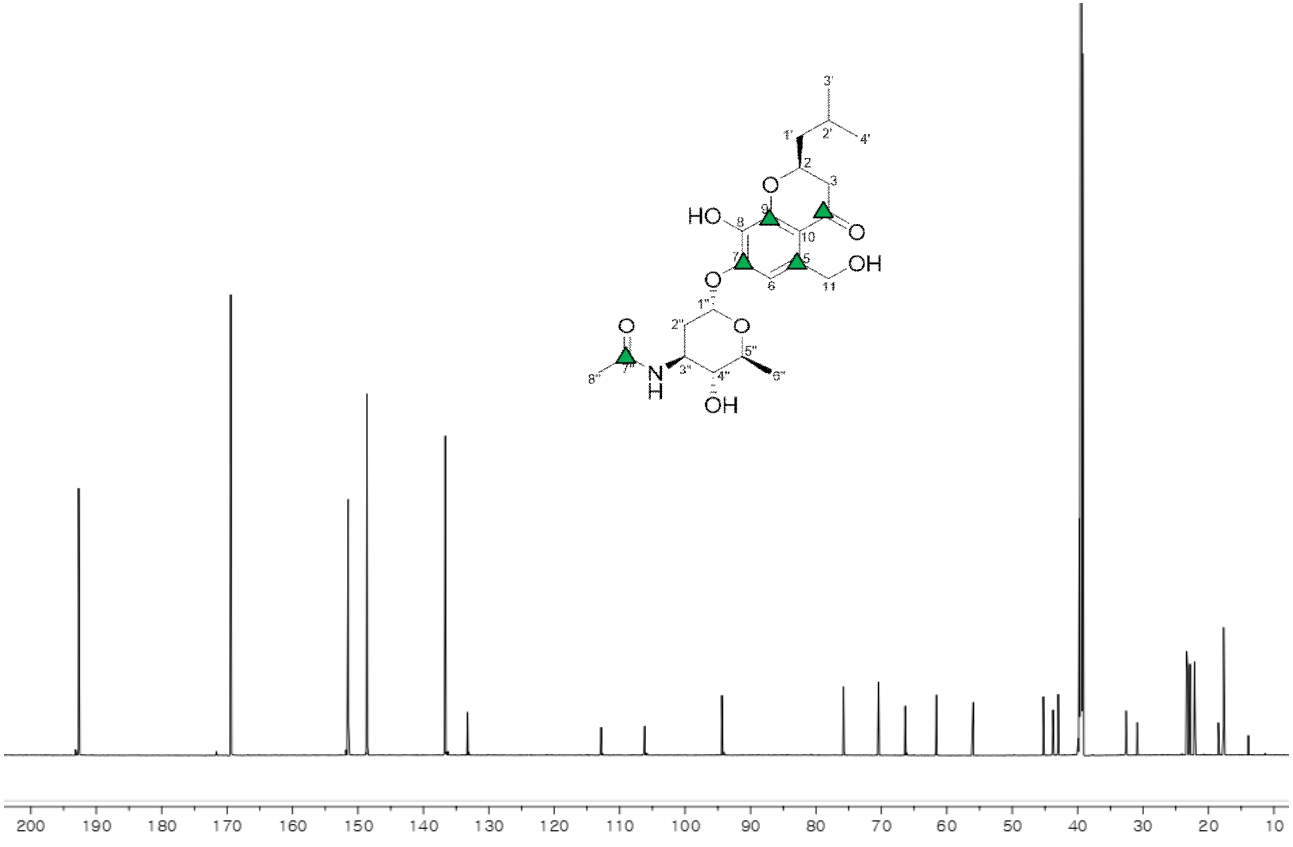

Figure S16. ^{1}H NMR spectrum (900 MHz) of actinomadurol (**13**) in CD_3OD.

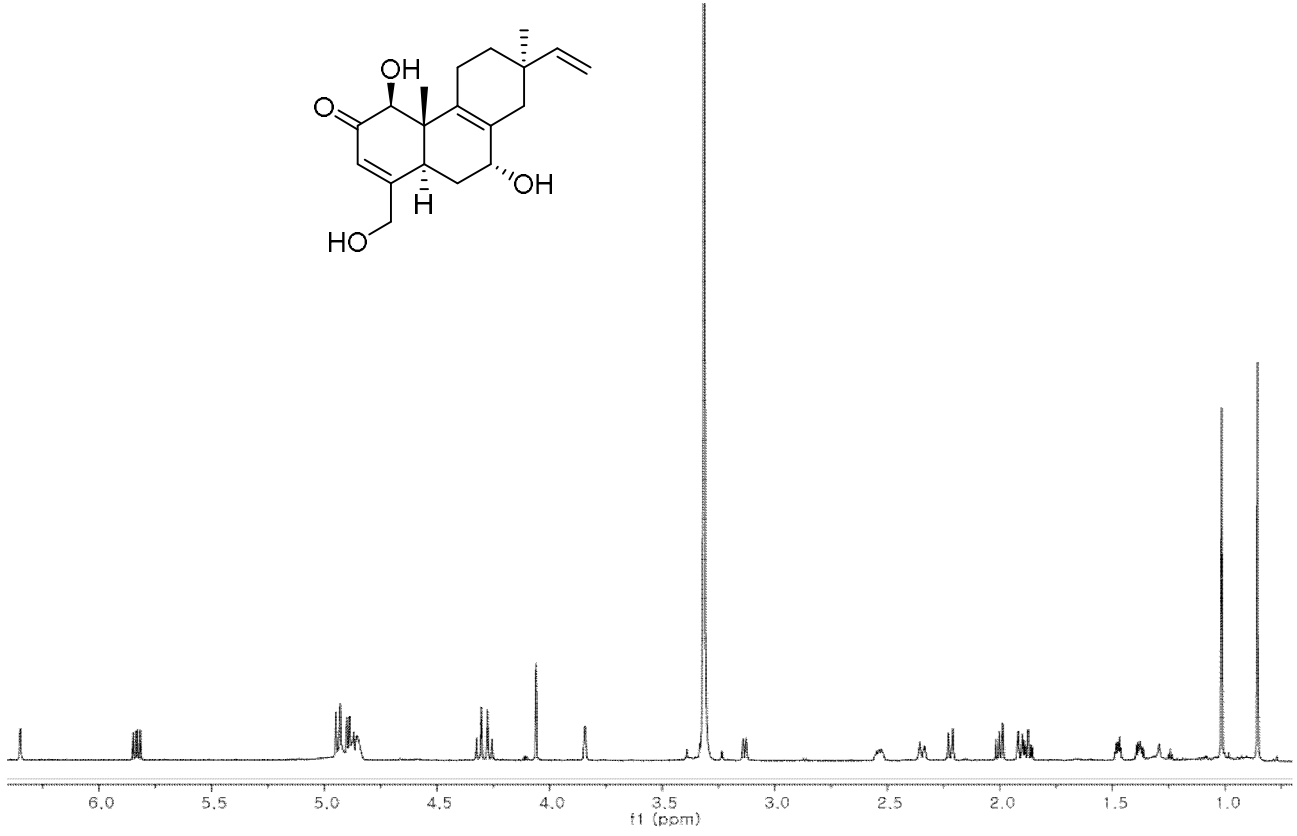

Figure S17. ^{13}C NMR spectrum (225 MHz) of actinomadurol (**13**) in CD_3OD.

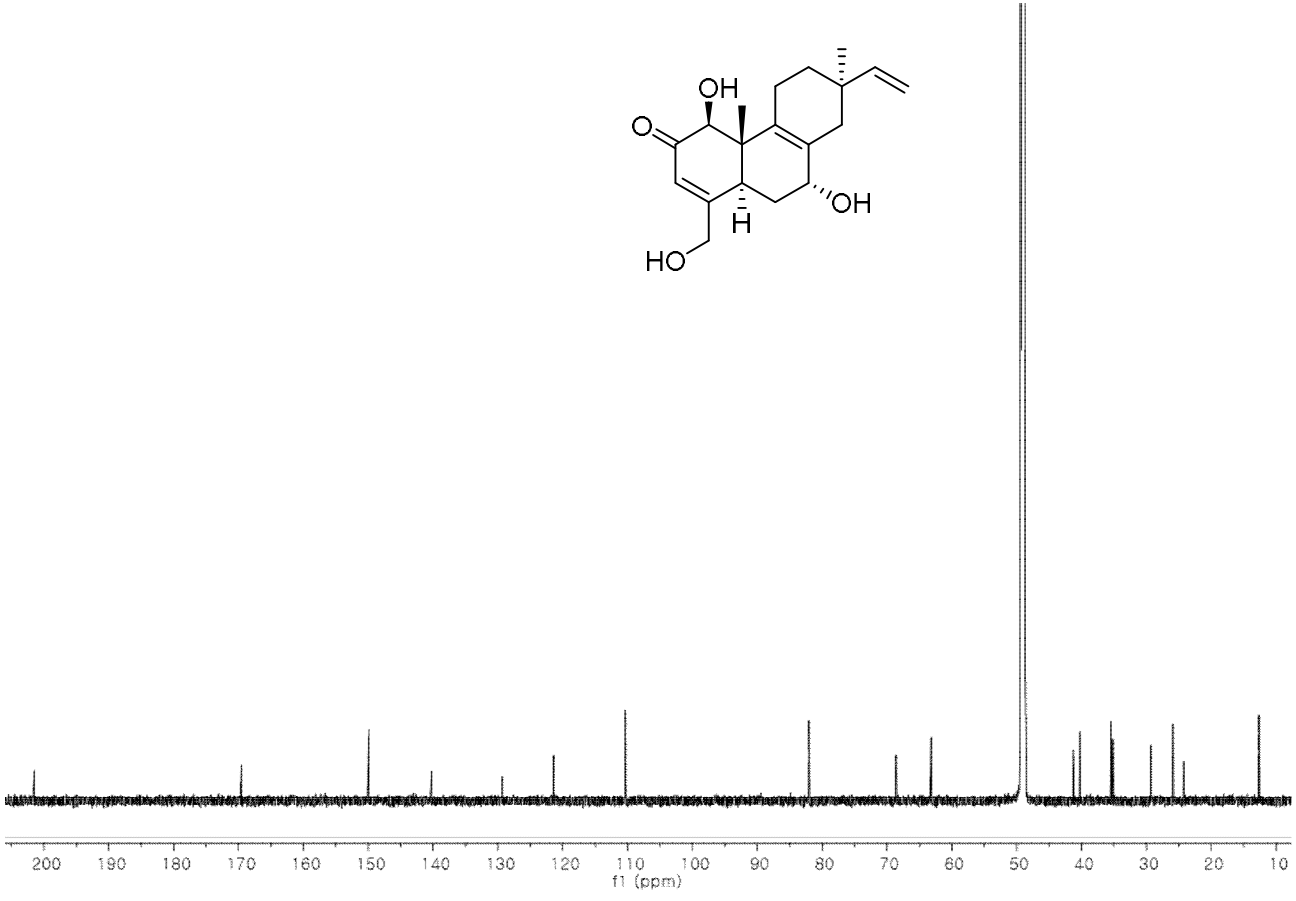

Figure S18. DEPT NMR spectrum (225 MHz) of actinomadurol (**13**) in CD_3OD.

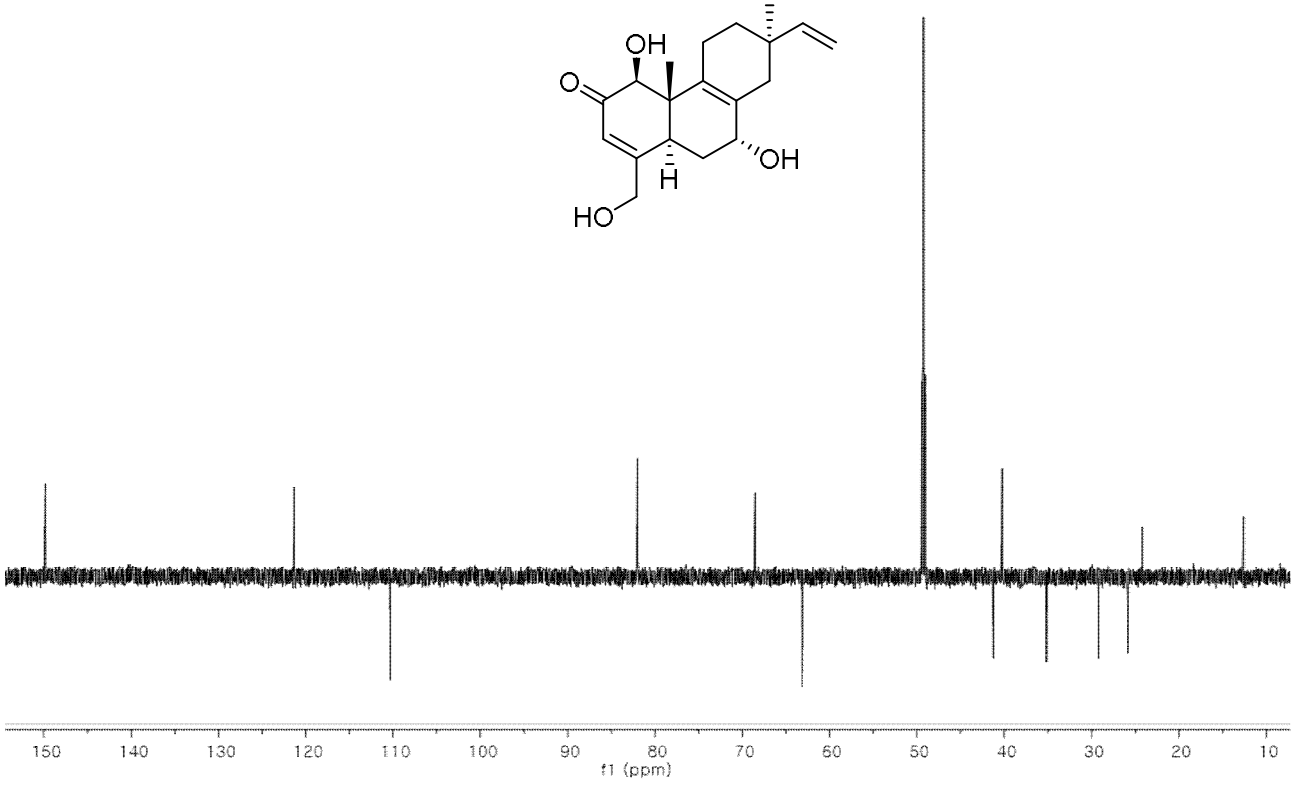

Figure S19. ^{1}H NMR spectrum (900 MHz) of JBIR-65 (**14**) in CD_3OD.

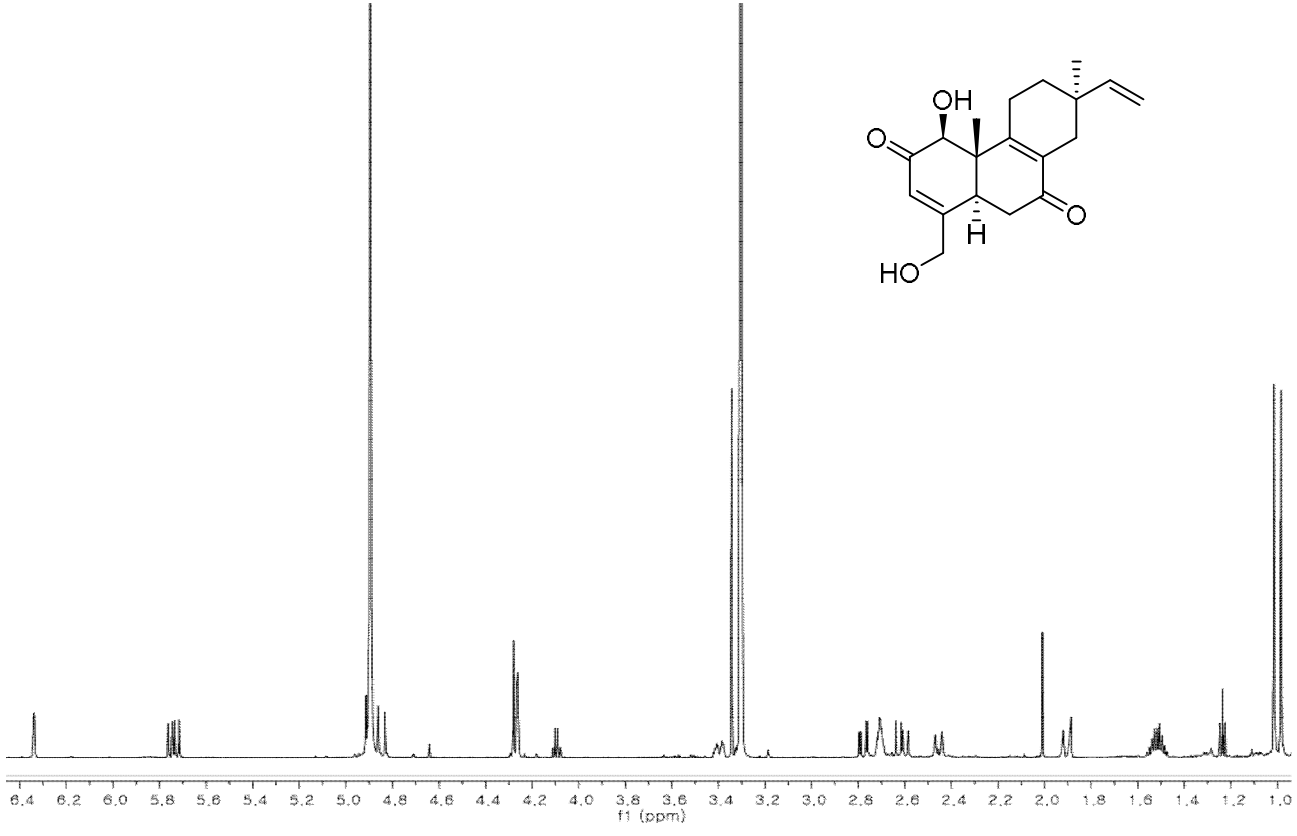

Figure S20. ^{13}C NMR spectrum (225 MHz) of JBIR-65 (**14**) in CD_3OD.

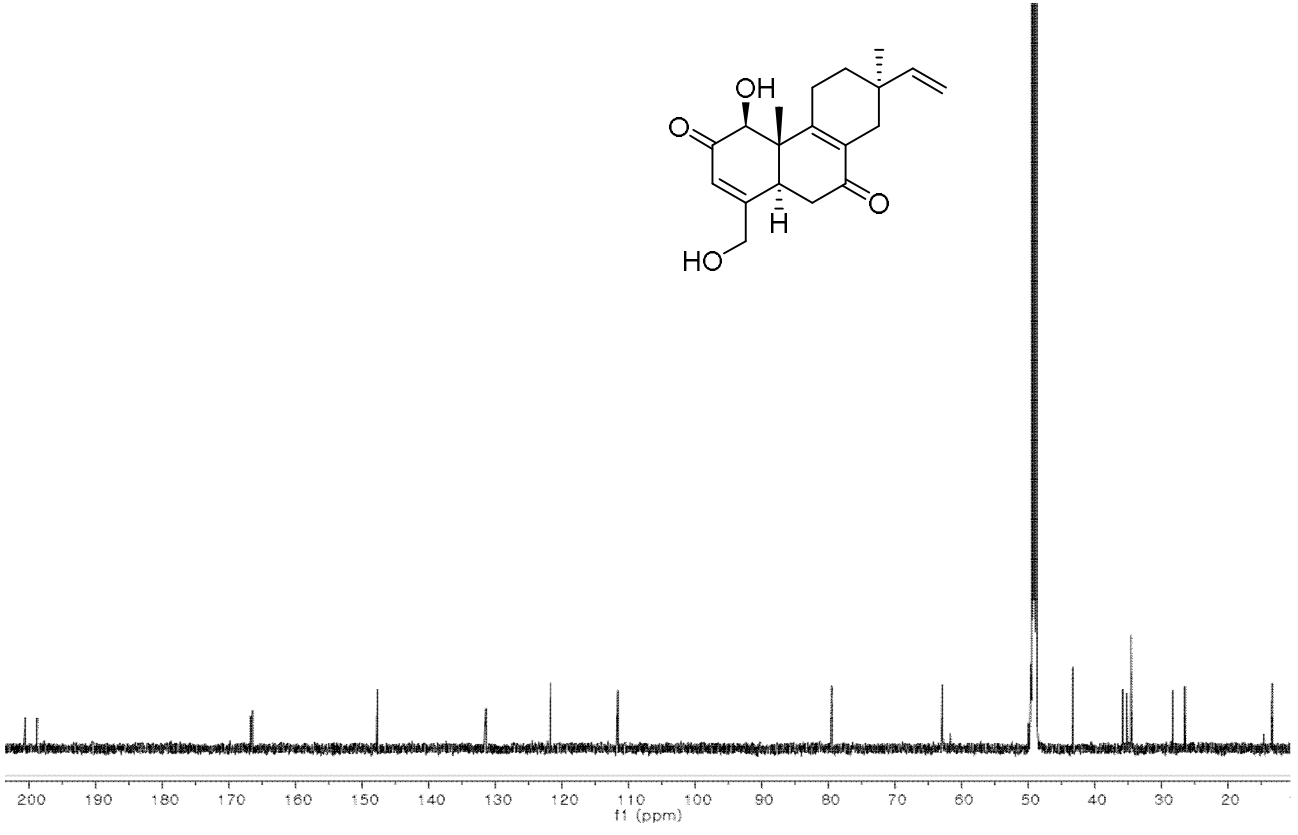

Figure S21. ^{1}H NMR spectrum (600 MHz) of acetate (**15**) of JBIR-65 (**14**) in CD_3OD.

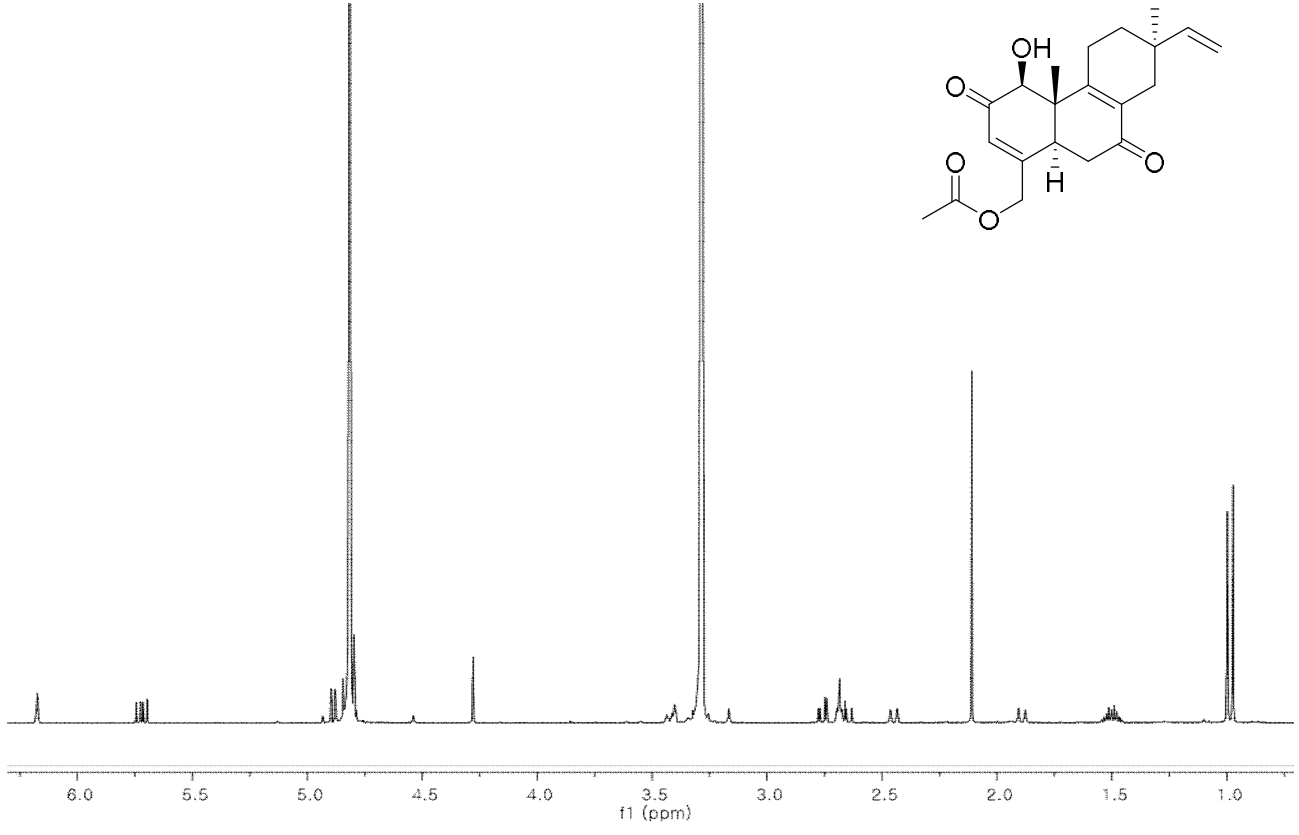

Figure S22. ^{1}H NMR spectrum (600 MHz) of *S*-MTPA ester (**16**) for JBIR-65 (**14**) in DMSO-d_6.

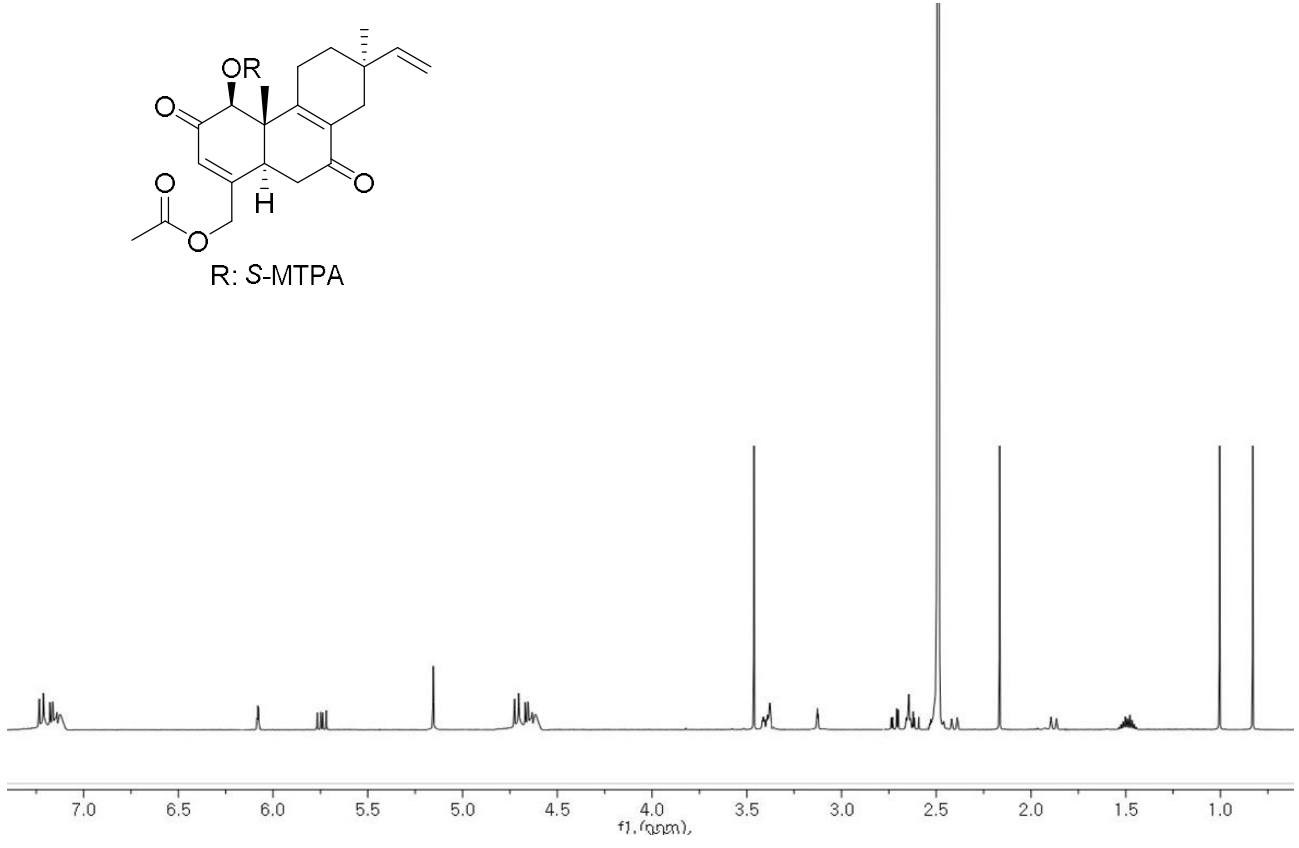

Figure S23. ^{1}H NMR spectrum (600 MHz) of *R*-MTPA ester (**17**) for JBIR-65 (**14**) in DMSO-d_6.

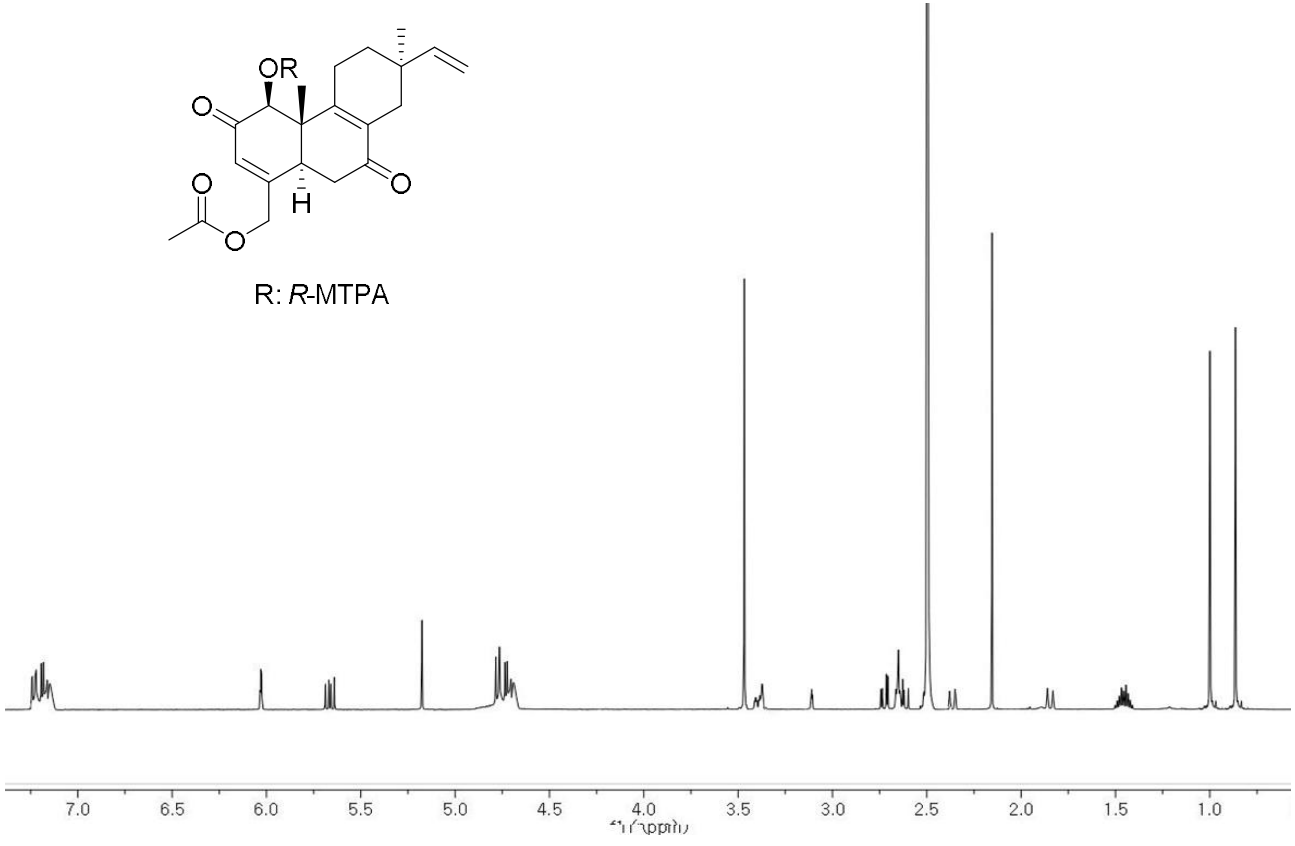

Figure S24. ^{1}H NMR spectrum (600 MHz) of deinococcucin A (**18**) in DMSO-d_6.

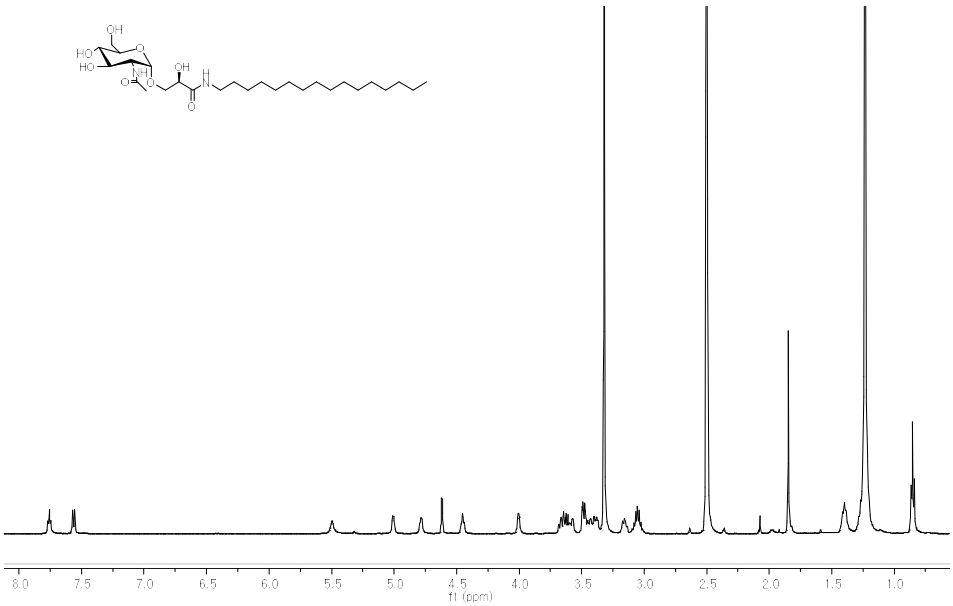

Figure S25. ^{13}C NMR spectrum (150 MHz) of deinococcucin A (**18**) in DMSO-d_6.

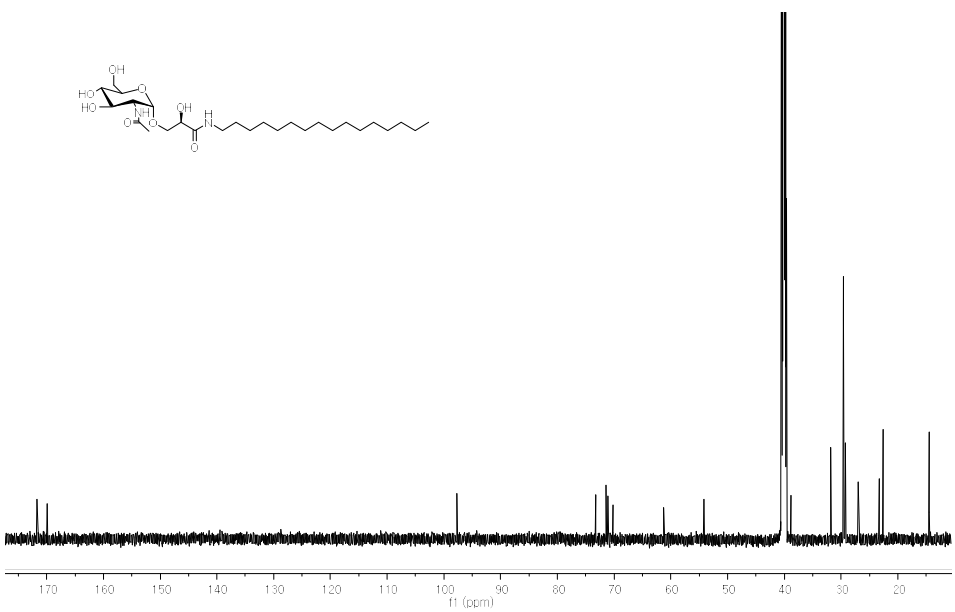

Figure S26. ^{1}H NMR spectrum (600 MHz) of deinococcucin B (**19**) in DMSO-d_6.

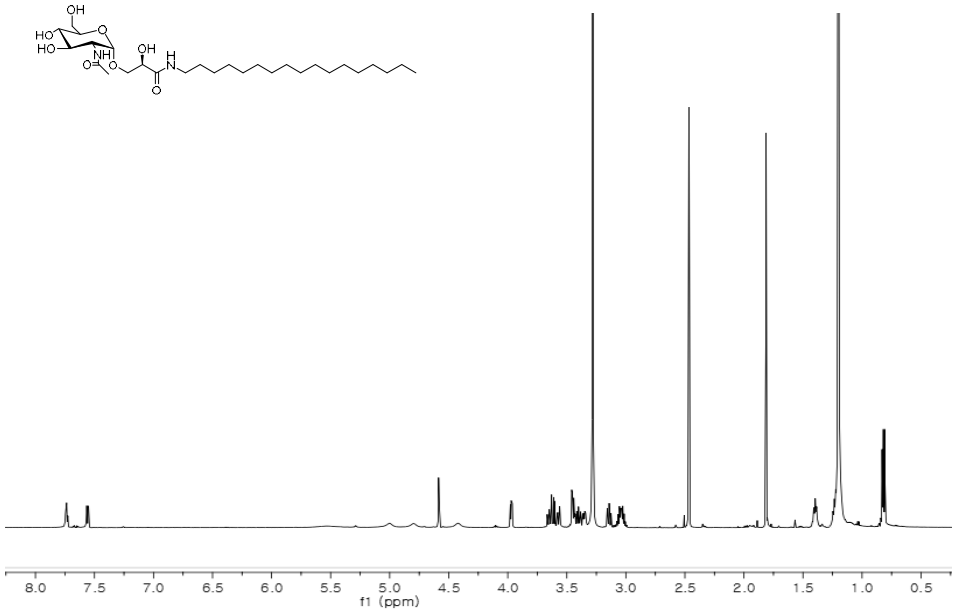

Figure S27. ^{13}C NMR spectrum (150 MHz) of deinococcucin B (**19**) in DMSO-d_6.

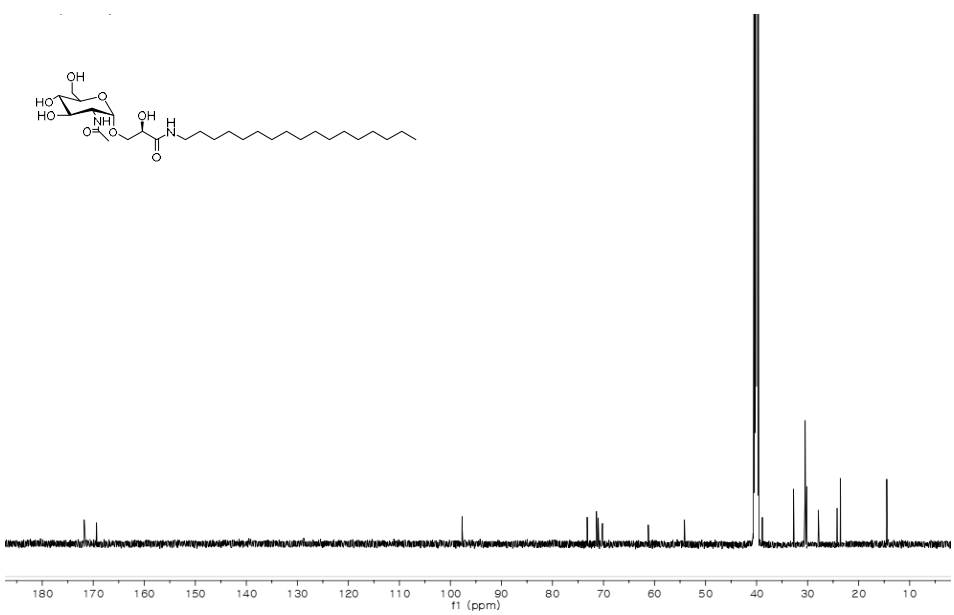

Figure S28. ^{1}H NMR spectrum (600 MHz) of deinococcucin C (**20**) in DMSO-d_6.

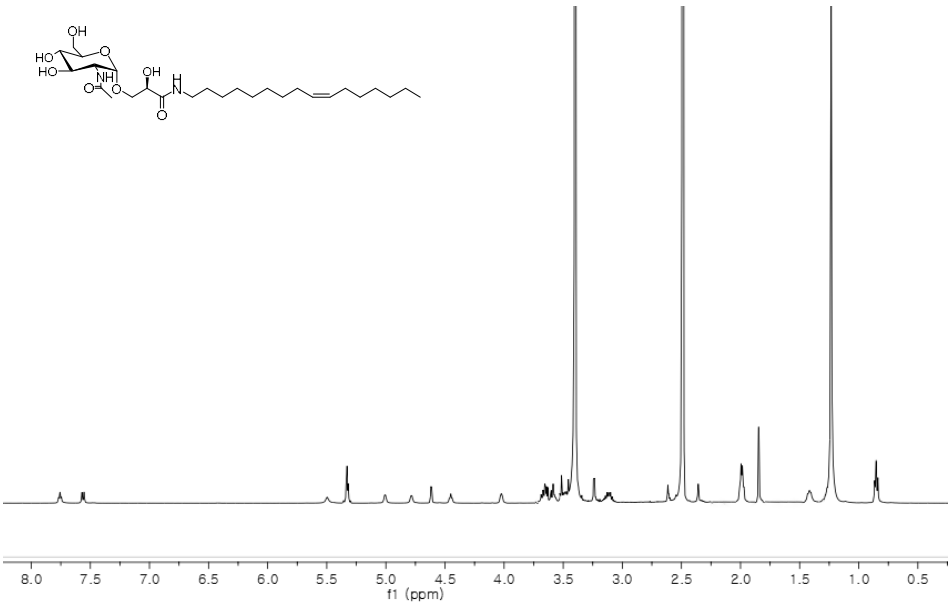

Figure S29. ^{13}C NMR spectrum (150 MHz) of deinococcucin C (**20**) in DMSO-d_6.

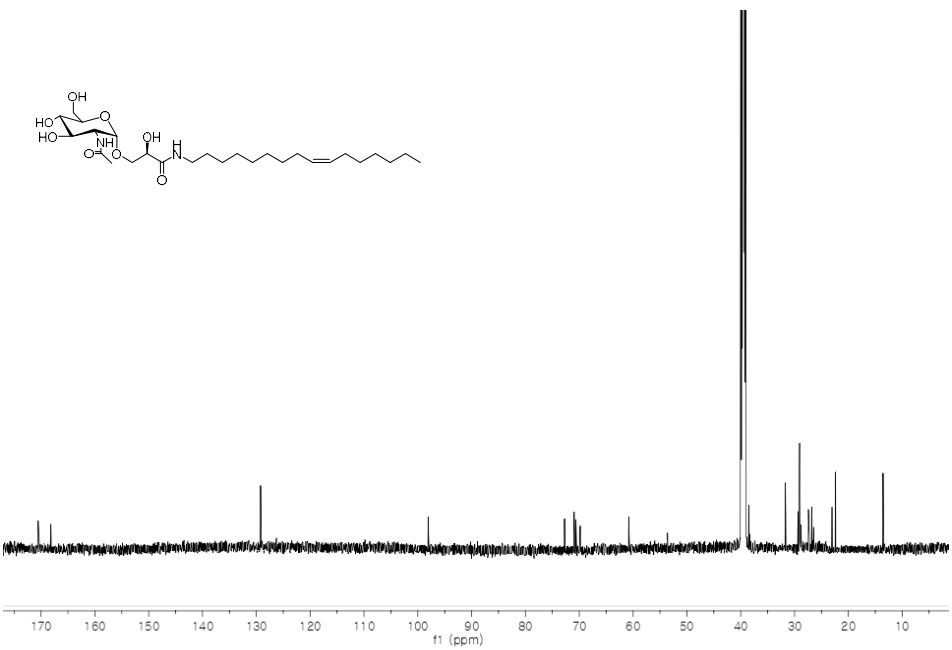

Figure S30. ^{1}H NMR spectrum (600 MHz) of deinococcucin D (**21**) in DMSO-d_6.

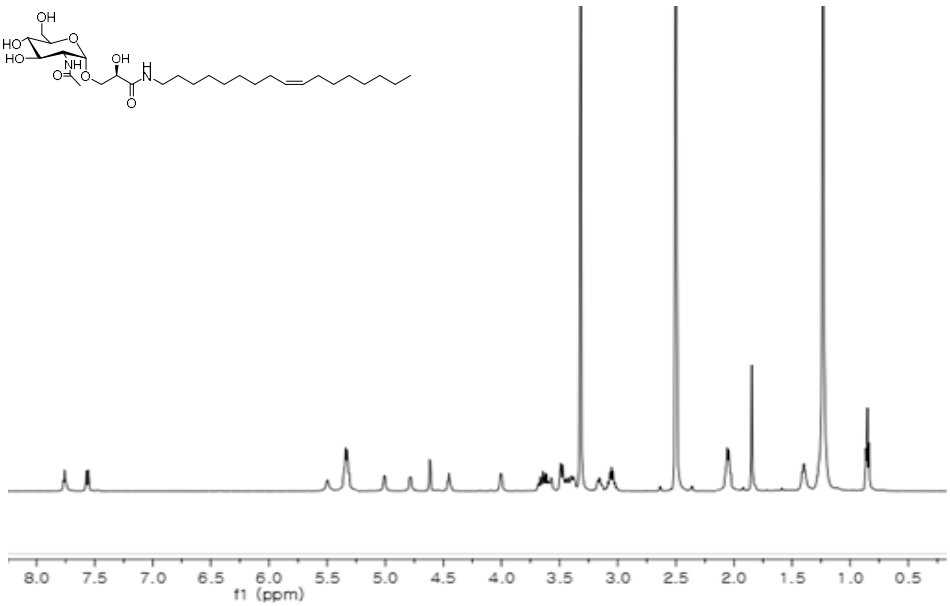

Figure S31. ^{13}C NMR spectrum (150 MHz) of deinococcucin D (**21**) in DMSO-d_6.

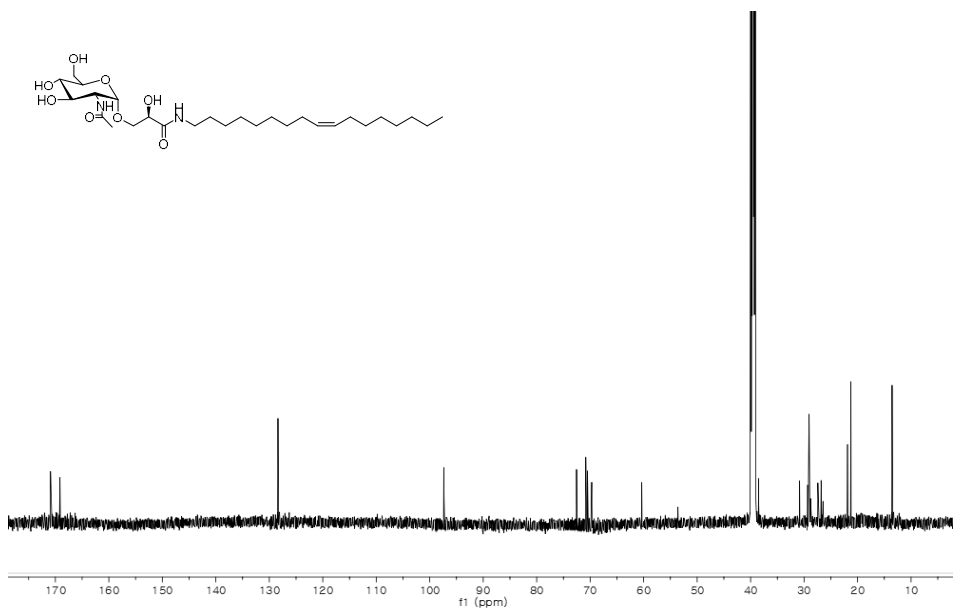

Figure S32. ^{1}H NMR spectrum (600 MHz) of 2,3-dihydroxy-propanoic acid (**22**) in DMSO-d_6.

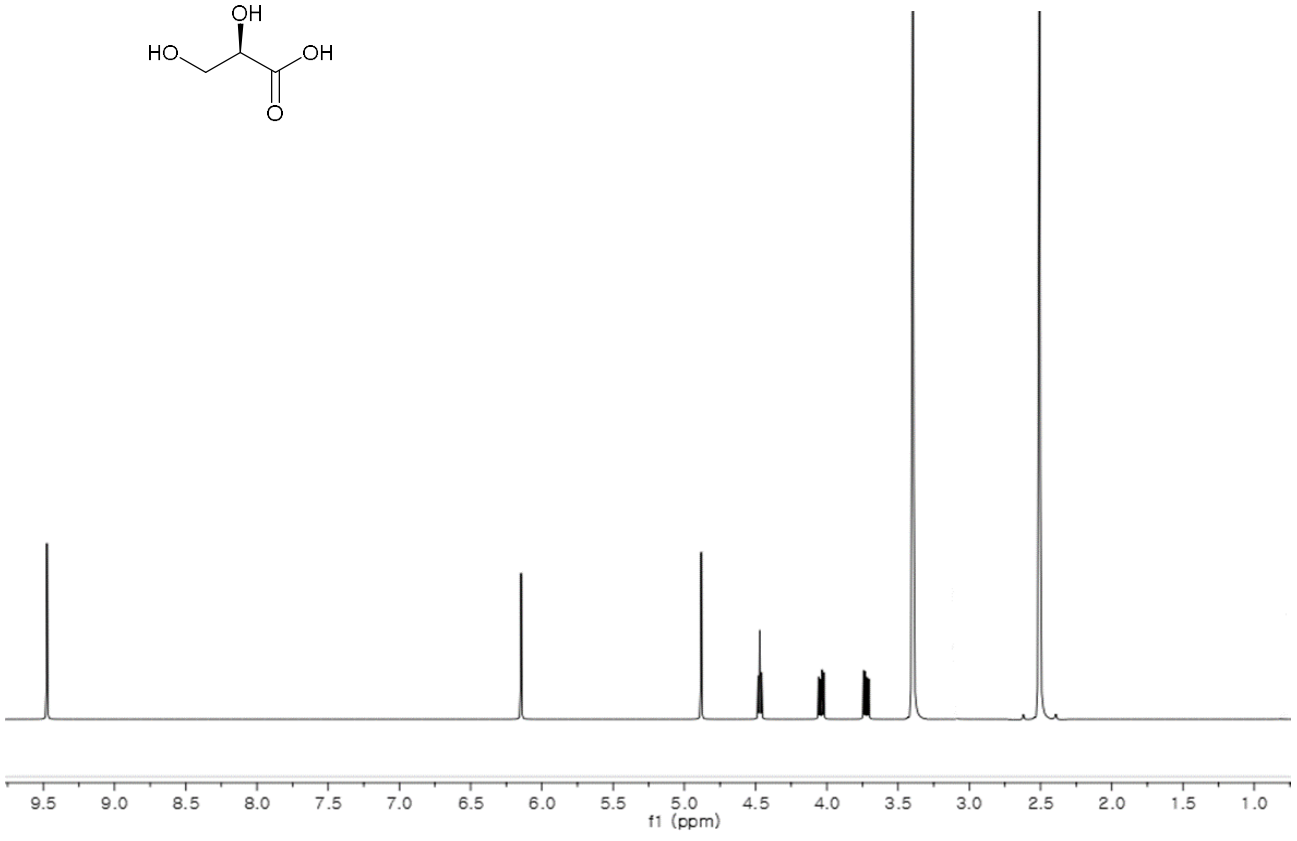

Figure S33. ^{1}H NMR spectrum (600 MHz) of (*S*)-PGME amide (**22a**) of 2,3-dihydroxy-propanoic acid (**22**) in DMSO-d_6.

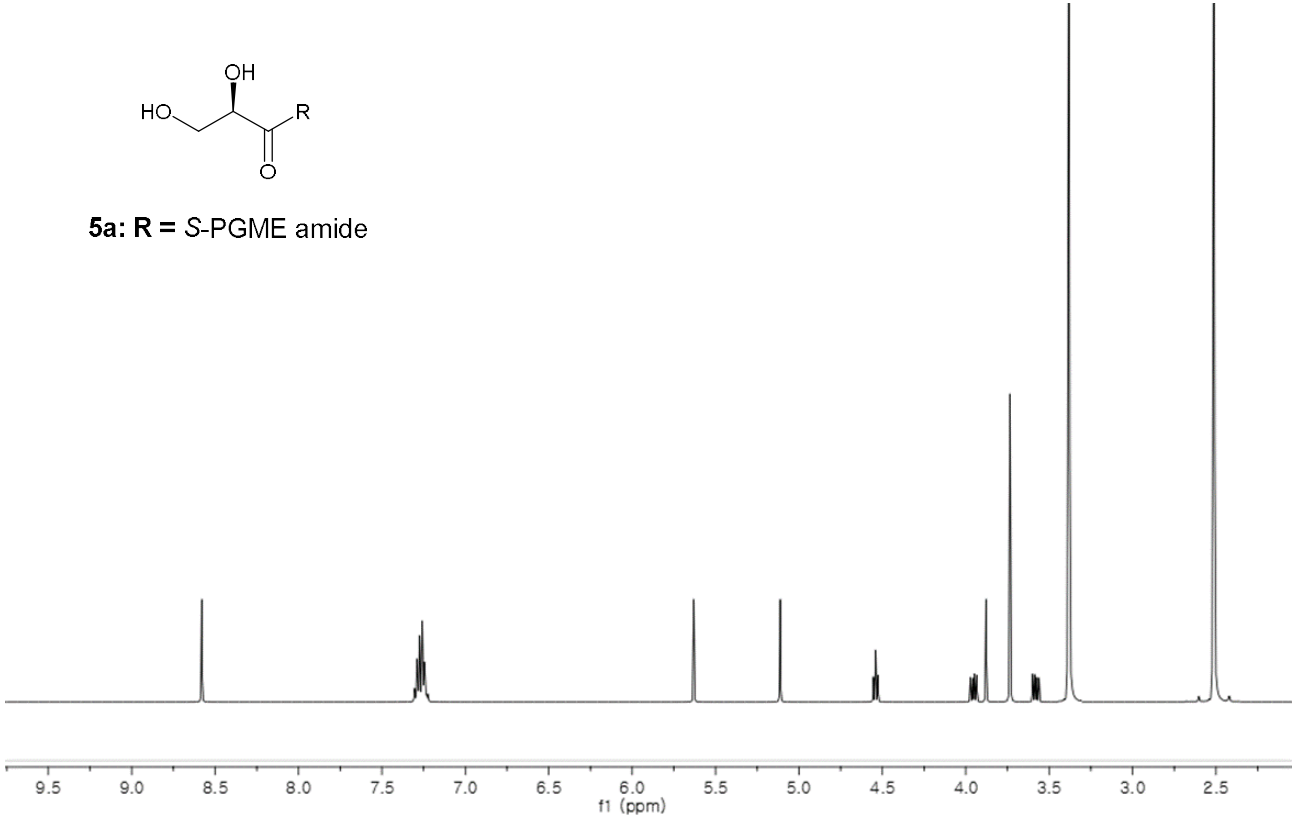

Figure S34. ^{1}H NMR spectrum (600 MHz) of (*R*)-PGME amide (**22b**) of 2,3-dihydroxy-propanoic acid (**22**) in DMSO-d_6.

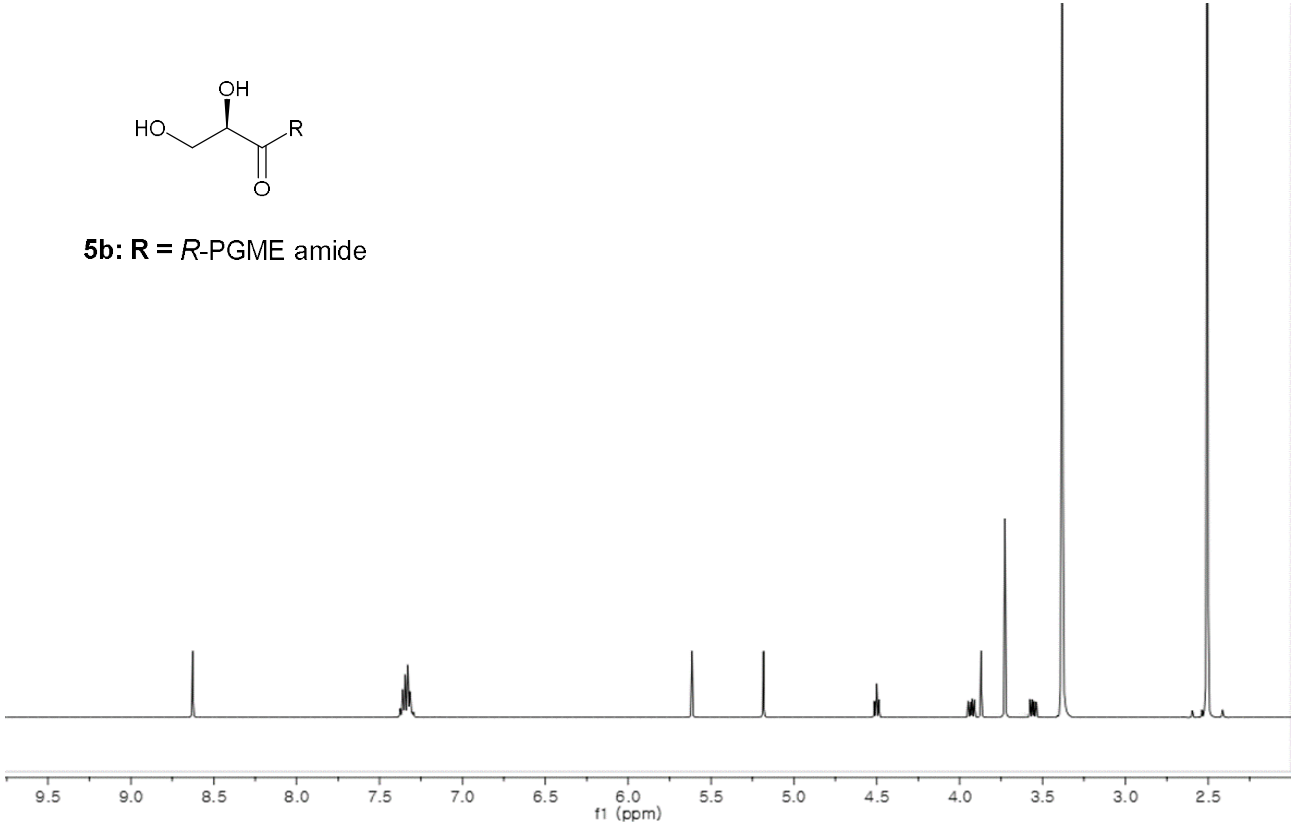

APPENDIX B:

Supporting information

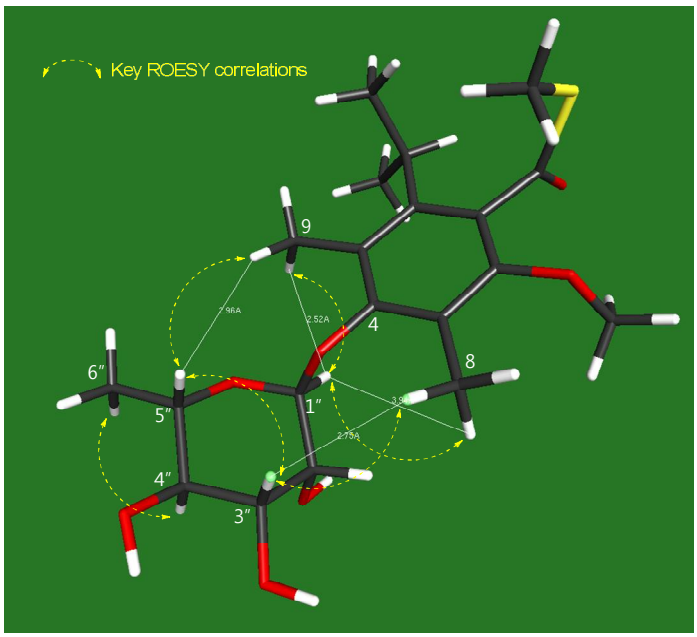

Figure S35. Minimum energy conformation of Suncheonoside C (**3**).

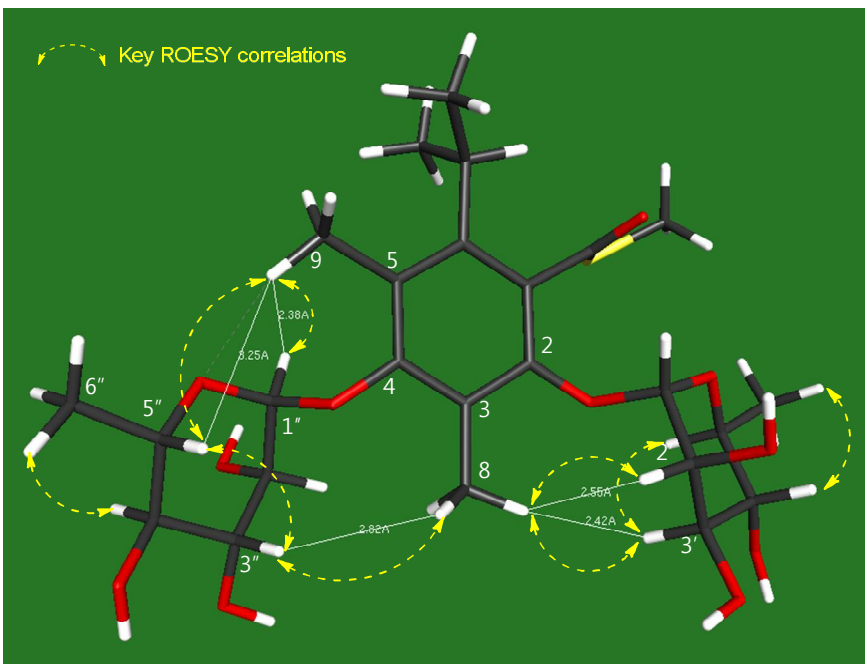

Figure S36. Minimum energy conformation of Suncheonoside D (**4**).

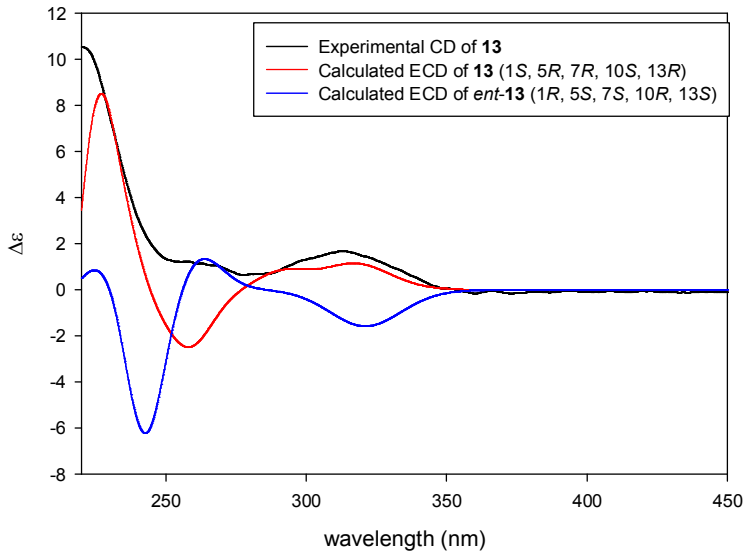

Figure S37. Experimental CD spectra of **13**, calculated ECD spectra of **13** (1*S*, 5*R*, 7*R*, 10*S*, 13*R*), and *ent*-**13** (1*R*, 5*S*, 7*S*, 10*R*, 13*S*).

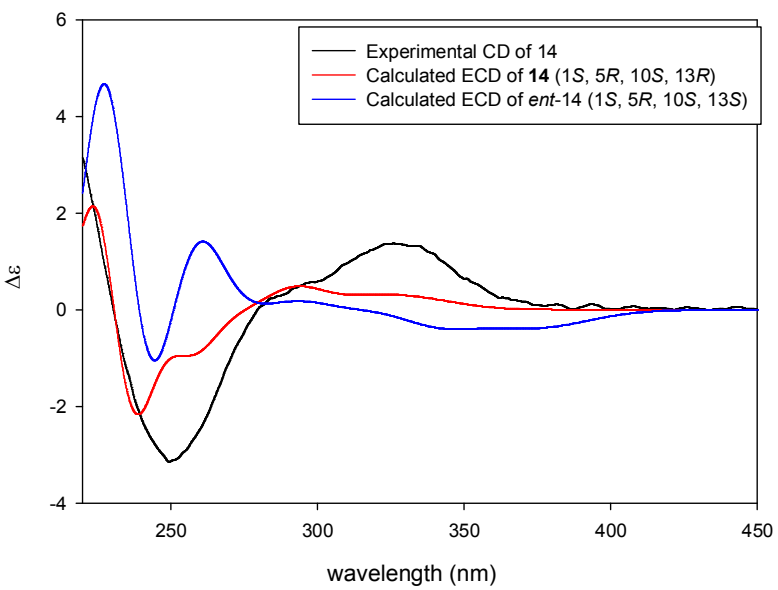

Figure S38. Experimental CD spectra of **14**, calculated ECD spectra of **14** (1*S*, 5*R*, 10*S*, 13*R*), and *ent*-**14** (1*S*, 5*R*, 10*S*, 13*S*).

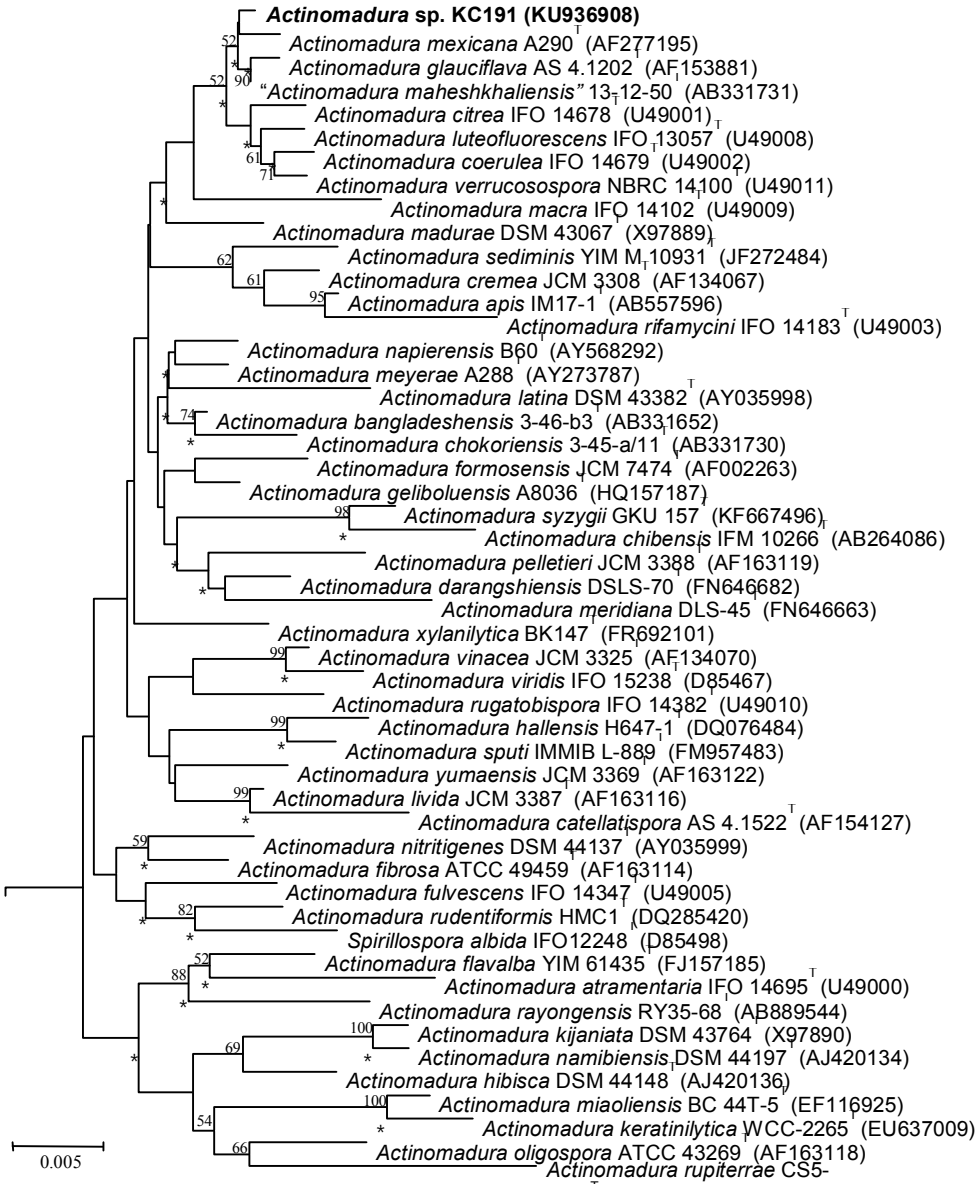

Figure S39. A neighbour-joining tree based on 16S rRNA gene sequences showing the relationship between isolate KC191 and the type strains of closely related species of the genus *Actinomadura*. Asterisks represent the corresponding branches that were also found in the trees created by both the maximum-likelihood and maximum-parsimony methods. *Actinomadura echinospora* IFO 14042T was used as an outgroup. Bootstrap values (>50 %) based on 1000 replications are shown at the nodes. Bar, 0.005 substitution per site.

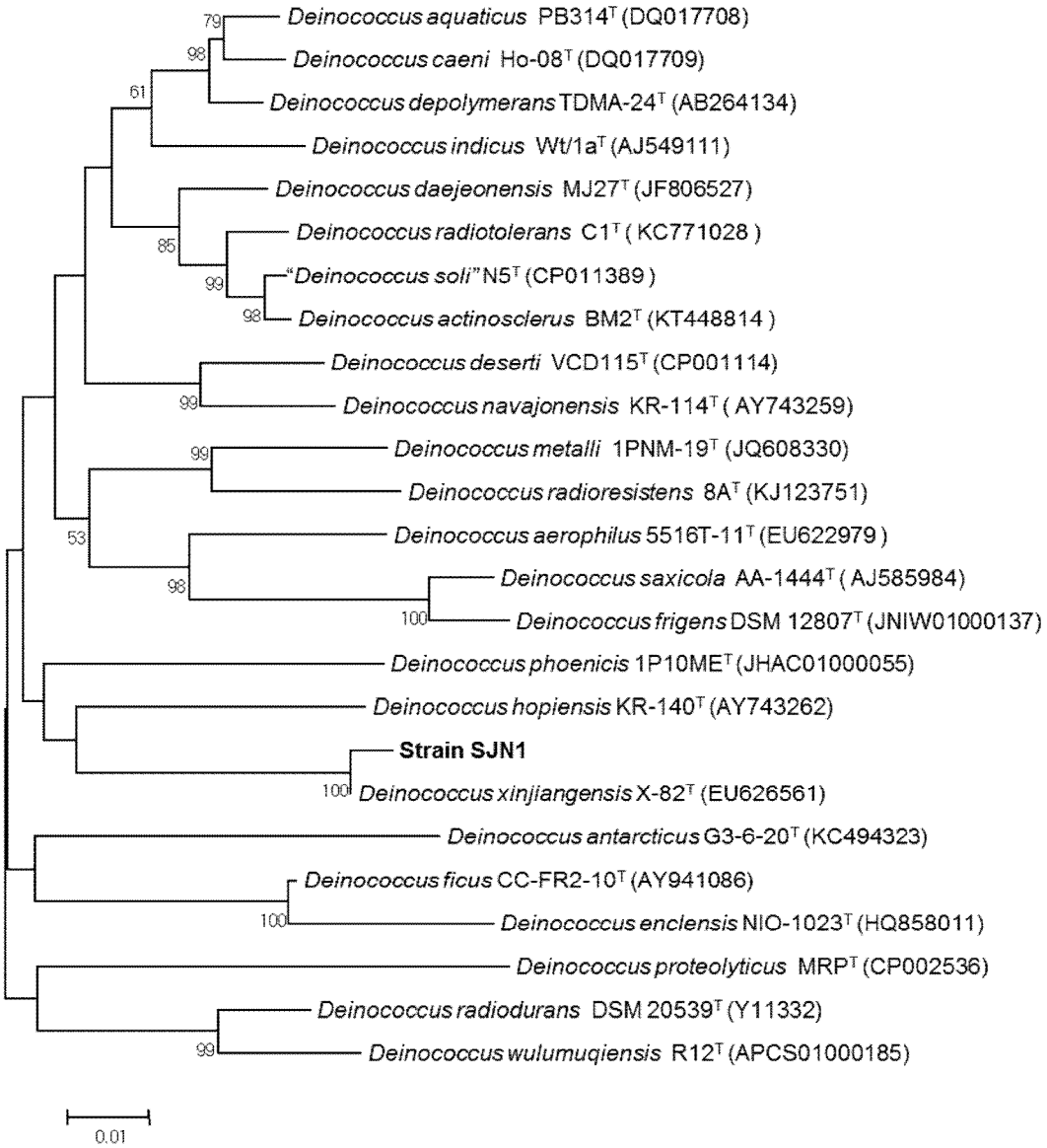

Figure S40. Phylogenetic tree reconstructed from a comparative analysis of 16S rRNA gene sequences showing the relationship between strain SJN1 and type strains of *Deinococcus* genus. Bootstrap values (expressed as percentages of 1000 replications) greater than 50 % are shown at branch points. Bar, 0.01 substitutions per nucleotide position.

Table S1. ECD calculation of actinomadurol (**13**)

total energy = -1039.04112
kinetic energy = 1029.42618
potential energy = -2068.46730

Parameters of Level DFT
DFT settings (Functional B3-LYP / Gridsize M3)
Geometry optimization options (Energy 10^{-6} Hartree, Gradient norm $\left|dE / dxyz\right| = 10^{-3}$ Hartree/Bohr)

Energy minimized coordinates of actinomadurol at the basis set def-SV(P) for all atoms (Å).

Atom	X	Y	Z	Atom	X	Y	Z
C	-3.1063	5.3704	0.7826	H	3.981	4.8719	1.1187
C	-3.2452	3.9263	0.9258	H	4.767	6.0644	-0.0805
C	-2.2488	3.1769	1.4458	C	-0.2587	5.0545	-0.2128
H	-4.1662	3.4727	0.5508	H	0.703	4.5393	-0.3688
C	-0.9644	3.8055	1.9553	H	-1.0399	4.5079	-0.7712
C	-0.6036	5.1791	1.2936	H	-0.1776	6.061	-0.6533
C	-1.8881	6.0569	1.43	H	-4.3578	1.6085	1.9071
H	-2.1185	6.1335	2.519	H	-2.6399	7.4784	0.4028
O	-1.7815	7.3329	0.8631	H	2.3142	3.0157	2.6085
O	-3.9108	6.0679	0.1804	H	1.232	2.3121	4.4315
C	0.6226	5.7707	2.0307				
C	1.5006	4.9874	2.6996				
C	1.3415	3.4911	2.8558				
C	0.2629	2.8874	1.9551				
H	0.6504	2.7471	0.9308				
H	0.0259	1.8835	2.3465				
H	-1.1569	4.0244	3.0276				
O	1.0483	3.2469	4.2387				
C	-2.4338	1.6814	1.6026				
O	-3.7183	1.2033	1.2963				
H	-2.1253	1.3909	2.6316				
H	-1.742	1.1546	0.9195				
C	0.8917	7.2609	1.8944				
C	1.9188	7.8083	2.8884				
H	1.2317	7.4603	0.8585				
H	-0.0434	7.8287	1.9905				
C	3.1854	6.9308	2.9861				
H	1.4628	7.8673	3.8956				
H	2.1888	8.8434	2.6048				
C	2.7212	5.5315	3.4233				
H	2.4914	5.5541	4.5057				
H	3.5548	4.81	3.3285				

C	3.902	6.9429	1.6457
C	4.1495	7.5146	4.0414
H	3.6456	7.6128	5.0209
H	4.508	8.5173	3.7437
H	5.0341	6.8651	4.1725
C	4.2303	5.9087	0.8635
H	4.186	7.9522	1.3093

Table S2. ECD calculation of JBIR-65 (**14**)

total energy = -1037.86773
kinetic energy = 1069.267634
potential energy = -2148.808023

Parameters of Level DFT
DFT settings (Functional B3-LYP / Gridsize M3)
Geometry optimization options (Energy 10^{-6} Hartree, Gradient norm $\left|dE / dxyz\right| = 10^{-3}$ Hartree/Bohr)

Energy minimized coordinates of JBIR-65 at the basis set def-SV(P) for all atoms (Å).

Atom	X	Y	Z	Atom	X	Y	Z
C	-6.1717	2.6558	-1.5063	H	-3.8901	1.061	0.3717
C	-7.4782	3.0777	-0.8246	H	-4.3835	1.3031	2.8676
C	-8.254	1.8659	-0.2952	H	-4.187	-4.5719	0.5733
C	-7.2826	3.7935	-0.0053	H	-5.1494	-2.529	1.0607
C	-8.1138	3.6184	-1.5491	C	-1.5024	-0.5173	2.3483
C	-7.4298	0.9775	0.689	H	-0.4598	-0.8517	2.2244
C	-9.1932	2.197	0.1877	H	-1.5201	0.25	3.1383
H	-8.5514	1.2403	-1.1581	H	-2.1041	-1.3742	2.7014
C	-5.2475	1.8529	-0.5616				
H	-5.632	3.5342	-1.8972				
H	-6.4095	2.0319	-2.3866				
C	-6.0503	0.657	0.0452				
C	-4.0887	1.2373	-1.405				
C	-3.2511	0.0655	-0.8212				
C	-4.137	-0.9455	-0.0451				
H	-5.1318	-0.2416	0.887				
H	-6.3191	0.0501	-0.8338				
C	-5.7118	-1.0131	1.4194				
H	-4.592	0.3265	1.6635				
H	-4.5939	2.8333	0.4514				
C	-5.3204	3.5763	0.8205				
H	-3.7848	3.3985	-0.0441				
H	-4.16	2.3366	1.333				
C	-7.3207	1.6269	2.088				
H	-6.7316	2.5548	2.0552				
H	-6.8373	0.9495	2.8132				
H	-8.3098	1.9035	2.5009				
C	-8.2092	-0.3601	0.7951				
C	-2.4073	-0.6231	-1.9322				
H	-1.0913	-1.0808	-1.2698				
H	-2.2015	0.1246	-2.7094				
H	-2.9682	-1.4485	-2.3927				

O	-0.88	-0.1093	-0.1156
C	-1.1725	-2.1097	-0.877
O	-0.2406	-1.065	-1.9751
H	-2.1562	0.5913	0.1285
H	0.2149	-0.3474	0.9215
O	-0.0115	-1.6553	1.6998
O	-0.0535	-2.5376	1.0376

국문논문요지

Streptomyces, Actinomadura, Deinococcus 박테리아로부터 유래한 생리활성 이차대사 물질 연구

신보라
서울대학교 약학대학 대학원
천연물과학전공

인류에게 있어서 미생물 기원 생리활성 천연물질은 질병 치료를 위한 신약 개발, 특히 항생제, 항암제 등의 개발의 중심축으로 자리한다. 2015 년, *Streptomyces avermitilis* 에서 유래한 천연물 아버맥틴(avermectin)의 발견과 이로부터 구충제 이버맥틴(ivermectin)의 개발에 대한 공로가 인정되어 물질 발견자인 일본 기타사토대학의 오무라 교수와 미국 드루대 캠벨 교수가 노벨 생리의학상을 수상하였다. 이러한 수상으로부터 천연물 유래 신약 개발의 중요성을 짐작해볼 수 있다. 뿐만 아니라 2012 년에 작성된 통계에 따르면 미생물 유래 생리활성물질은 약 70,000 종이 보고되었고 이들로부터 약 450~500 종류의 신약이 개발되었다. 이것은 약 0.64~0.71%의 비율로서 합성 화합물로부터 신약이 개발되는 비율인 약 0.025%, 전체 천연물로부터 신약이 개발되는 비율인 0.25%에 비하여 월등히 높다고 볼 수 있으며 이는 미생물 유래 천연물의 우수성을

입증하는 것이라 여겨진다. 이러한 미생물로부터 유래한 신규 생리 활성 물질을 발견하고자 하는 노력의 일환으로 다양한 환경 (해양, 농토, 곤충의 장내)에서 얻어진 다양한 종류의 박테리아 균주 (*Streptomyces*, *Actinomadura*, *Deinococcus* sp.)로부터 유력한 이차대사산물 생산 물질들을 분리, 구조 규명하였다.

1. 순천만에서 분리된 *Streptomyces* sp.가 생산하는 생리활성 이차대사물질 연구

Streptomyces 에 속하는 SSC21 균주는 전라남도 순천시 순천만에서 채집된 퇴적물에서 분리 되었다. 순천만은 강물을 따라 유입된 토사와 유기물 등이 바닷물의 조수 작용으로 퇴적되어 생긴 곳으로 오염원이 적어 다양한 생물이 풍부하게 발달되어있는 습지보존지역이다. 따라서 이러한 지형적, 환경적 특이성이 새로운 균주를 얻을 수 있는 적절한 장소라 생각되어 채집이 시행되었다. LC/MS 를 이용한 화학적 분석을 통해 SSC21 균주가 생산하는 신규 물질 4 개를 발견할 수 있었고, 이를 Suncheonosides A-D 라 명명하였다. 특히, 특이한 mass spectrum 의 분석을 통해 이 물질이 황을 포함하는 것임을 예측할 수 있었다. Suncheonoside 의 평면구조는 ^{1}H, ^{13}C, COSY, HSQC, HMBC, ROESY 등의 NMR 자료 및 MS 등의 다양한 분광학적 분석을 통해 hexasubstituted benzothioate glycoside 임이 밝혀졌다. 당의 입체구조를 분석하기 위해서 ROESY 분석, $^{1}H-^{13}C$ 결합상수 분석, 화학 반응이 적용되었으며 그 결과 L-rhamnose 임을 밝힐 수 있었다 (Figure 1). Sunchenosides A, B 와 D 는 농도의존적으로 아디포넥틴의 생산을 증진하는 항당뇨병 활성을 보인다.

(a)

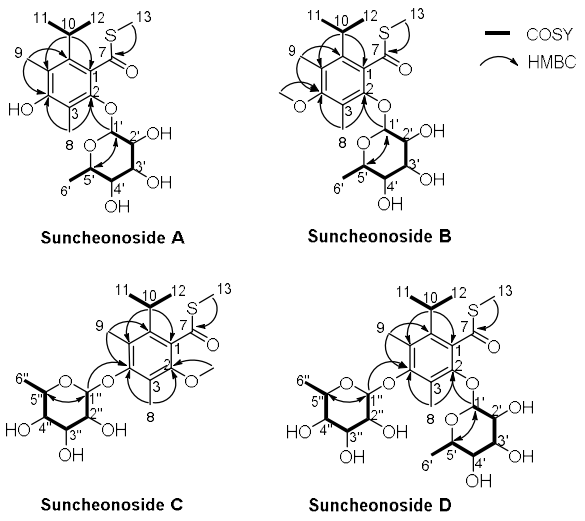

(b)

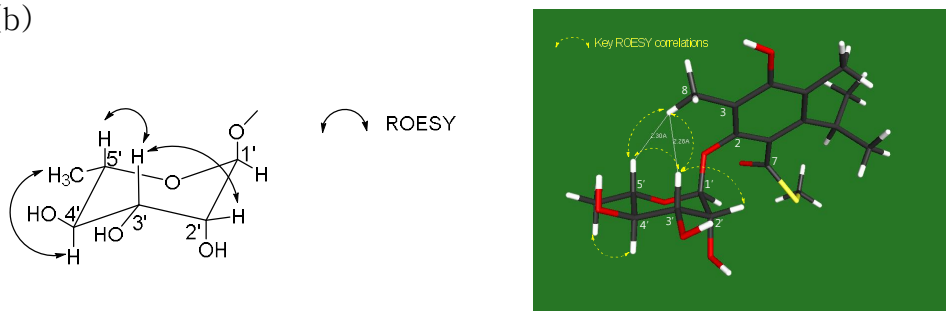

Figure 1. (a) The structures of suncheonosides A, B, C and D. (b) The observed strong ROESY correlations in the hexose moiety and key ROESY correlations and distances between protons of suncheonoside A.

2. 흰점박이꽃무지 애벌레의 장에서 분리된 *Streptomyces* sp.가 생산하는 생리활성 이차대사물질 연구

Streptomyces 균주인 JS8 은 흰점박이꽃무지 애벌레의 장에서 분리되었다. 흰점박이꽃무지 애벌레는 초가지붕에서 채집되거나 일부 농가에서 사육해 판매하던 곤충으로, 주로 약용으로 이용된다. 조선시대에 편찬된 의학서적인 <동의보감>에는 “간 질환 등 성인병 치료

효과가 있다.” 고 기술돼 있다. 따라서 약용곤충으로부터 새로운 생리활성 물질을 찾고자 실험을 진행하였다. 흰점박이꽃무지 애벌레로부터 약 80 개의 균주를 얻을 수 있었으며 그 중 균주 JS8 는 LC/MS 의 화학적 분석을 통해 신규 물질을 생산함을 예상할 수 있었다. ^{1}H, ^{13}C, COSY, HSQC, HMBC, ROESY 등의 NMR 자료 및 MS 등의 다양한 분광학적 기법을 사용하여 새로운 플라보노이드 계열 물질 JS8 A 와 B 를 생산함을 밝힐 수 있었다. 특히, JS8 A 와 B 는 에피머 관계를 이루고 있어 카이랄 HPLC 를 이용하여 분리될 수 있었다. 입체구조 결정을 위해서는 time-controlled acetylation 과 MTPA 를 이용한 modified Mosher 방법이 적용되었다 (Figure 2). 두 물질의 생리활성 연구가 진행 중에 있다.

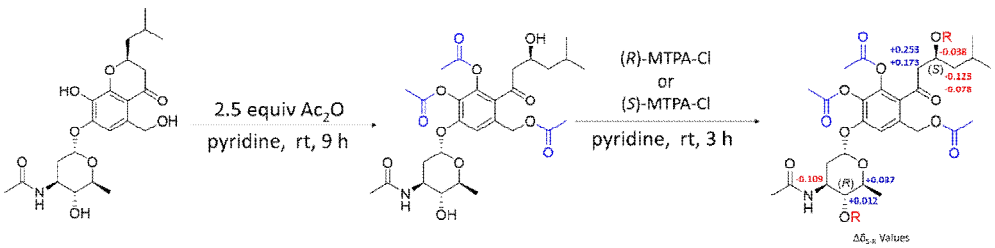

Figure 2. Using time-controlled acetylation and modified Mosher method to determine the absolute configuration of JS8 A.

3. 영국 농토에서 분리된 *Actinomadura* sp.가 생산하는 생리활성 이차대사물질 연구

새로운 이차대사물질인 actinomadurol 은 희소방선균인 *Actinomadura* 균주 KC 191로부터 기지 물질인 JBIR-65와 함께 분리되었다. 균주 KC 191은 영국 New castle 지역의 농토에서 얻어진 균주로써 균주 동정 결과 희소방선균인 *Actinomadura* sp. 로 결정되었다. 희소방선균에서 생산되는 물질 Actinomadurol의 평면 구조는 ^{1}H, ^{13}C, COSY, HSQC, HMBC, NOESY 등의 NMR 자료를 바탕으로 하여 매우 드물게 존재하는 탄소 19개의 norditerpenoid 구조를 가지는 것으로 결정되었다. 또한 입체구조는 ECD 계산을 통하여 결정할 수 있었다

(Figure 3). 또한 기지물질인 JBIR-65의 입체구조를 결정하기 위하여 time-controlled acetylation, modified Mosher 방법과 ECD 계산이 수행되었고, 이를 통해 이전에 밝혀지지 않았던 입체구조를 밝히는데 성공하였다. Actinomadurol은 *Staphylococcus aureus*, *Kocuria rhizophila*, *Proteus hauseri* 등에 대하여 항박테리아 효과를 보이는 것으로 보인다.

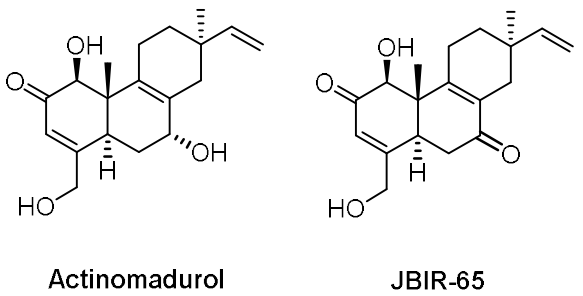

Actinomadurol JBIR-65

Figure 3. The structures of actinomadurol and JBIR-65.

4. 일본 왕개미의 장내에서 분리된 *Deinococcus* sp. 가 생산하는 생리활성 이차대사물질 연구

일본왕개미(*Camponotus japonicus*)의 여왕개미의 장으로부터 분리된 SJN1 균주에서 네 종의 신규 aminoglycolipid를 발견하였다. 일본왕개미는 우리나라에서 서식하는 가장 흔하고 큰 개미 중 하나로 여왕개미가 짝짓기를 위해 혼인비행을 하는 시점인 5월에 채집되었다. 이러한 여왕개미의 장에서 분리된 균주 SJN1은 *Deinococcus* sp. 로 동정되었으며 여기서 분리된 deinococcucins A-D라 명명된 네 개의 물질 구조는 1D, 2D NMR 분석과 질량 분석을 통해 밝혀 졌다. 분석 결과 deinococcucins은 *N*-acetyl glucosamine, 2,3-dihydroxypropanoic acid, 16~17개의 하이드로카본 체인을 가진 alkyl amine을 포함하는 것으로 분석되었다. Deinococcucins C와 D에 포함되어 있는 olefinic double bond의 위치를 확인하기 위하여 olefin metathesis를 진행한 후 LC/MS로 분석하였다. *N*-acetyl glucosamine 와 2,3-

dihydroxypropanoic acid의 입체구조는 기준 시료와의 GC/MS 분석과 phenylglycine methyl ester derivatization의 반응을 통해 밝혀낼 수 있었다 (Figure 4). Deinococcucins A와 C는 murine Hepa-1c1c7 cell에 대하여 quinone reductase 활성을 나타내는 것으로 보인다.

(a)

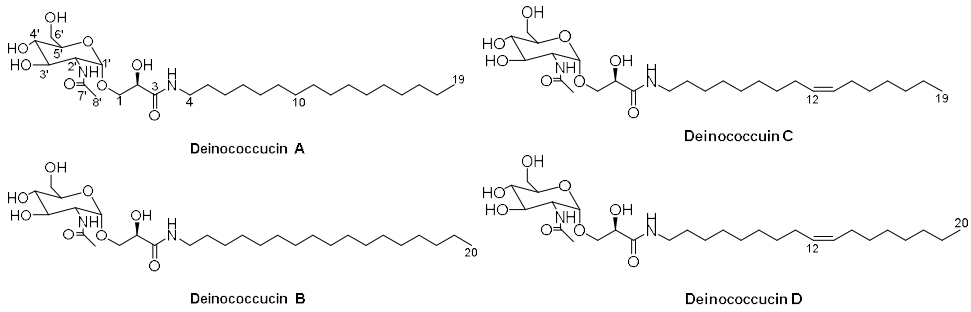

(b)

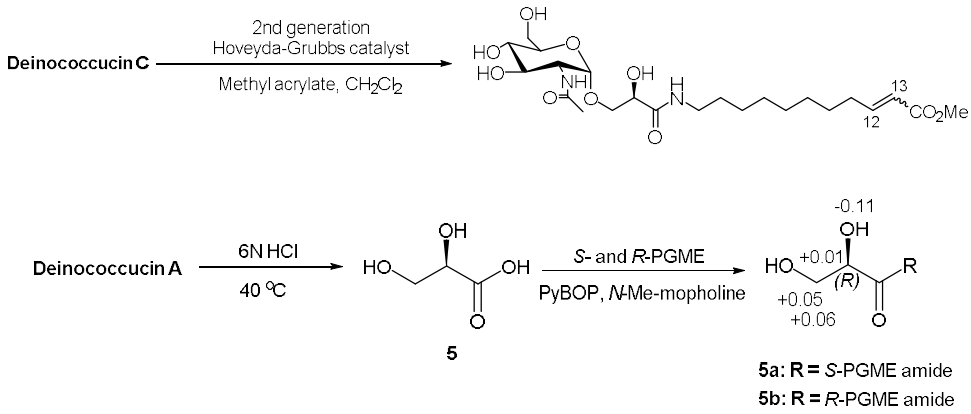

Figure 4. (a) The structures of deinococcucins A, B, C and D. (b) Various chemical reactions to determine the absolute configuration of deinococcucins.

주요어 : 희소방선균, 공생미생물, 구조결정, 생리활성, 생합성
학번 : 2012-23593

Publication List

1. Shin, B.; Park, S. H.; Kim, B.-Y.; Jo, S.-I.; Lee, S. K.; Shin, J.; Oh, D.-C. Deinococcucins A-D, aminoglycolipids from *Deinococcus* sp., a gut bacterium of the carpenter ant *Camponotus japonicus*. *J. Nat. Prod.* **2017**, *80*, 2910-2916.

2. Kim, T. I.; Shin, B.; Kim, G. J.; Choi, H.; Lee, C. S.; Woo, M. H.; Oh, D.-C.; Son J. K. DNA topoisomerase inhibitory activity of constituents from the fruits of *Illicium verum*. *Chem. Pharm. Bull.* **2017**, *55*, 6504-6507.

3. Park, H. B.; Park, J.-S.; Lee, S. I.; Shin, B.; Oh, D.-C.; Kwon, H. C. Gordonic acid, a polyketide glycoside derived from bacterial coculture of *Streptomyces* and *Gordonia* species. *J. Nat. Prod.* **2017**, *80*, 2542-2546.

4. Um, S.; Bach, D.-H.; Shin, B.; Ahn, C.-H.; Kim, S.-H.; Bang, H.-S.; Oh, K.-B.; Lee S. K.; Shin, J.; Oh, D.-C. New naphthoquinone-oxindole alkaloids, coprisidins A and B, from a gut-associated bacterium in the dung beetle, *Copris tripartitus*. *Org. Lett*. **2016**, *18*, 5792-5795.

5. Shin, B.; Kim, B.-Y.; Cho, E.; Oh, K.-B.; Shin, J.; Goodfellow, M.; Oh,

D.-C. Actinomadurol, an antibacterial norditerpenoid from a rare actinomycete, *Actinomadura* sp. *J. Nat. Prod.* **2016**, *79*, 1886-1890.

6. Kim, M. C.; Lee, J. H.; Shin, B.; Subedi, L.; Cha, J. W.; Park, J.-S.; Oh, D.-C.; Kim S. Y.; Kwon, H. C. Salinazinones A and B: pyrrolidinyl-oxazinones from solar saltern-derived *Streptomyces* sp. KMF-004. *Org. Lett*. **2015**, *17*, 5024-5027.

7. Shin, B.; Ahn, S.; Noh, M.; Shin, J.; Oh, D.-C. Suncheonosides A-D, benzothioate glycosides from a marine-derived *Streptomyces* sp. *J. Nat. Prod.* **2015**, *78*, 1390-1396.

8. Jo, Y. H.; Shin, B.; Liu, Q.; Lee, K. Y.; Oh, D.-C.; Hwang, B. Y.; Lee, M. K. Antiproliferative prenylated xanthones and benzophenones from the roots of *Cudrania tricuspidata.* in HSC-T6 cells. *J. Nat. Prod.* **2014**, *77*, 2361-2366.

9. Kim, C. S.; Shin, B.; Kwon, O. W.; Kim, S. Y.; Choi, S. U.; Oh, D.-C.; Kim, K. H.; Lee, K. R. Holophyllin A, a rearranged abietane-type diterpenoid from the trunk of *Abies holophylla. Tetrahedron Lett.* **2014**, *55*, 6504-6507.

Permissions for republication of the published papers in thesis

"Reproduced from [**Shin, B**.; Ahn, S.; Noh, M.; Shin, J.; Oh, D.-C. *Journal of Natural Products*. **2015**, *78*, 1390-1396.]."

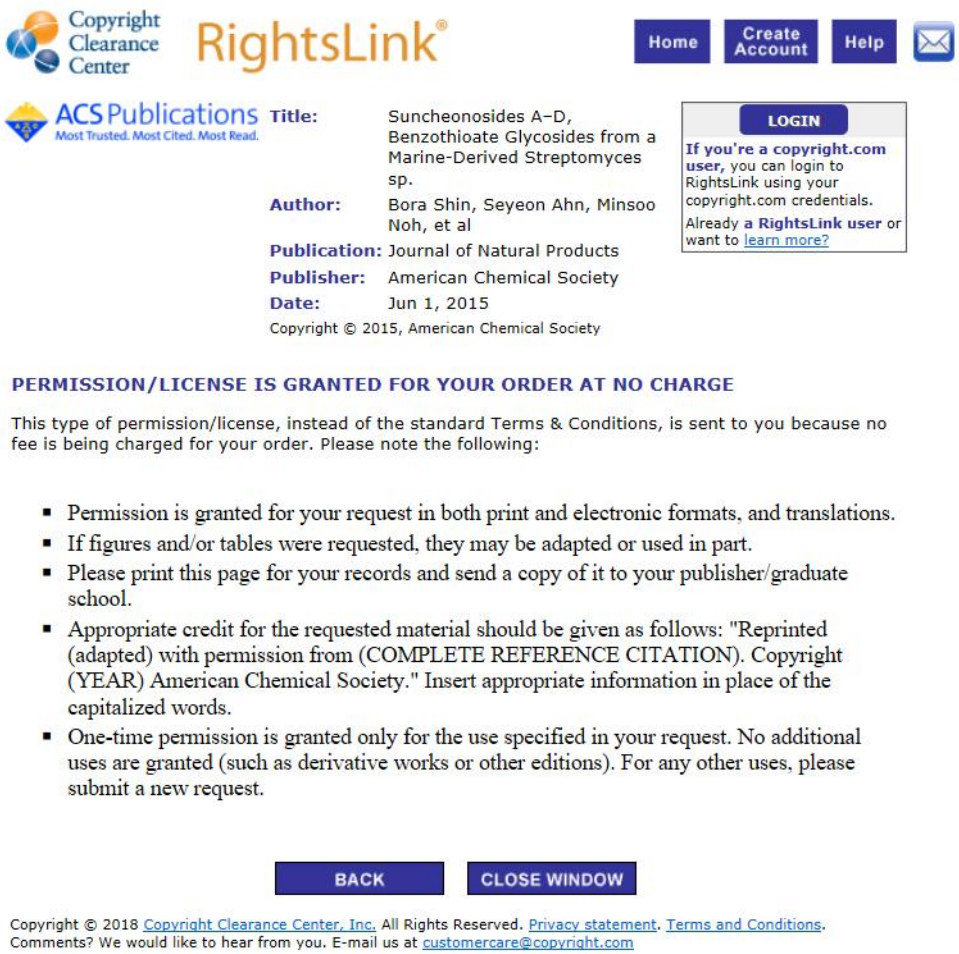

Copyright Clearance Center RightsLink®

Home | Create Account | Help

ACS Publications
Most Trusted. Most Cited. Most Read.

Title: Suncheonosides A–D, Benzothioate Glycosides from a Marine-Derived Streptomyces sp.
Author: Bora Shin, Seyeon Ahn, Minsoo Noh, et al
Publication: Journal of Natural Products
Publisher: American Chemical Society
Date: Jun 1, 2015
Copyright © 2015, American Chemical Society

LOGIN
If you're a copyright.com user, you can login to RightsLink using your copyright.com credentials.
Already a RightsLink user or want to learn more?

PERMISSION/LICENSE IS GRANTED FOR YOUR ORDER AT NO CHARGE

This type of permission/license, instead of the standard Terms & Conditions, is sent to you because no fee is being charged for your order. Please note the following:

- Permission is granted for your request in both print and electronic formats, and translations.
- If figures and/or tables were requested, they may be adapted or used in part.
- Please print this page for your records and send a copy of it to your publisher/graduate school.
- Appropriate credit for the requested material should be given as follows: "Reprinted (adapted) with permission from (COMPLETE REFERENCE CITATION). Copyright (YEAR) American Chemical Society." Insert appropriate information in place of the capitalized words.
- One-time permission is granted only for the use specified in your request. No additional uses are granted (such as derivative works or other editions). For any other uses, please submit a new request.

BACK | CLOSE WINDOW

Copyright © 2018 Copyright Clearance Center, Inc. All Rights Reserved. Privacy statement. Terms and Conditions.
Comments? We would like to hear from you. E-mail us at customercare@copyright.com

Permissions for republication of the published papers in thesis

"Reproduced from [**Shin, B**.; Kim, B.-Y.; Cho, E.; Oh, K.-B.; Shin, J.; Goodfellow, M.; Oh, D.-C. *Journal of Natural Products*. **2016**, *79*, 1886-1890.]."

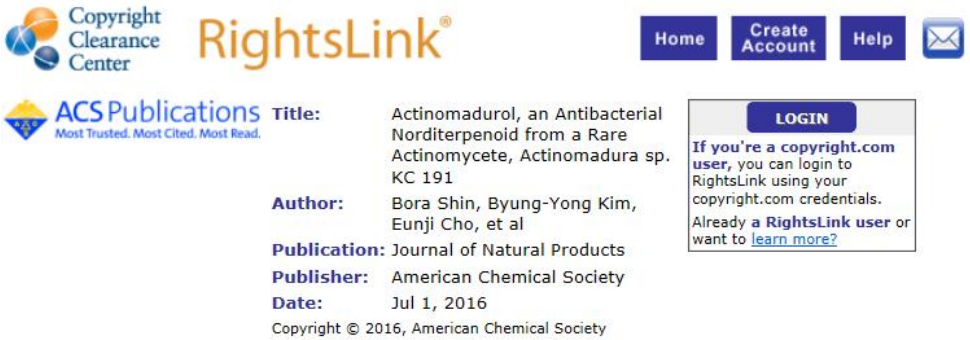

Copyright Clearance Center RightsLink®

Home | Create Account | Help

ACS Publications
Most Trusted. Most Cited. Most Read.

Title: Actinomadurol, an Antibacterial Norditerpenoid from a Rare Actinomycete, Actinomadura sp. KC 191

Author: Bora Shin, Byung-Yong Kim, Eunji Cho, et al

Publication: Journal of Natural Products

Publisher: American Chemical Society

Date: Jul 1, 2016

Copyright © 2016, American Chemical Society

LOGIN

If you're a copyright.com user, you can login to RightsLink using your copyright.com credentials.

Already a RightsLink user or want to learn more?

PERMISSION/LICENSE IS GRANTED FOR YOUR ORDER AT NO CHARGE

This type of permission/license, instead of the standard Terms & Conditions, is sent to you because no fee is being charged for your order. Please note the following:

- Permission is granted for your request in both print and electronic formats, and translations.
- If figures and/or tables were requested, they may be adapted or used in part.
- Please print this page for your records and send a copy of it to your publisher/graduate school.
- Appropriate credit for the requested material should be given as follows: "Reprinted (adapted) with permission from (COMPLETE REFERENCE CITATION). Copyright (YEAR) American Chemical Society." Insert appropriate information in place of the capitalized words.
- One-time permission is granted only for the use specified in your request. No additional uses are granted (such as derivative works or other editions). For any other uses, please submit a new request.

BACK | CLOSE WINDOW

Copyright © 2018 Copyright Clearance Center, Inc. All Rights Reserved. Privacy statement. Terms and Conditions.
Comments? We would like to hear from you. E-mail us at customercare@copyright.com

Permissions for republication of the published papers in thesis

"Reproduced from [**Shin, B**.; Park, S. H.; Kim, B.-Y.; Jo, S.-I.; Lee, S. K.; Shin, J.; Oh, D.-C. *Journal of Natural Products*, **2017**, *80*, 2910-2916.]."

Copyright Clearance Center RightsLink®

Home | Create Account | Help

ACS Publications
Most Trusted. Most Cited. Most Read.

Title: Deinococcucins A–D, Aminoglycolipids from Deinococcus sp., a Gut Bacterium of the Carpenter Ant Camponotus japonicus

Author: Bora Shin, So Hyun Park, Byung-Yong Kim, et al

Publication: Journal of Natural Products

Publisher: American Chemical Society

Date: Nov 1, 2017

Copyright © 2017, American Chemical Society

LOGIN

If you're a copyright.com user, you can login to RightsLink using your copyright.com credentials.

Already a RightsLink user or want to learn more?

PERMISSION/LICENSE IS GRANTED FOR YOUR ORDER AT NO CHARGE

This type of permission/license, instead of the standard Terms & Conditions, is sent to you because no fee is being charged for your order. Please note the following:

- Permission is granted for your request in both print and electronic formats, and translations.
- If figures and/or tables were requested, they may be adapted or used in part.
- Please print this page for your records and send a copy of it to your publisher/graduate school.
- Appropriate credit for the requested material should be given as follows: "Reprinted (adapted) with permission from (COMPLETE REFERENCE CITATION). Copyright (YEAR) American Chemical Society." Insert appropriate information in place of the capitalized words.
- One-time permission is granted only for the use specified in your request. No additional uses are granted (such as derivative works or other editions). For any other uses, please submit a new request.

BACK | CLOSE WINDOW

Copyright © 2018 Copyright Clearance Center, Inc. All Rights Reserved. Privacy statement. Terms and Conditions.
Comments? We would like to hear from you. E-mail us at customercare@copyright.com